

1966

# The behavior of a folded plate roof system

Frederick Mitchell Graham  
*Iowa State University*

Follow this and additional works at: <https://lib.dr.iastate.edu/rtd>



Part of the [Civil Engineering Commons](#)

## Recommended Citation

Graham, Frederick Mitchell, "The behavior of a folded plate roof system " (1966). *Retrospective Theses and Dissertations*. 2898.  
<https://lib.dr.iastate.edu/rtd/2898>

This Dissertation is brought to you for free and open access by the Iowa State University Capstones, Theses and Dissertations at Iowa State University Digital Repository. It has been accepted for inclusion in Retrospective Theses and Dissertations by an authorized administrator of Iowa State University Digital Repository. For more information, please contact [digirep@iastate.edu](mailto:digirep@iastate.edu).

**This dissertation has been  
microfilmed exactly as received 66-10,421**

**GRAHAM, Frederick Mitchell, 1921-  
THE BEHAVIOR OF A FOLDED PLATE ROOF  
SYSTEM.**

**Iowa State University of Science and Technology,  
Ph.D., 1966  
Engineering, civil**

**University Microfilms, Inc., Ann Arbor, Michigan**

**THE BEHAVIOR OF A FOLDED PLATE ROOF SYSTEM**

by

**Frederick Mitchell Graham**

**A Dissertation Submitted to the  
Graduate Faculty in Partial Fulfillment of  
The Requirements for the Degree of  
DOCTOR OF PHILOSOPHY**

**Major Subject: Structural Engineering**

**Approved:**

Signature was redacted for privacy.

**In Charge of Major Work**

Signature was redacted for privacy.

**Head of Major Department**

Signature was redacted for privacy.

**Dean of Graduate College**

**Iowa State University  
Of Science and Technology  
Ames, Iowa**

**1966**

## TABLE OF CONTENTS

	Page
I. INTRODUCTION AND SUMMARY	1
II. REVIEW OF LITERATURE	2
A. Brief Statements on Various Theories	2
B. Primary Theory (No Cross-Sectional Distortion)	3
C. Secondary Theory	5
1. Solution by arbitrarily induced $\Delta$ -values	
2. Iterative procedure	
3. Particular solution procedure	
D. Present Experimental Status	8
E. Published Literature	9
III. DEVELOPMENT OF THEORY	10
A. Fundamental Concepts and Assumptions	10
B. Primary Theory	12
C. Secondary Theory	23
1. Iterative procedure	
2. Particular solution procedure	
D. Development of Secondary Theory	26
E. Additional Analytical Refinements	36
F. Buckling Analysis of Edge Plate	37
G. Manipulative Techniques for Computations	40
IV. THEORETICAL INVESTIGATION	41
A. Criteria for Parameter Choice	41
B. Pilot Model Considerations and The Analysis of a Typical Test Model	42
C. Dimensionless Parameter - $\lambda$	60
D. Check System for Theoretical Calculations	61

E. Stress and Moment Determination at Gage Location	64
F. Beam Analysis	65
V. EXPERIMENTAL INVESTIGATION	66
A. Loading System	66
B. Deflection Measurement	74
C. Stress and Moment Measurement	74
D. Property Tests of Model Material (Aluminum 1100-H-14)	89
E. Effect of Gage and Adhesive Thickness on Moment Determination	90
F. Testing Procedure	92
G. Typical Set of Model Data and Data Reduction	92
VI. TEST RESULTS - INTERPRETATIONS AND OBSERVATIONS	116
A. $\sigma_x$ - values	116
B. $\delta^v$ - values	120
C. $m_y$ - values	120
D. Experimental Observations on Buckling Behavior	127
E. Final Comments	128
VII. SELECTED REFERENCES	140
VIII. ACKNOWLEDGEMENTS	141

## I. INTRODUCTION AND SUMMARY

The popularity of folded plate roof structures has prompted a study to be made of an 8 plate simply supported roof system. This study was made with 8 aluminum models of varying plate thickness, span length and roof slope. The models were loaded until pronounced yielding had taken place and concurrently a continuous record of strains and deflections at strategic locations was kept.

The object was to discern the correlation between the ordinary folded plate theory and the experimental observations when the various parameters were varied. The anticipated information to be gained was the effect of certain parameters on the theoretical prediction of stresses and deflections, the behavior of the structural system at ultimate loads, the buckling behavior of the edge plates and ultimately, how these factors could be incorporated into the design procedure.

The problem proved to be a very interesting one both from the theoretical and experimental standpoint and in conclusion answered several questions and provided an insight into others.

## II. REVIEW OF LITERATURE

### A. Brief Statements on Various Theories

It is the thinking of the writer that the various folded plate theories can be broadly grouped into two categories - the Engineering Theory of Elasticity and the Mathematical Theory of Elasticity. Theories employing the Engineering Theory of Elasticity fall into the majority group that make the familiar assumption regarding planar distribution of flexural, torsional and axial strains with their consequent planar distribution of stresses. Of course this assumption is only made in regards to individual elements of the structure and not to the structure as a whole.

On the other hand the Mathematical Theory of Elasticity utilizes the general equations of equilibrium and the equation of strain compatibility. The problem is then executed without the usual simplifying assumptions.

Insofar as the vast majority of folded plate theories fall into the category of Engineering Elasticity, the following brief statements will emphasize this group of theories.

Since all of the Engineering Elasticity theories are based on the same fundamental assumptions one would expect to obtain the same conclusions from all. As an analogy to this situation, the common beam can be analyzed by slope deflection, moment distribution, conjugate beam, strain energy etc. with the consequence of identical results - the only stipulation being that the calculations be carried out to the same degree of refinement. The degree of refinement encompasses such considerations as accuracy of computation, inclusion or exclusion of shearing strains and axial strains,

temperature compensation, the importance of secondary stresses, non-linear material properties etc. Likewise the folded plate theories can be expected to yield identical results with identical refinements.

#### B. Primary Theory (No Cross-Sectional Distortion)

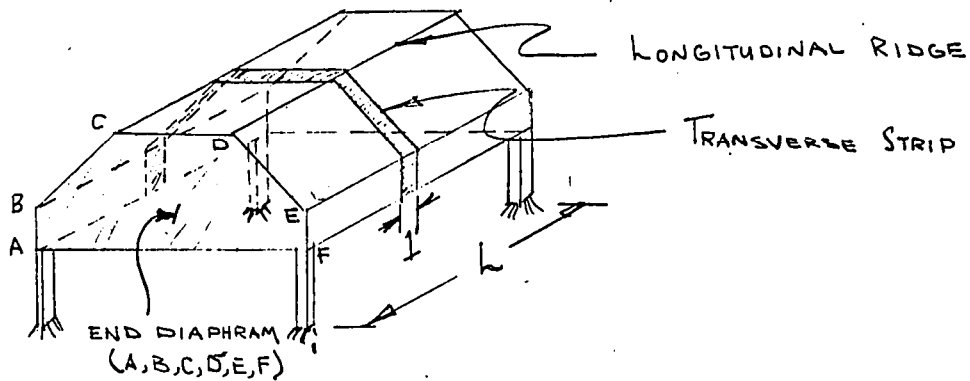
This theory has at times been referred to as the membrane theory but in light of the familiarity that American engineers have with the primary and secondary analysis of structures, it is thought that this terminology would be very appropriate. The first Primary Theory published was by G. Ehlers and H. Craemer (3,4) in Germany in 1930, and later the theory was further developed by E. Gruber (7) and others, mostly German. Insofar as all of their theories made the same simplifying assumption of no relative deflection between the ridges, the only difference between theories was in the manner of computing the unknown stresses and moments.

In 1947 G. Winter and M. Pei (14) made the first contribution to American Literature in the form of a more streamlined version of the same theory. It is this version of the Primary Theory that will be briefly outlined in the subsequent statements.

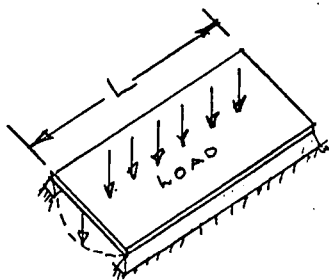
The paper make no claims as to the originality of the basic theory but does take credit for the development of the distribution system that eliminates the necessity of solving several simultaneous equations.

A folded plate structure is formed when several flat plates are joined at the edges and are supported by end diaphragms. This, of course, is the simplest case because it is possible to have intermediate diaphragms and have continuous spans. In the development of the Primary Theory the following plate configuration was used by Winter and Pei:





The basic theory assumes that since an individual plate is long and thin it is capable of only two modes of structural participation which are designated as slab action and plate action e.g.



SLAB ACTION

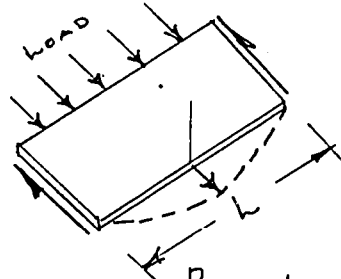


PLATE ACTION

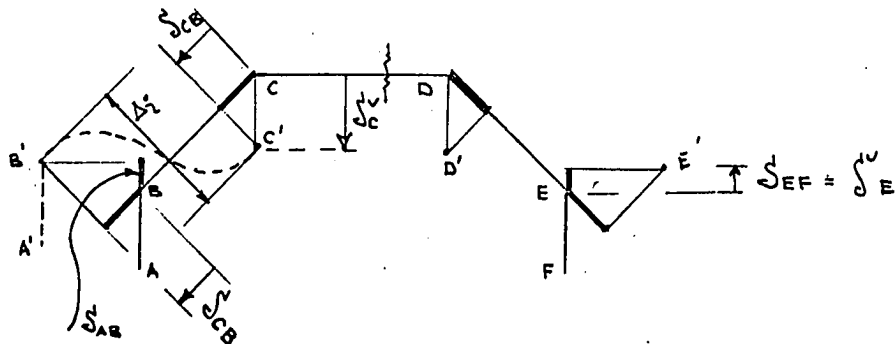
It also assumes that the structure is homogeneous, elastic and that the lines of intersection between the individual plates (the ridges) do not undergo any relative displacement. The moments and stresses in the structure are found by the following procedure:

1. A transverse strip of unit width is cut from the mid-span of the structure and analyzed as a continuous beam loaded with the deadload and superimposed live load and supported at the ridge lines that are assumed to be unyielding. This approach is justified on the premise that all slabs have similar longitudinal load distribution with the consequence that any other unit strip loading would be similar in form.

2. The reactions of this transverse strip of slab form the mid-ordinate of the ridge line-loads and are resolved into components parallel to the plates, thusly forming the plate loads.
3. The total individual plate load is computed by adding the component contributions from the boundary ridges of the plate and is then used to compute the longitudinal plate stresses, assuming each plate to be a long, thin, independently acting deep beam that is supported by the end diaphragms.
4. Now observing that the common edges of adjacent plates do not have equal stresses, proceed to establish continuity by employment of the stress distribution process.
5. The structure is now designed on the basis of the transverse slab moments and the longitudinal plate stresses.

### C. Secondary Theory

In compliance with common American terminology the Secondary Theory considers the moments and stresses existing by virtue of primary deformations. In this respect we are primarily concerned with the effect that relative deflection of adjacent ridges has on transverse moments and longitudinal stresses e.g.



### 1. Solution by arbitrarily induced $\Delta$ -values

This technique was introduced by I Gaafar (5) in 1954 and constitutes one of the first practical solutions to the secondary problem to appear in American Literature. Mr. Gaafar's procedure is briefly given in the following statements:

- (a) Determine the primary transverse moments and longitudinal stresses in compliance with the Winter and Pei procedure and compute the plate deflections ( $\delta$ ) that result.
- (b) Arbitrarily induce a relative deflection ( $\Delta_1$ ) between any two ridges. This will create a translational fixed end slab moment that can be distributed. The distributed moments are used to compute ridge loads that can as before be resolved into plate loads. These will be in terms of  $\Delta_1$ . This operation is repeated for the  $\Delta$ -value of each individual plate.
- (c) The  $\Delta$  induced plate stresses can now be computed in terms of the various  $\Delta$ -values and used to determine the plate deflections ( $\delta$ ). These deflections when combined with the deflections from step (a) form the individual total plate  $\delta$ -values i.e.  $\delta_i = f$  (primary stresses,  $\Delta_1, \Delta_2, \dots, \Delta_n$ )
- (d) A set of simultaneous equations can now be formulated by realizing that any plate- $\Delta(\Delta_1)$ , is a manifestation of the  $\delta$ -values existing at its boundary ridges. Consequently for  $n$  plates bounded by ridges at both edges, there will in general be  $n$  equations in the nature of  $\Delta_1 = g(\delta_1, \delta_2, \dots, \delta_n)$  which from above reduce to  $\Delta_1 = \phi$  (primary stresses,  $\Delta_1, \Delta_2, \Delta_3, \dots, \Delta_n$ ).

Solving the equations simultaneously for  $\Delta$ -values constitutes the solution from which all transverse moments and longitudinal (plate) stresses can be determined.

H. Simpson (11) has used a system very similar in principle to that of Gaafar where he has arbitrarily induced a rotation ( $\frac{\Delta}{L}$ ) in each successive plate. Each arbitrary rotation case gives rise to a translational fixed end moment that when distributed and used to compute the ridge and consequent plate loads, enable one to determine the plate deflections ( $\delta$ ) that are uniquely associated with this arbitrary rotation. Since an arbitrary numerical rotation was induced and not an unknown  $\Delta$ -value, it is necessary to multiply each case by an unknown factor ( $K$ ) which is essentially a way of saying we are going to use  $K$ -amount of this particular case for superposition purposes. Simultaneous equations are now formulated according to the following statements.

Define  $K$  such that  $(\frac{\Delta}{L})_{\text{existing}} = K (\frac{\Delta}{L})_{\text{arbitrary}}$

Then:  $K_i (\frac{\Delta}{L})_{\text{arbitrary}} = f \left[ \delta_{\text{primary}} \text{ - values, } K_1 (\delta_{\text{case 1}} \text{ - values}), \right.$   
 $K_2 (\delta_{\text{case 2}} \text{ - values}), \dots \dots \dots K_n (\delta_{\text{case n}} \text{ - values)} \left. \right]$

A set of  $n$  simultaneous equations are formed and solved for  $K$ -values which in turn dictate what portion of each case shall be superimposed on the primary case to yield final results.

## 2. The iterative procedure

After computing the primary stresses and the consequent  $\delta$ -values, we can proceed to determine the change in transverse slab moment and therefore

the change in ridge loading. These load changes can be used to repeat the process which will in turn result in another change in ridge loading.

This process works very well with certain structural configurations but with others the convergence is slow if not divergent, as is the case of plates intersecting at very small angles.

### 3. Particular solution procedure

This technique of solution was devised by D. Yitzhaki (15) and is based on the principle that any structure that is indeterminate to the  $n^{\text{th}}$  degree can be analysed by superimposing  $n$  particular solutions in combinations such that the given problem conditions will be satisfied. The procedure is very orderly, very general and is adaptable to a wide variety of conditions. It also lends itself to tabularization and the inclusion of additional refinements that are sometimes dictated by certain structural configurations. It is this process of analysis that will be exhibited in the theoretical development in this dissertation.

There have been many other approaches to folded plate theory in the literature, the inclusion of which is thought to be prohibitive. In the opinion of the writer the fundamental principles of all of the theories are included in this brief survey.

#### D. Present Experimental Status

At the time the writer established his initial proposal there was very little experimental evidence to substantiate any of the theories. I. Gaafar seems to have made the first published contribution (5) to the experimental side of the ledger when he tested a five-plate aluminum model with concentrated live loads.

Another experimental contribution (10) was made by A. C. Scordelis, E. L. Croy and I. R. Stubbs in which a simple-span aluminum folded plate model consisting of 3 north light shells was analyzed theoretically and experimentally using ridge line loads. Analytical results obtained by the ordinary folded plate theory, the theory of elasticity and the elementary beam theory are compared with experimental results and the validity of the assumptions used in the analytical methods is examined.

The "Report of a Research Survey Regarding Folded Plate Construction" conducted by the A.S.C.E. Task Committee on folded plate construction, discloses the fact that there is currently rather extensive activity, both theoretical and experimental, taking place but most of the results are unpublished.

#### E. Published Literature

There is a considerable amount of European published literature but the majority of American literature is in the form of Engineering Society Papers. There is one book in English that is devoted in its entirety to folded plate considerations and this is written by David Yitzhaki (15).

It is a very thorough and orderly treatment and is presented with the option of including many of the refinements that are usually neglected in the process of simplifying the assumptions.

### III. DEVELOPMENT OF THEORY

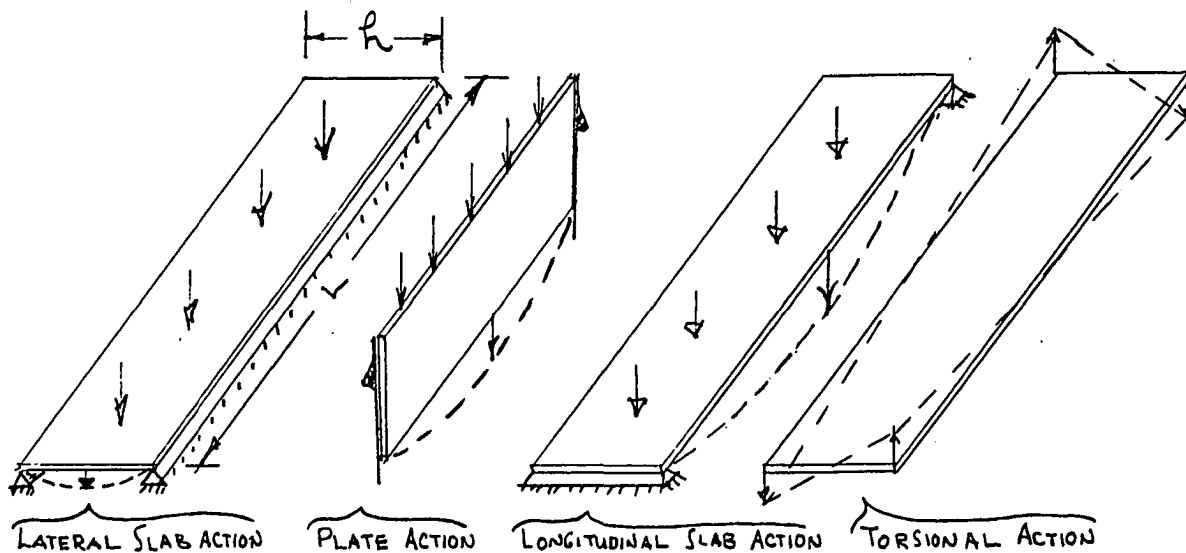
#### A. Fundamental Concepts and Assumptions

The Theoretical Development that has been chosen for exposition in this dissertation can be thought of as being composed of two major parts:

- (1). Primary folded plate theory with no cross-sectional distortion.
- (2). Secondary theory which takes into account the effect of distortion.

The basic concepts and tools of the method are commonly known to all engineers but the structural interaction is very complex and consequently destroys the problem's simplicity. An attempt will hereby be made to execute an imaginative development that will promote an intuitive feeling for the structural interaction. All symbols will be introduced as needed.

The heart of the theory lies in the behavior of the most basic structural element - the individual plate, which can behave as follows:



The basic theory assumes that since an individual plate is long and thin, it is capable of only two modes of structural participation, which are designated as slab action and plate action. The longitudinal slab

action is neglected due to the high  $\frac{L}{h}$  ratio. If longitudinal slab action were considered it would immediately be seen that there exists an extreme flexibility in this respect.

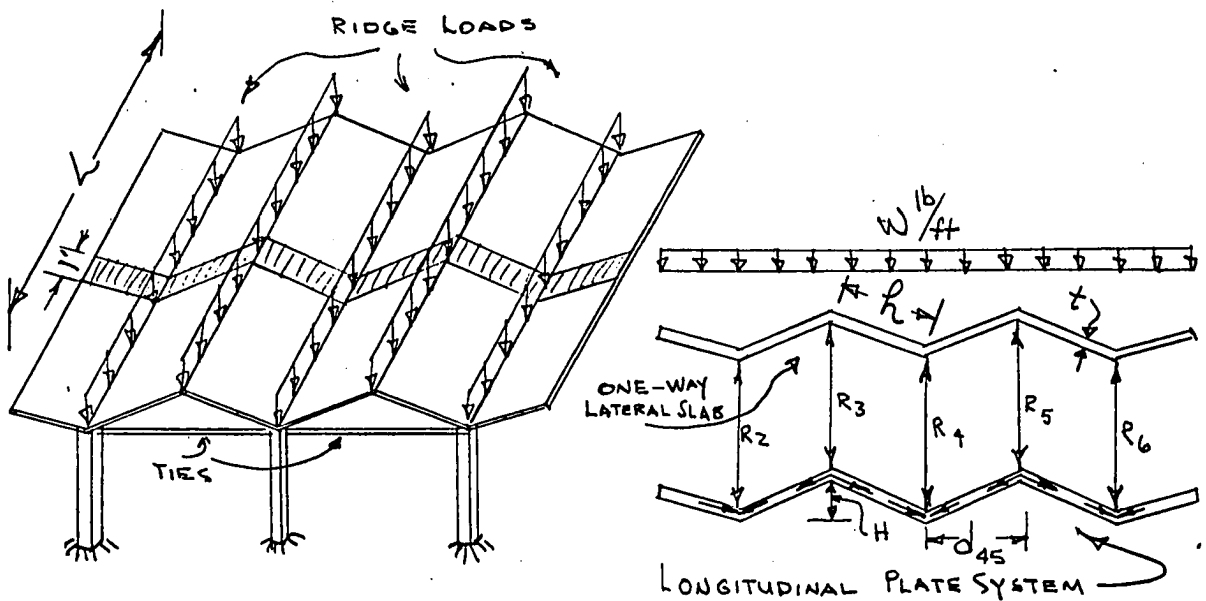
Since these plates are assumed to be capable of only two modes of structural participation, the plates are worthless as individuals but when connected along their common edges and framed into end diaphragms, a very rigid structure is formed. These end diaphragms restrict all lateral movements in the end plane but offer no restriction normal to the end plane. The mechanism of load transfer is as follows: the surface loads are transferred to the ridges through transverse slab action, each ridge load is resolved into components parallel to the plane of the plates intersecting at the ridge and through plate action these components are carried out to the end supports. This is the general scheme of behavior and the specific execution of this scheme will now be developed. The assumptions underlying the theory development are as follows:

1. There are two modes of structural participation
  - (a) lateral slab action
  - (b) plate action
2. Longitudinal slab action and torsional rigidity of the plates are neglected.
3. The structure is composed of continuous, elastic homogeneous elements
4. The principles of superposition are applicable.
5. In regards to the individual plate, plane sections remain plane, i.e., a linear relationship exists between the longitudinal strains and the distance from an edge of the plate.

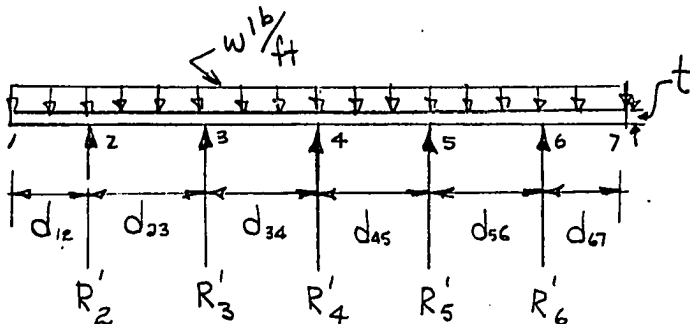


### B. Primary Theory

In the primary analysis of the plate system the assumption is made that each slab is subjected to a similar longitudinal load distribution with the consequent effect of producing a set of similar ridge loads. This fact makes it possible to isolate a typical unit strip of the folded system, as follows:



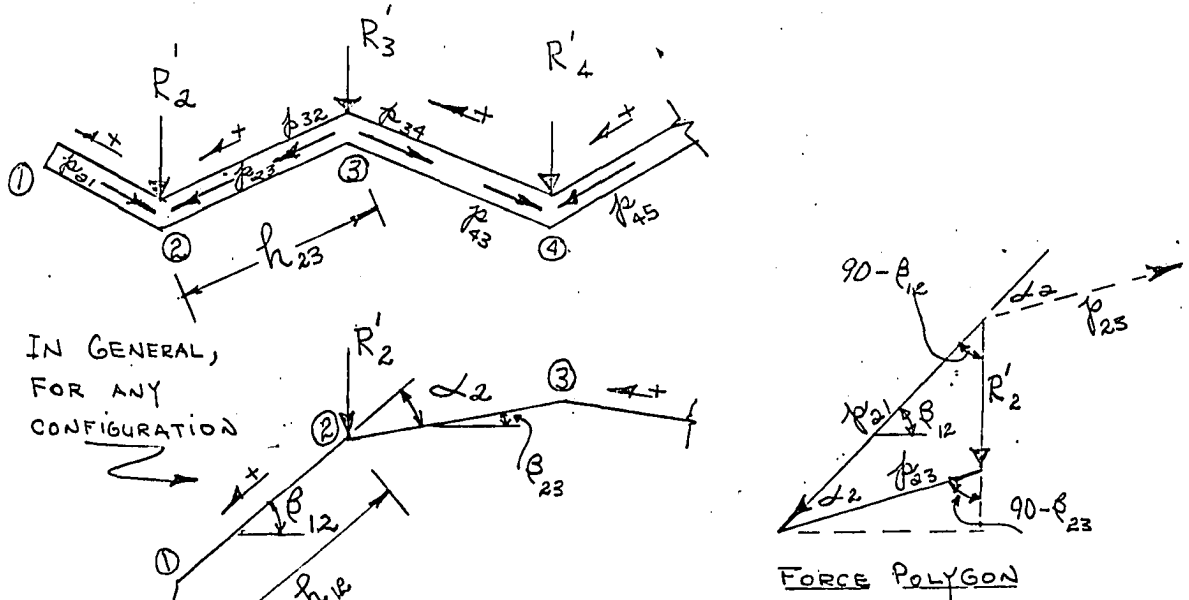
The isolated strip is analogous to the following continuous beam, with the exception being - for all stiffness computations it is necessary to use  $h$  rather than  $d$ .



Note! The  $R'$ -values are primed because they are the initial values resulting from moment distribution

and are correct only if no relative settlement takes place between ridges. They can be thought of as ridge loads, later  $R''$  will signify loads required to make the slab system conform to the plate system.

These  $R'$  values are now resolved into components parallel to the plates at respective plate intersections, i.e.



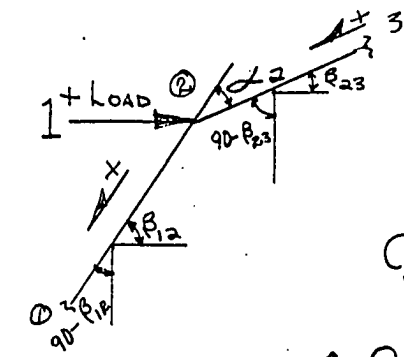
$$\frac{\sin \alpha_2}{R'} = \frac{\sin 90 - \beta_{12}}{p_{23}} = \frac{\sin 90 - \beta_{23}}{p_{21}}$$

$$\therefore p_{23} = \frac{\cos \beta_{12}}{\sin \alpha_2} R'_2 \quad p_{21} = \frac{\cos \beta_{23}}{\sin \alpha_2} R'_2$$

OR  $p_{23} = C_{23}^V R'_2$  AND  $p_{21} = C_{21}^V R'_2$

-c	+c
+c	-c

These  $C^V$  values are coefficients that when multiplied by the ridge loads, will yield the contribution of the ridge load to the specified plate load. The next development will involve  $C^H$  values, that can be used for the resolution of a horizontal ridge load (Fig. 1) into components ll to the plates. Even if these values are seldom needed for horizontal ridge loads, they will later prove expedient in the calculation of horizontal ridge movements, if required.

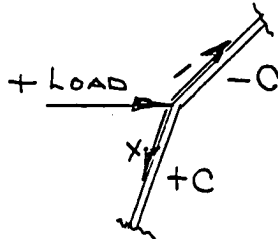


IF WE MERELY TRANSLATE OUR THINKING BY 90°, IT IS POSSIBLE TO WRITE  $C_{12}^H$  &  $C_{23}^H$  DIRECTLY

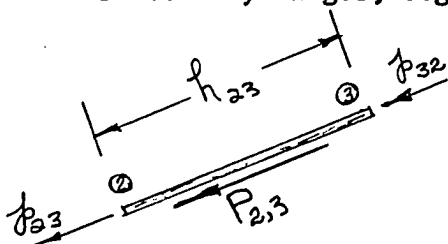
$$C_{21}^H = \frac{\cos(90 - \beta_{23})}{\sin \alpha_2}, \quad C_{23}^H = \frac{\cos(90 - \beta_{12})}{\sin \alpha_2}$$

FIG. 1. Signs  $\therefore C_{21}^H = \frac{\sin \beta_{23}}{\sin \alpha_2}, \quad C_{23}^H = \frac{\sin \beta_{12}}{\sin \alpha_2}$

The sign of C may be determined by simply observing statically the component directions of a plus load i.e.

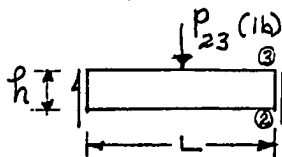


Each individual plate load is arrived at by combining the contributions from its boundary ridges, e.g.

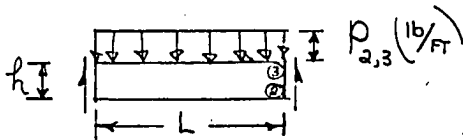


WHERE  $P_{2,3} = p_{32} + p_{23}$

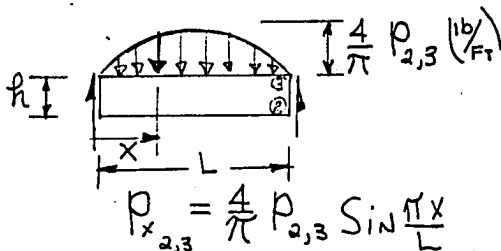
The computed  $P_{2,3}$  will be the maximum ordinate of the plate load-distribution which could presumably be distributed in a number of ways - the most probable of which are:



This is possible when the only loads are those applied directly to the ridges, such as a possible crane load.



Result of uniform slab loading



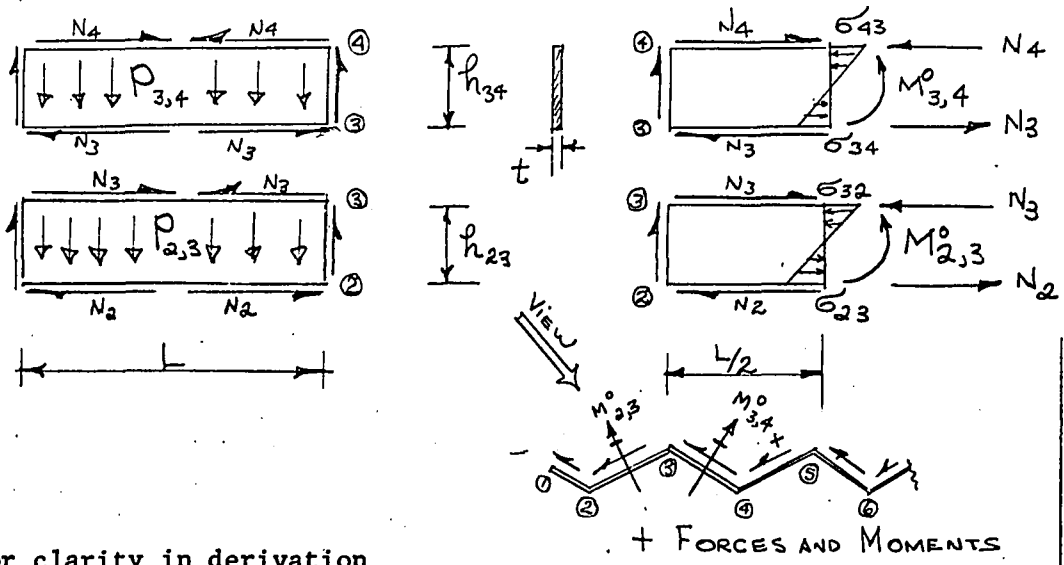
Equivalent sinusoidal loading which

is quite often used to facilitate certain types of calculations.

This  $P_{2,3}$  - value is now used for computation of  $M_{2,3}^0$  which is the maximum moment that would exist if the plate were free to behave independently.  $M_{2,3}^0$  is now used to compute  $\sigma_{2,3}^0$  the corresponding free edge stress, e.g.  $\sigma_{2,3}^0 = \frac{M_{2,3}^0}{th^2/6}$

On completion of this step it will be observed that the free edge plate stresses at common edges are not equal and therefore introduce the problem of establishing continuity. This is accomplished by a stress distribution method that is analogous to the Hardy Cross moment distribution method. The writer develops this method by first demonstrating the analogy to regular slope deflection equations and with this analogy as a tool, proceeding to execute other developments.

To initiate the development, use is made of the free bodies of two adjacent plates, the applied forces being the  $M^0$  - values and the continuity-restoring edge shearing forces:



Note: For clarity in derivation positive stress is considered a manifestation of positive forces or positive moments. This induces simplicity into the equations. Later we will resort to the more normal -comp. + tension convention, with its inherent design advantages.

$M^o$  = Moment caused by plate loads

$\sigma_{34}$ , etc = Stress at 3 in plate 3,4

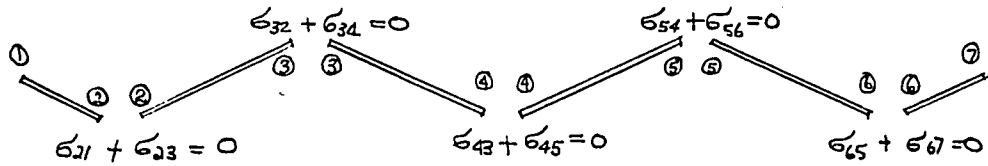
The longitudinal stress equations can now be expressed in terms of the designated forces and moments.

$$\sigma_{23} = \frac{M_{2,3}^o}{y_{23} h_{23}^2 / 6} + \frac{N_2}{t_{23} h_{23}} + \frac{(N_2) \left( \frac{h_{23}}{2} \right)}{t_{23} h_{23}^2 / 6} - \frac{N_3}{t_{23} h_{23}} + \frac{(N_3) \left( \frac{h_{23}}{2} \right)}{t_{23} h_{23}^2 / 6}$$

$$\sigma_{23} = \frac{6M_{2,3}^o}{A_{23} h_{23}} + \frac{N_2}{A_{23}} + \frac{3N_2}{A_{23}} - \frac{N_3}{A_{23}} + \frac{3N_3}{A_{23}}$$

$$\sigma_{23} = \frac{2}{A_{23}} (2N_2 + N_3) + \frac{6M_{2,3}^o}{A_{23} h_{23}} \quad \text{or} \quad \frac{M_{2,3}^o}{z_{23}} \tag{1}$$

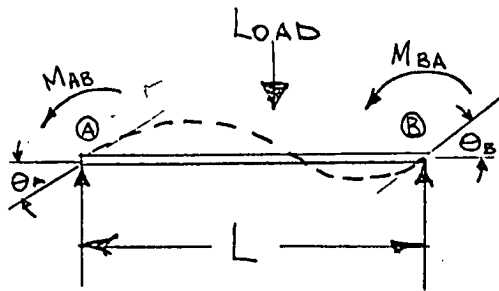
A set of equations can now be written, utilizing (1) i.e.



from which, in the case of the illustrated configuration, there are 5 equations and 5 unknowns ( $N_2, N_3, \dots, N_6$ ). Solving these equations simultaneously and substituting the acquired N values back into (1) will yield the longitudinal stresses existing at the plate edges.

When there are several equations to solve simultaneously the task becomes rather formidable and the use of an iterative procedure can greatly ease the solution. If the stress equations are carefully scrutinized it is seen that there is a strong resemblance to the slope deflection equations for ordinary beams, thereby making the following analogy possible.

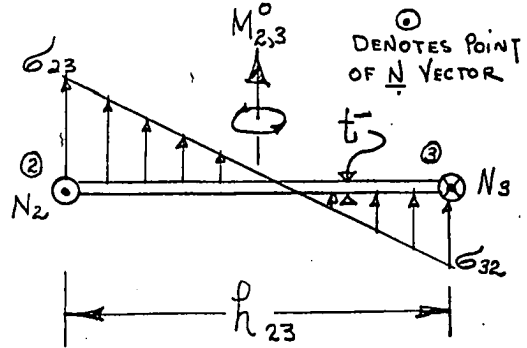
Beam



$$M_{AB} = \frac{2EI}{L} [2\theta_A + \theta_B] + \text{F.E.M.}_{AB}$$

$$M_{BA} = \frac{2EI}{L} [2\theta_B + \theta_A] + \text{F.E.M.}_{BA}$$

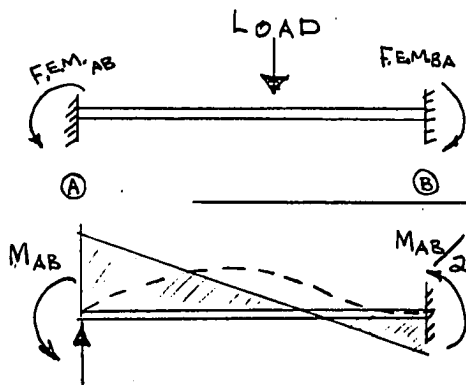
Analogous Plate Cross-section



$$\sigma_{23} = \frac{2}{A_{23}} [2N_2 + N_3] + \frac{M_{2,3}^0}{z_{23}}$$

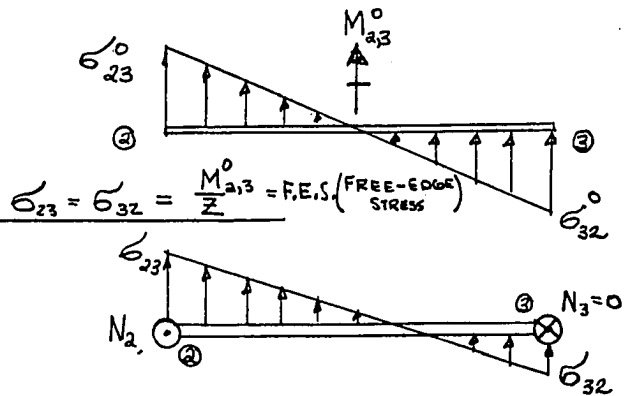
$$\sigma_{32} = \frac{2}{A_{23}} [2N_3 + N_2] + \frac{M_{2,3}^0}{z_{23}}$$

Moment Distribution



$$\text{C.O.F.} = \frac{1}{2}$$

Stress Distribution

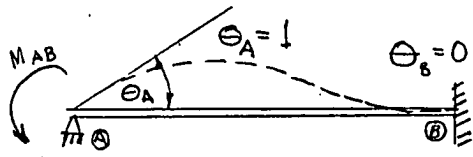


Apply a  $\sigma_{23}$  with corresponding  $N_2$ ;  $N_3 = 0$

$$\sigma_{23} = \frac{2}{A_{23}} [2N_2 + 0] + 0 = \frac{4N_2}{A_{23}}$$

$$\sigma_{32} = \frac{2}{A_{23}} [0 + N_2] + 0 = \frac{2N_2}{A_{23}}$$

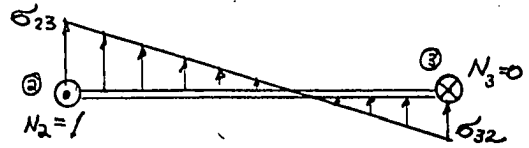
$$\sigma_{32} = \frac{1}{2} \sigma_{23} \text{ and C.O.F.} = \frac{1}{2}$$



Stiffness Factor

$$M_{AB} = \frac{2EI}{L} [(2)(1) + 0] + 0 = \frac{4EI}{L}$$

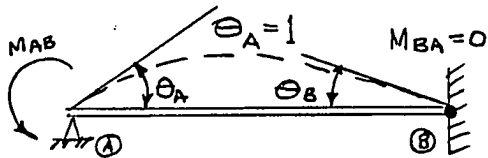
$$\text{Distribution Factor} = \frac{K_{AB}}{\Sigma K}$$



$$\sigma_{23} = \frac{2}{A_{23}} [(2)(1) + 0] = \frac{4}{A_{23}} = \text{S.F.} = K$$

$$\text{Relative Stiffness} = \frac{1}{A_{23}}$$

$$\text{D.F.} = \frac{1/A}{\Sigma 1/A}$$



Stiffness Factor for hinged end

$$M_{AB} = \frac{2EI}{L} [2\theta_A + \theta_B]$$

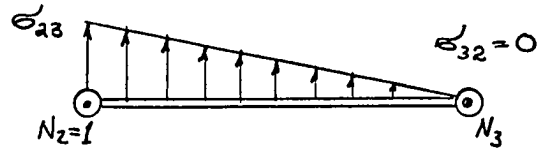
$$\text{But } M_{BA} = 0 = [2\theta_B + \theta_A]$$

$$\theta_B = -\frac{\theta_A}{2}$$

$$M_{AB} = \frac{2EI}{L} \left[ \frac{3}{2} \theta_A = \frac{3}{2} \right] = \frac{3EI}{L}$$

So for hinge condition

$$\text{S.F.} = \frac{3}{4} \text{ the fixed end-S.F.}$$



This condition arises at the center ridge of an anti-symmetrically loaded system, where the common edges are tending in opposition to each other and thereby nullify the stress.

$$\sigma_{23} = \frac{2}{A_{23}} [2N_2 + N_3] = \frac{2}{A_{23}} [2(1) + N_3]$$

$$\sigma_{32} = 0 = \frac{2}{A_{23}} [2N_3 + N_2]; N_3 = -\frac{N_2}{2} = -\frac{1}{2}$$

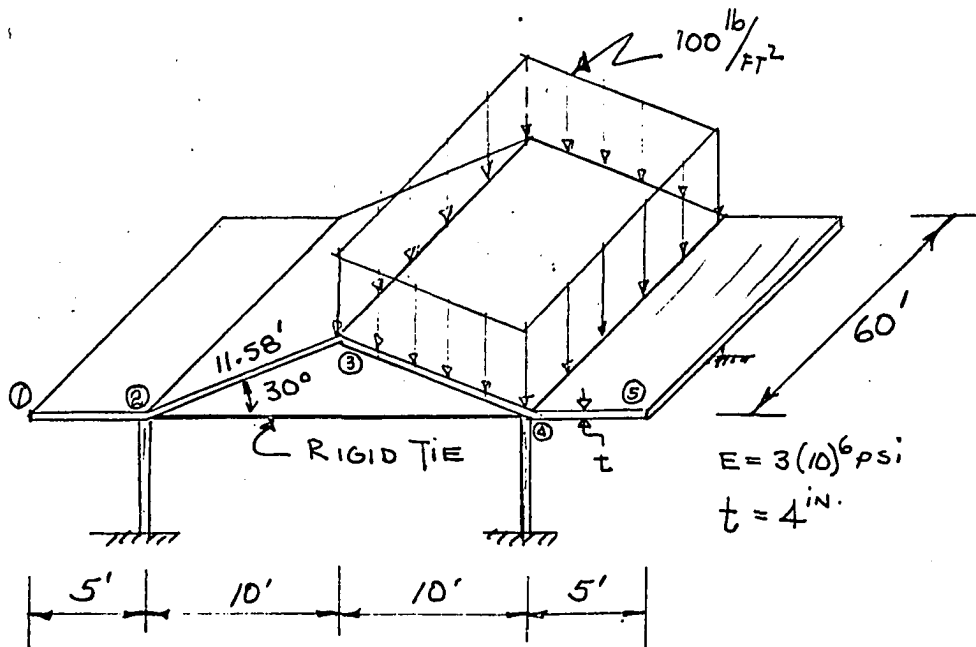
$$\sigma_{23} = \frac{2}{A_{23}} \left[ 2 - \frac{1}{2} \right] = \frac{2}{A_{23}} \cdot \frac{3}{2} = \frac{3}{A_{23}}$$

i.e. 3/4 free edge stiffness factor

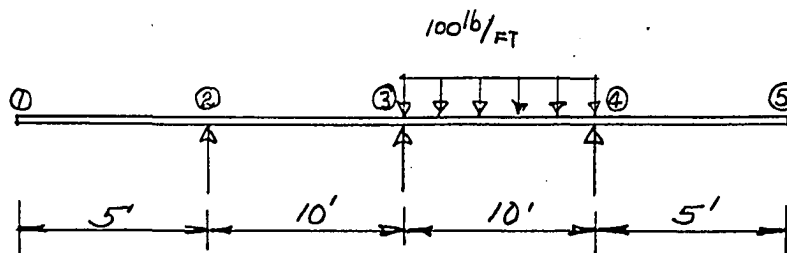
= restrained edge stiffness factor



As an illustration of the developed Primary Theory the following example is presented:



Load on horizontal projection of a 1' unit strip of transverse slab

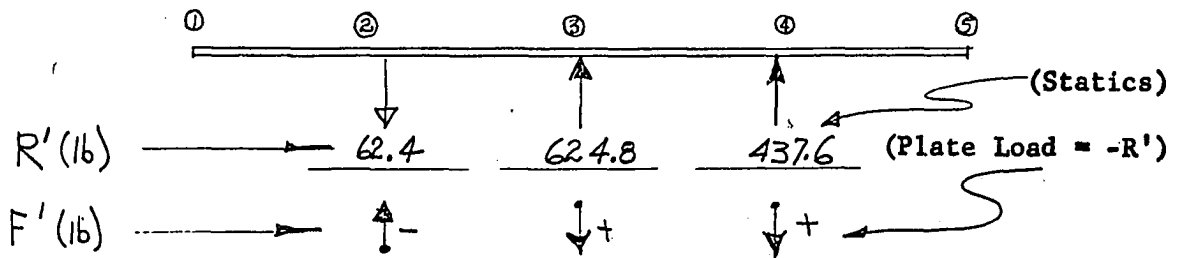


Determine primary slab moments:

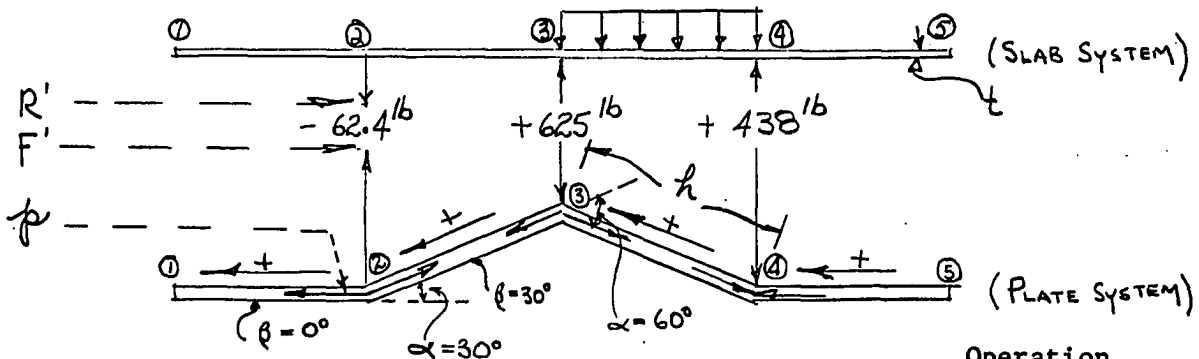
	①	②	③	④	⑤	
D.F.		0	1	0		
F.E.M. (ft-lb)			0.5	0.5	1	0
			-833	-833		
			-416	+416	+833	
			-416			
			-208	+208		
M' (ft-lb)			-624	-624		

(wl<sup>2</sup>/12)

Determine slab reactions and plate loads



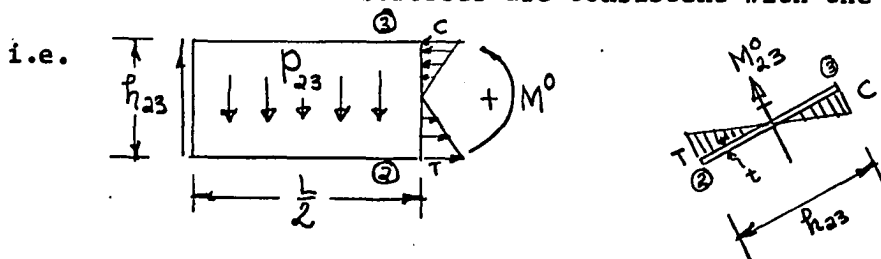
Determine the effect of primary ridge loads on the plate-system



Operation

$F'(lb)$	-62.4	+625	+438	
$C^v$	-1.732+2.00	+1-1	-2+1.732	$C_{n,n+1}^v = \frac{\cos \beta_{n,n-1}}{\sin \alpha_n}$
$p$	+108-125	+625-625	-876+758	$F' \times C^v$
$P$	+108	+500	-1501	$p_{23} + p_{32}$ etc.
$M^o$ (in-lb)	$+5.82 \times 10^5$	$+27 \times 10^5$	$-81 \times 10^5$	$1/8 PL^2 \times 12$
$\sigma$ (psi)	+242	+211	-632	$M^o / z \quad z = 1/6th^2$

Note! The above stresses are consistent with the loads and moments,



But for the actual distribution of these stresses, the (+ ten, -comp.) sign convention will be utilized.

Stress Distribution

	①	②	③	④	⑤		
S.F.		1/5	1/11.58	1/11.58	1/11.58	1/5	1/ht or 1/A
D.F.	0	0.70.3	0.50.5	0.30.7	0	S.F./ΣS.F.	
C.O.	0	0.350.15	0.250.25	0.150.35	0	1/2 D.F.	
F.E.S. ( $\sigma^0$ )	+242	-242+211	-211-632	+632+1710	-1710	Just carry-over	
	-159	+162	+68-162	-162	+377	distribute later	
	-57	+12	+24-24	-12	+57		
	-4	+1	+2-2	-1	+4		
$\Sigma$	+22	-242+386	+117-820	+457+1710	-1272		
Distribute	0	+440-189	-351+351	+376-876	0		
	+22	+198+197	-468-469	+833+834	-1272		
Final ( $\sigma'$ )	<u>+22</u>	<u>+198</u>	<u>-468</u>	<u>+834</u>	<u>-1272</u>		

The analysis of the given structure would now be complete if the implied assumptions were true, i.e. the validity of the slab moment distribution process is dependent upon a structural behavior that is limited to ridge rotations with no accompanying relative ridge deflections.

This immediately suggests that an investigation of relative ridge deflections be made and that the findings be utilized to effect a correction in the primary transverse slab moments and the primary plate stresses.

### C. Secondary Theory

The secondary phase of folded plate theory involving the analysis and disposition of these movements has at times been designated as the Bending-Theory. Here the use of the term secondary in conjunction with the lateral moments and longitudinal plate stresses induced by deflection phenomena is thought to be quite consistent with terminology common to the American Engineering profession.

#### 1. Iterative procedure

Hence the iterative approach to secondary analysis will consist of the determination of (a) Ridge deflections that are consistent with primary plate stresses, (b) Transverse slab moments that are induced by a, (c) Additional ridge loads induced by b, (d) Longitudinal plate stresses induced c, (e) Repeat a,b,c and d..... The structural behavior of the system might be such as to obviate the secondary operations beyond step (a), the implication being that the distortion in structural configuration is too slight to produce any secondary effects e.g.-all ridges undergo the same vertical deflection.

On the other hand there might be a substantial inducement of slab moments without a consequent substantial inducement of ridge loads - the implication being that observation of step (c) dictates that operations cease.

Contrary to this structural characteristic of rapid convergence, there are certain structural configurations that are very sensitive to secondary effects, a condition favoring slow convergence or even divergence. When confronted with this situation the iterative technique must be abandoned in favor of some exact procedure employing a set of simultaneous equations.

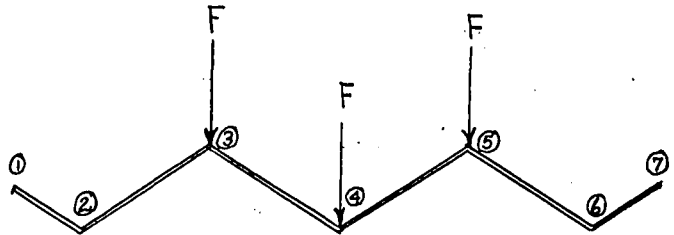
## 2. Particular solution procedure

The technique herein presented is founded on the basic premise that if the true loading, consisting of  $N$  concentrated loads, is known and if a set of  $N$  particular solutions can be found, each set consisting of  $N$  arbitrary loads then the true solution will exist in the form of a superposition of the particular solutions.

### Example:

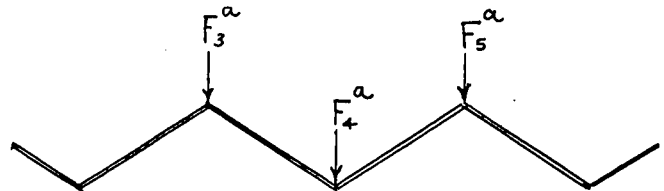
#### Basic system

The load for which it is desired to find associated longitudinal stresses and slab moments.



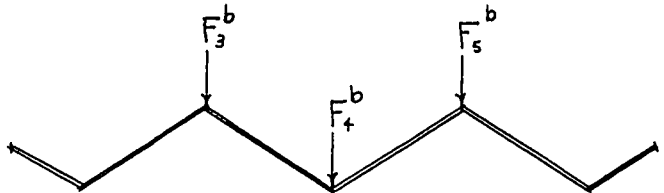
#### Particular load system (a)

A loading for which there is a uniquely associated set of  $\sigma$ -values and  $m$ -values.



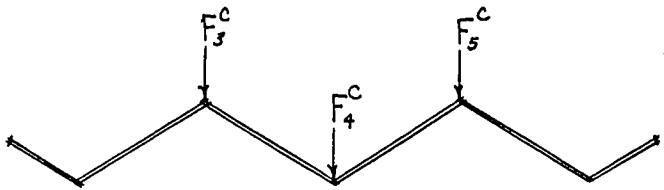
#### Particular load system (b)

A loading for which there is a uniquely associated set of  $\sigma$ -values and  $m$ -values.



#### Particular load system (c)

A loading for which there is a uniquely associated set of  $\sigma$ -values and  $m$ -values.



The systems are superimposed using a-amount of system (a), b-amount of system (b), etc., which results in the following set of equations:

$$aF_3^a + bF_3^b + cF_3^c = F_3$$

$$aF_4^a + bF_4^b + cF_4^c = F_4$$

$$aF_5^a + bF_5^b + cF_5^c = F_5$$

The coefficients a, b and c can now be determined and they will dictate the % of each corresponding element of the various particular load systems that must be superimposed to construct the desired basic system.

The philosophy of this method is somewhat analogous to the well known "General Method of Structural Analysis" or the "Maxwell Method" wherein a solution is assumed that satisfies the statics of the problem and subsequently the geometry is corrected by means of a superposition of individual effect solutions. The particular solution technique does not, however, involve the individual-effect solutions in a strict sense insofar as it is impossible to apply the conventional unit load to a specified ridge without simultaneously introducing other secondary ridge loads during the execution of the computation procedure. Therefore a particular load system can be constructed by adding these secondary effects to the arbitrarily assumed primary ridge loads. It is somewhat analogous to saying that if the holding forces in a bent subject to sideway were superimposed on the original actuating forces, the result would be a system of loads that would be uniquely associated with the computed moments and the observed geometry.

The basic system loads directly related to the superposition procedure are not, however, formed by this type of superposition. They are, in fact, the holding forces that exist by consequence of the primary deflection phenomena. We herein are essentially determining the effect of the absence

of these holding forces when we superimpose the particular systems in the manner specified above.

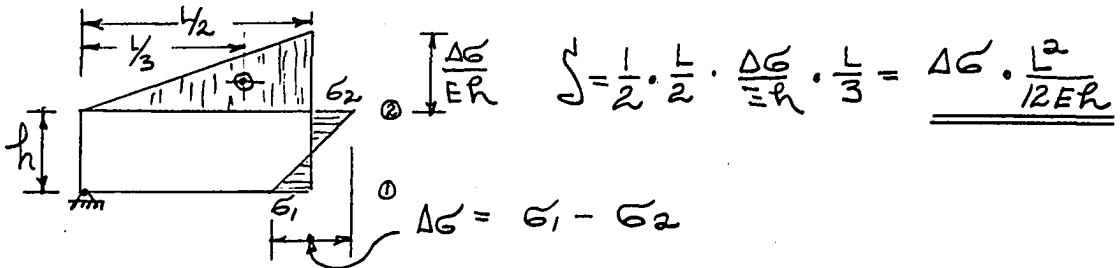
#### D. Development of Secondary Theory

1. Determination of ridge deflections that are consistent with the primary plate stresses:

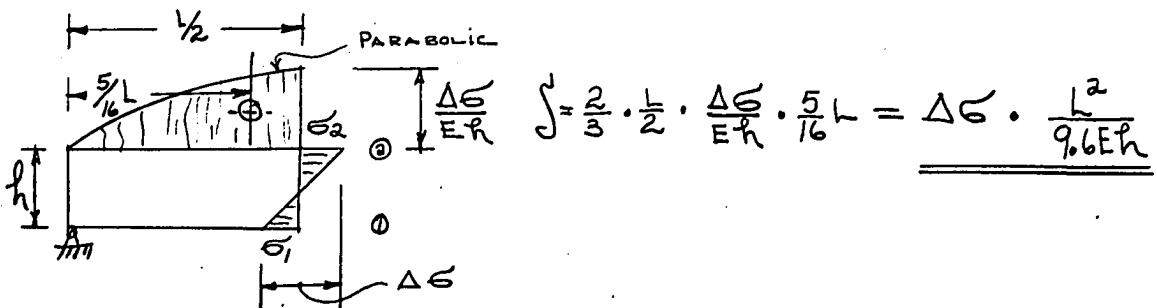
The deflection of a plate in its own plane could normally be calculated on the basis of loads and moments but the known primary ridge stresses suggest a method utilizing angle changes, i.e. double integration -  $y'' = \frac{M}{EI} = \frac{\Delta\phi}{\text{unit length}}$ , where  $\phi$  is the slope or conjugate beam - beam with a load of  $\frac{\Delta\phi}{\text{unit length}}$ . The choice will naturally be determined by computational expedience.

The angle change per unit of length is a function of the stress differential existing between the two edges of a plate. The foregoing ideas are illustrated in the following cases:

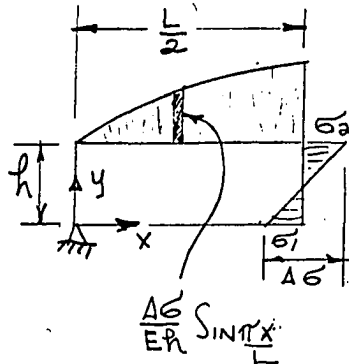
Concentrated load case: (conjugate beam)



Uniform load case: (conjugate beam)

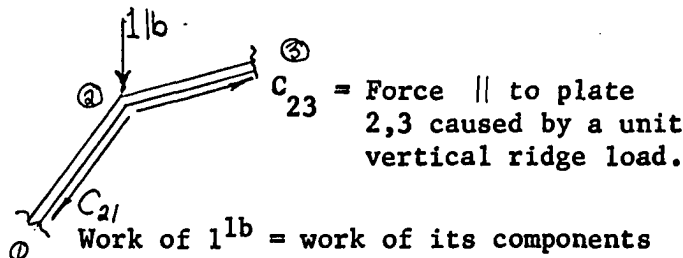


Sinusoidal load case: (double integration)



$$\textcircled{2} \quad \int \frac{\Delta \sigma}{Eh} \cdot \int = \frac{L^2}{\pi^2} \cdot \frac{\Delta \sigma}{Eh} = \underline{\underline{\Delta \sigma \cdot \frac{L^2}{9.86 E h}}}$$

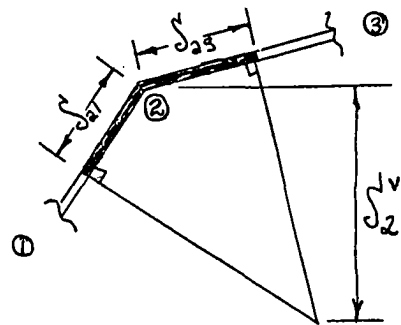
The individual plate deflections are used to calculate vertical ridge deflections by making use of the already known C-values coupled with energy principles. Thusly,



WORK OF  $1^{lb} =$  WORK OF ITS COMPONENTS

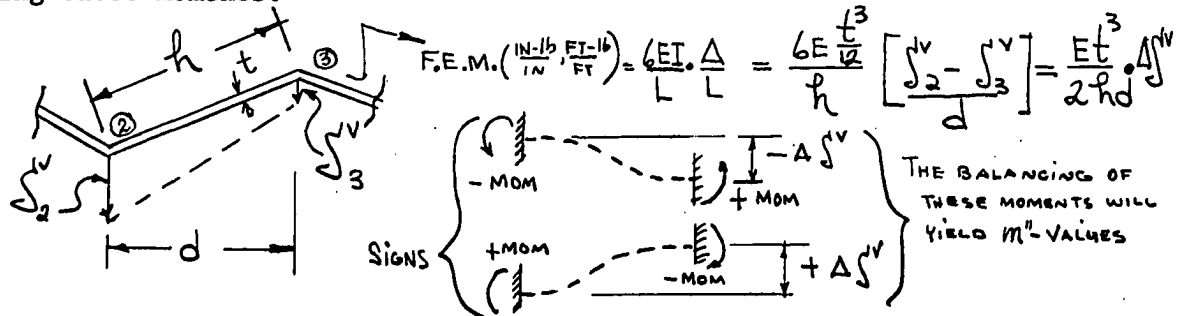
$$\therefore 1 \cdot \int_2 = C_{21} \int_{21} + C_{23} \int_{23}$$

$\delta_2^v$  can also be determined by the following williot geometry



2. Determination of secondary moments induced by relative ridge deflections:

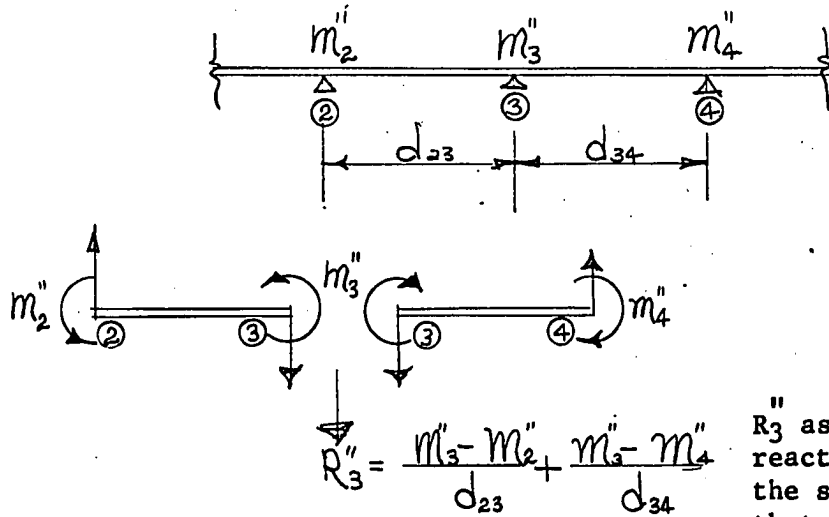
This step consists of finding the fixed-end moments resulting from relative ridge deflections i.e., plate rotations, as follows, and distributing these moments.





3. Determination of secondary ridge loads induced by the secondary moments ( $m''$ ):

Just use horizontal projection of the system as follows:



$R_3''$  as shown is the ridge reaction required to hold the slabs in a position that is consistent with plate movements

$$F'' = \text{Ridge Load} = -R''$$

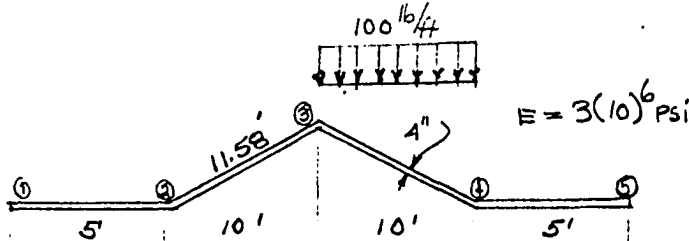
4. Determination of secondary longitudinal plate stresses induced by secondary ridge loads

This is accomplished in identical manner as were stresses in the primary system.

5. Repeat 1, 2, 3, 4 and 5 until scheme converges.
6. An alternate to the above procedure would be to follow step 3 with the establishment of the various particular load systems and thereby directly determine the effect of the secondary ridge loads.

It is obvious that the secondary effects for this rather peculiar loading condition are quite pronounced which suggests that convergence may be slow. With this in mind a solution will be sought utilizing the

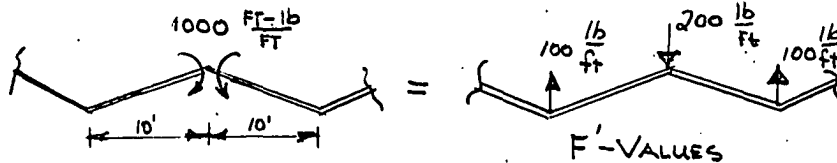
EXAMPLE OF ITERATIVE SECONDARY THEORY



OPERATION

$\delta'$ (Psi)	+24	+197	-468	-833	-1272	RESULT FROM PRIMARY CALC.	
$\Delta \delta'$	-173	+665	-1301	+2105		$\delta'_n - \delta'_{n+1}$	
$E/9.6Eh$	3	1.4	1.3	3		$\frac{E}{9.6Eh} \cdot (10)^4$	
$\delta$ (in)	-5.18	+8.64	-16.9	+63.1		$\Delta \delta' \cdot \frac{E}{9.6Eh} \cdot (10)^2$	
C	-1.732+2	+1-1	-2+1.732			ENTER CONSTANT	
CS	0.0895	0.173	0.0814	0.169	0.338	1.046	CS
$\delta''$ (in)		0.2625	0.2554	1.384		$C_{n,n-1} \delta''_{n-1} + C_{n,n} \delta''_n$	
$\Delta \delta''$		0.0071	-1.129			$\delta''_n - \delta''_{n+1}$	
F.E.M. ( $\frac{PL^2}{16}$ )		+41	-41	-6500	+6500	$\frac{Et^3}{2hd} \cdot \Delta \delta''$	
D.F.		0 1	0.5 0.5	1 0		MOMENT DISTRIBUTION	
		+41	-41	-6500	+6500		
		-41	-3230	+3230	-6500		
		0	+20	+3250	0		
			+1615	-1615			
$M''$ ( $\frac{Et \cdot lb}{ft}$ )			-1636			$\sum M$	
$R''$ ( $\frac{lb}{ft}$ )		+163	-326	+163		$\frac{M''_n - M''_{n-1}}{d_{n,n-1}} + \frac{M''_n - M''_{n+1}}{d_{n,n+1}}$	
$F''$ ( $\frac{lb}{ft}$ )		-163	+326	-163		$-R''$	
C		-1.732+2	+1-1	-2+1.732		ENTER CONSTANT	
$p$ ( $\frac{lb}{ft}$ )		+283-326	+326-326	+326-283		C X F	
P ( $\frac{lb}{ft}$ )		+283	0	0	-283	$p_{n,n+1} + p_{n+1,n}$	
$M^0$ (in-lb)		+1.24	0	0	-1.24	$\frac{1}{4.87} PL^2 \cdot 12 \cdot (10)^6$	
$\sigma^0$ (Psi)		+516	0	0	-516	$M^0/Z$ ( $Z = 2400$ )	
D.F.		1 0	0.703	0.505	0.307	0 1	STRESS DISTRIBUTION
		+516	-516	0	0	+516	
		0	+360-155	0	0	-155+360	
		-180	0	0	+77	+77	
		0	0	0	0	0	
$\sigma''$		+336	-155	+77	-155	+336	$\sum \sigma$

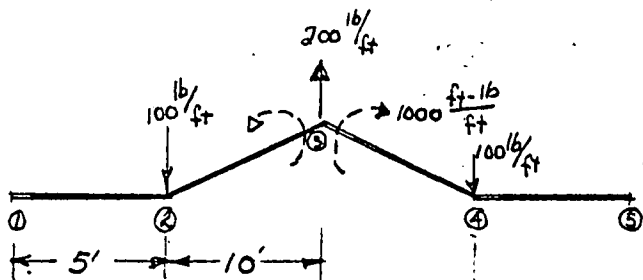
particular load technique. The philosophy of the arbitrary selection of a particular loading is arrived at by observing that the  $R''$ -values are functions of the ridge moments and thereby form a balanced set of forces ( $\Sigma R'' = 0$ ). In light of this fact it is expedient to assume arbitrary loadings in the form of mutually balanced forces that can be thought of as being manifestations of arbitrarily assumed ridge moments, e.g.



Choosing thusly will result in a set of particular loadings equal in number to the number of redundant ridge moments rather than the number of  $R''$ -values. In the case at hand the ridge moment at 3 is the only redundant quantity, so one arbitrary loading will suffice. The particular load will be assumed as  $1000 \frac{\text{ft-lb}}{\text{ft}}$ , distributed sinusoidally in the longitudinal direction. The reason for the sinusoidal variation lies in the fact that the secondary effects that are being studied are functions of the elastic curves of the ridges. Of course the elastic curves of uniformly loaded members are not sine curves but the difference is negligible. Therefore, in light of the ease with which normal functions can be manipulated, all particular solutions will be constructed on the basis of normal variation of loads.

The significance of the calculations (Page 31) lies in the fact that the F-values constitute a set of actual loads that are uniquely associated with the  $\sigma'$ ,  $\delta^v$  and  $m''$  values of this particular system (a). Now insofar as our problem originated from the fact that the  $R''$ -values

EXAMPLE OF PARTICULAR SOLUTION TECHNIQUE  
 PARTICULAR LOAD SYSTEM (a):



OPERATIONS FOR  
 CONSTRUCTING A  
 PARTICULAR SOLUTION

$F' (\frac{lb}{ft})$	+100	-200	+100		ARBITRARY LOADING		
C	-1.732+2	+1-1	-2+1.732		ENTER CONSTANT		
$R' (\frac{lb}{ft})$	-1732+200	-200+200	-200+173.2		$C \cdot F'$		
$P (\frac{lb}{ft})$	-173.2	0	0	+173.2	$f_{n,n+1} + f_{n+1,n}$		
$M^o (IN-lb)$	-7.58	0	0	+7.58	$\frac{PL^3}{9.87} \cdot 12 \cdot 10^5$		
$\sigma^o (PSI)$	-316	0	0	+316	$\frac{M^o}{Z} \cdot 12$		
D.F.	0	0.703	0.505	0.307	0.1	STRESS DISTRIBUTION	
	-3/6	+316	0	0	+316		-3/6
	0	-221+95	0	0	+95-221		0
	+110	0	0	0	0		+110
$\sigma' (PSI)$	-206	+95	-47	+95	-206		$\sum \sigma$
$\Delta \sigma' (PSI)$	-301	+142	-142	+301		$\sigma'_n - \sigma'_{n+1}$	
$\frac{L^3}{9.86Eh}$	2.9	1.27	1.27	2.9		$\frac{L^3}{9.86Eh} \cdot 10^{-4}$	
$S' (IN)$	-8.72	1.803	-1.803	+8.72		$\Delta \sigma' \cdot \frac{L^3}{9.86Eh} \cdot 10^2$	
C	-1.732+2	+1-1	-2+1.732			ENTER CONSTANT	
$C S' (IN)$	+0.151+0.036	+0.018+0.018	+0.036+0.151			$C S'$	
$\Delta S' (IN)$	+0.187	+0.036	+0.187			$C_{n,n-1} S'_{n,n-1} + C_{n,n+1} S'_{n,n+1}$	
$\Delta S^v (IN)$		+0.151	-0.151			$S^v_n - S^v_{n+1}$	
F.E.M. ( $\frac{ft-lb}{ft}$ )		+870	-870			$\Delta S^v \cdot Et^3/2hd$	
D.F.	0.1	0.505	1.0			MOMENT DISTRIBUTION	
	+870	-870	-870	+870			
	-870	0	0	-870			
		+435	+435				
		0	0				
$M'' (\frac{ft-lb}{ft})$		-435	0			$\sum M$	
$R'' (\frac{lb}{ft})$	+43.5	-87	+43.5			$\frac{m''_n - m''_{n-1}}{d_{n,n-1}} + \frac{m''_n - m''_{n+1}}{d_{n,n+1}}$	
$F'' (\frac{lb}{ft})$	+143.5	-287	+143.5			$F' + R''$	

of the basic load system are fictitious holding forces and we are seeking the effect of their absence, we are lead to the following indicial equation:

$$aF + R'' = 0$$

$$a(-287) + (-326) = 0$$

Particular Basic

$$a = \frac{326}{-287} = \underline{\underline{-1.137}}$$

Superposition of the basic and particular systems now yield the following solutions:

$$\sigma = \sigma'_{\text{basic}} + a\sigma'_{\text{particular}} \quad \Rightarrow \quad \text{parabolic} + \text{sinusoidal}$$

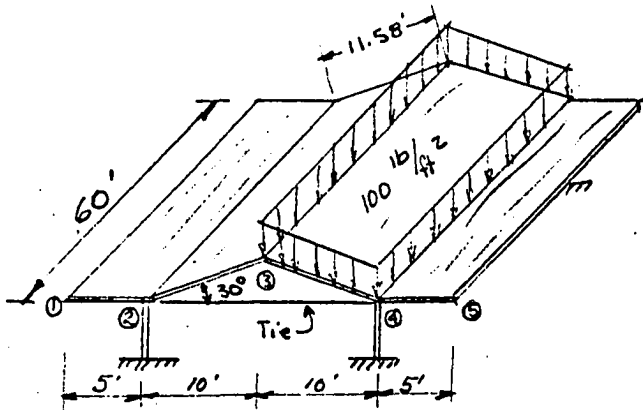
$$\delta^v = \delta^v_{\text{basic}} + a\delta^v_{\text{particular}} \quad \Rightarrow \quad \text{very close to sinusoidal} + \text{sinusoidal}$$

$$m = m'_{\text{basic}} + m''_{\text{basic}} + am''_{\text{particular}} \quad \Rightarrow \quad \text{uniform} + \text{very close to sinusoidal} + \text{sinusoidal}$$

Results

Max. mid-span values	①	②	③	④	⑤
$\sigma'_{\text{basic}}$	24	197	-468	+833	-1272
$a\sigma'_{\text{part.}}$	234	-108	+53	-108	+234
$\sigma$ (psi)	258	+89	-415	+725	-1038
$\delta^v_{\text{basic}}$		0.2625	0.2554	1.384	
$a\delta^v_{\text{part.}}$		-0.212	-0.041	-0.212	
$\delta^v$ (in)		+0.05	+0.214	1.172	
$m'_{\text{basic}}$		0	-624	0	
$m''_{\text{basic}}$		0	-1636	0	
$am''_{\text{part.}}$		0	+495	0	
$m$ ( $\frac{\text{ft-lb}}{\text{ft}}$ )		0	-1765	0	

CONSOLIDATION OF EXAMPLE PROBLEM



SLAB THICKNESS =  $t = 4''$   
 $E = 3(10)^6$  PSI  
 $h =$  PLATE WIDTH  
 $d =$  HORIZONTAL PROJ. OF PLATE  
 $A = ht$

WANTED: LATERAL SLAB MOMENTS, LONGITUDINAL PLATE STRESSES AND VERTICAL RIDGE DEFLECTIONS

1-ft STRIP AT MID-SPAN

	①	5'	②	10'	③	④	⑤	OPERATIONS			
SLAB D.F. →		0.1	0.5	0.5	10'	1	0				
F.E.M. →			-416	+416	-834	+834		MOMENT DISTRIBUTION			
			-416		-208	+208					
$M'(ft-lb)$			-62.4					$\sum M$			
$R'(DUE TO LOAD) lb$		0	-500		-500			$R' = w d / 2$			
$R'(DUE TO MOMENT)$		+62.4	-125		+62.4			$\frac{m_n - m_{n-1}}{d_n - d_{n-1}} + \frac{m_n - m_{n+1}}{d_n - d_{n+1}}$			
$F'(lb)$		-62.4	+625		+437.6			$-\sum R'$			
C		-1.732	+2	+1	-1	-2	+1.732	ENTER CONSTANT			
$\phi'(lb)$		+108	-125	+625	-625	-876	758	$C \times F'$			
$P'(lb)$		108	500		-1501		758	$\phi_{n,n+1} + \phi_{n+1,n}$			
$M^0(IN-lb)$		5.82	27		-81		+40.9	$1/8 PL^2 \cdot 12 \cdot 10^5$			
$\sigma^0(Psi)$		242	211		-632		1,710	$M^0 / Z$			
PLATE D.F.	1	0	0.7	0.3	0.5	0.5	0.3	0.7	0	1	$4/A / \sum 4/A$
C. O.	0	0.35	0.15	0.25	0.25	0.15	0.35	0			
	+242	-242	+211	-211	-632	+632	+1710	-1710			
			+105				-105				
	-195			+84	-177			+414			
			+65				-65				
	-23			+10	-10			+23			
			+5				-5				
	-2			+1	-1			+2			
	+22	-242	+386	-116	-820	+457	+1710	-1271			
	0	+440	-188	-352	+352	+376	-877				BALANCE
$\sigma'(Psi)$	+22	+198	-468		+833		-1271				$\sum \sigma$

STRESS DISTRIBUTION  
 + TENSION  
 - COMPRESSION

$\Delta \epsilon$ (psi)	-173	+665	-1301	+2,105	$G_n - G_{nt}$
$L^2/9.6 E h$	3	1.3	1.3	3	$L^2/9.6 E h \cdot 10^{-4}$
$S$ (in)	-5.18	+8.64	-16.9	+63.1	$\Delta G' \cdot L^2/9.6 E h \cdot 10^{-2}$
$C$	-1732+2	+1-1	-2	+1732	ENTER CONSTANT
$C S$	0.08950173	0.08640169	0.3381046		$C S$
$\Delta S^V$ (in)	0.2625	0.2554	1.384		$C_{n,n-1} S_{n,n-1} + C_{n,n+1} S_{n,n+1}$
$\Delta S^V$	0.0071	-1.129			$S_n - S_{n+1}$
F.E.M. (ft-lb)	+41	-41	-6500+6500		$\Delta S^V \cdot E h^3/24d$
D.F.	0.1	0.5	1.0		MOMENT DISTRIBUTION
	+41	-41	+6500		
	-41	-3230	+3230	-6500	
	0	+20	+3250	0	
		+1615	-1615		
$M''$ (ft-lb)			-1636		$S M$
$R''$ (lb)	+163	-326	+163		$\frac{M_n - M_{n+1}}{S_{n,n-1}} + \frac{M_{n+1} - M_{n+2}}{S_{n,n+1}}$

PARTICULAR LOAD SYSTEM (a)

$F'$ (lb)	+100	-200	+100		ARBITRARY LOADING		
$C$	-1732+2	+1-1	-2	+1732			
$p$ (lb)	-173.2	+2.00	-2.00	-300+173.2	$C \cdot F'$		
$P$ (lb)	-173.2	0	0	+173.2	$p_{n,n+1} + p_{n,n+2}$		
$M^0$ (in-lb)	-758	0	0	+7.58	$P L^2/9.87 \cdot 12 \cdot 10^5$		
$G^0$ (psi)	-316	0	0	+316	$M^0/z$		
D.F.	1.0	0.703	0.505	0.307	0.1		
	-316	+316	0	0	+316	-316	
	0	-221	+95	0	+95	-221	0
	+110	0	-47	-47	0	0	+110
$G'$ (psi)	-206	+95	-47	+95	-206	$\Sigma G$	
$\Delta G'$	-301	+142	-142	+301	$G'_n - G'_{nt}$		
$L^2/9.87 E h$	2.9	1.27	1.27	2.9	$L^2/9.87 E h \cdot 10^{-4}$		
$S'$ (in)	-8.72	+1.803	-1.803	+8.72	$\Delta G' \cdot L^2/9.87 E h \cdot 10^{-2}$		
$C$	-1732+2	+1-1	-2	+1732	ENTER CONSTANT		
$C S$	+0.151	+0.036	+0.036	+0.151	$C S$		
$\Delta S^V$ (in)	+0.187	+0.036	+0.187		$C_{n,n-1} S_{n,n-1} + C_{n,n+1} S_{n,n+1}$		
$\Delta S^V$ (in)	+0.151	-0.151			$S_n - S_{n+1}$		
F.E.M. (ft-lb)	+870	-870			$\Delta S^V \cdot E h^3/24d$		

D.F.	0	1	0.505	1	0	
		+870	-870	-870	+870	MOMENT DISTRIBUTION
		-870	0	0	-870	
		+435, 435				
M''(ft-lb)	0	0	-435	0	0	$\sum 17L^2$
R''(lb)		+43.5	-87	+43.5		$\frac{m_k - m_{k-1}}{d_{k-1}} + \frac{m_k - m_{k+1}}{d_{k+1}}$
F(lb)		+143.5	-287	+143.5		F' + R''

INITIAL EQUATION:  $aF_{PART}'' + R_{BASIC}'' = 0 \Rightarrow a(-287) + (-326) = 0 \Rightarrow a = -1.137$

FINAL VALUES						
	0	1	0.505	1	0	
$\delta$ (psi)	+258	+89	-415	+725	-1038	$\delta_{BASIC} + a \delta_{PART}''$
$\delta_v$ (in)		+0.05	+0.214	+1.172		$\delta_{BASIC} + a \delta_{PART}''$
M(ft-lb)		0	-1765	0		$m_{BASIC} + m_{BASIC} + a m_{PART}''$

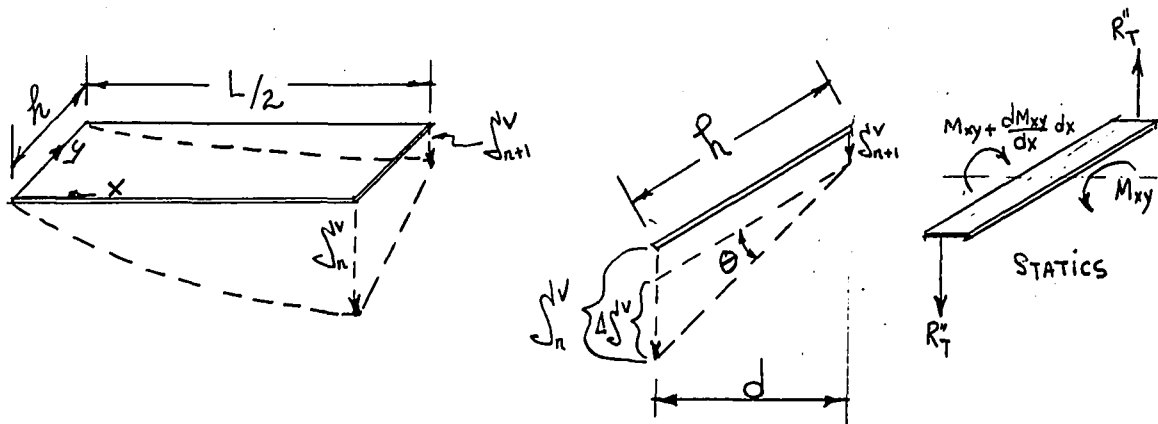


### E. Additional Analytical Refinements

The original assumptions used for the development of the theory neglected the torsional stiffness of the individual plate as being insignificant and in the majority of cases it seems to be. But in event the structural configuration makes torsional stiffness important, the particular solution technique is well adapted for these additional corrections.

The additional corrections will exist in the form of a secondary ridge load ( $R_T''$ ) due to torsion that is to be added to the  $R_{\text{basic}}''$ -values and the  $R_{\text{part}}''$ -values respectively.

The torsional ridge loads are a result of asking oneself what distributed edge forces are associated with a specified twisted configuration of a thin plate. The development stems from the consideration of the following twisted plate configuration:



Geometry

The problem is to derive an expression for  $R_T''$  in terms of  $\theta$  or  $\frac{\Delta\delta v}{d}$ . (Use analogy to twisting of thin bar)

Geometry

$$\theta = \frac{\Delta\delta^v}{d} \sin \frac{\pi x}{L}$$

$$\frac{d\theta}{dx} = \frac{\pi}{L} \frac{\Delta\delta^v}{d} \cos \frac{\pi x}{L}$$

$$\frac{d^2\theta}{dx^2} = -\frac{\pi^2}{L^2} \frac{\Delta\delta^v}{d} \sin \frac{\pi x}{L}$$

$$\text{Equate } \frac{d^2\theta}{dx^2} = \frac{R_T'' d}{JeG} = \frac{\pi^2}{L^2} \cdot \frac{\Delta\delta^v}{d} \sin \frac{\pi x}{L}$$

$$\therefore R_T'' = \Delta\delta^v \cdot \frac{\pi^2 JeG}{L^2 d^2} \sin \frac{\pi x}{L} = \Delta\delta^v \cdot \frac{\pi^2 t^3 hG}{3L^2 d^2} \sin \frac{\pi x}{L}$$

$$\underline{\underline{(R_T'' )_{\max} = \Delta\delta^v \cdot \frac{\pi^2 Gt^3 h}{3L^2 d^2}}}$$

Statics

$$dM_{xy} = R_T'' dx d, \quad \frac{dM_{xy}}{dx} = R_T'' d$$

Relationship between Statics and Geometry

$$d\theta = \frac{M_{xy} dx}{JeG}, \quad \frac{d\theta}{dx} = \frac{M_{xy}}{JeG}$$

$$\frac{d^2\theta}{dx^2} = \frac{dM_{xy}}{dx} \cdot \frac{1}{JeG} = R_T'' d / JeG$$

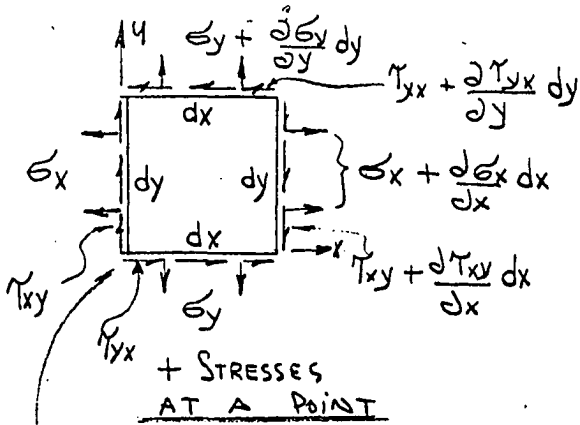
To add refinement to the analysis, this value is merely superimposed on  $R''$  existing by virtue of secondary moment.

Further refinement in analysis could be had by considering the longitudinal slab stiffness but this value has been shown to be insignificant throughout the literature.

#### F. Buckling Analysis of Edge Plate

It is anticipated that certain structural configurations will cause buckling of the edge plates to be a significant consideration and therefore the writer is moved to develop a rational approach to the prediction of this phenomenon.

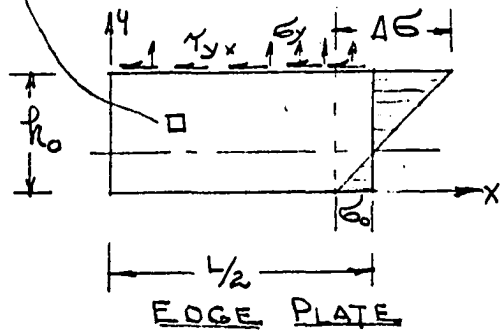
The first step in the analysis of the edge plate is to ascertain the distribution of normal and shearing stresses throughout the plate. This is done as follows:



$$\textcircled{1} \frac{\partial \sigma_x}{\partial x} = \frac{\partial \tau_{yx}}{\partial y}$$

$$\textcircled{2} \frac{\partial \sigma_y}{\partial y} = \frac{\partial \tau_{xy}}{\partial x}$$

EQUILIBRIUM EQUATIONS



$$\sigma_x = \sigma_0 + \frac{\Delta \sigma}{h} y = \sigma_0 \left[ 1 + \frac{\Delta \sigma}{\sigma_0 h} y \right] \sin \frac{\pi x}{L}$$

$$\text{LET } \frac{\Delta \sigma}{\sigma_0 h} = \alpha, \text{ THEN } \sigma_x = \sigma_0 \left[ 1 + \alpha y \right] \sin \frac{\pi x}{L}$$

NORMAL STRESS VARIATION ACROSS PLATE

$$\textcircled{1} \frac{\partial \sigma_x}{\partial x} = \frac{\partial \tau_{yx}}{\partial y} = \sigma_0 \left[ 1 + \alpha y \right] \frac{\pi}{L} \cos \frac{\pi x}{L} \Rightarrow \tau_{yx} = \sigma_0 \left[ y + \frac{\alpha}{2} y^2 \right] \frac{\pi}{L} \cos \frac{\pi x}{L}$$

$$\tau_{yx} = \sigma_0 \left[ y + \frac{\alpha}{2} y^2 \right] \frac{\pi}{L} \cos \frac{\pi x}{L} + C_1 \quad \begin{cases} \tau = 0 \\ y = 0 \end{cases}$$

$$\textcircled{2} \frac{\partial \sigma_y}{\partial y} = \frac{\partial \tau_{xy}}{\partial x} = \frac{\partial \tau_{yx}}{\partial x} = -\sigma_0 \left[ y + \frac{\alpha}{2} y^2 \right] \frac{\pi^2}{L} \sin \frac{\pi x}{L}$$

$$\sigma_y = \dots = -\sigma_0 \left[ \frac{y^2}{2} + \frac{\alpha}{6} y^3 \right] \frac{\pi^2}{L} \sin \frac{\pi x}{L} + C_2 \quad \begin{cases} \sigma_x = 0 \\ y = 0 \end{cases}$$

COMPILING:

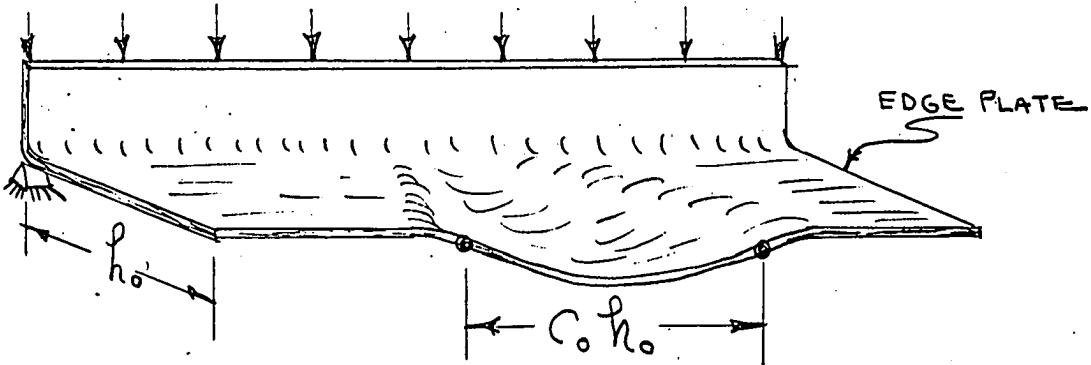
$$\underline{\sigma_x = \sigma_0 \left[ 1 + \alpha y \right] \sin \frac{\pi x}{L}}$$

$$\underline{\sigma_y = -\sigma_0 \left[ \frac{y^2}{2} + \frac{\alpha}{6} y^3 \right] \frac{\pi^2}{L} \sin \frac{\pi x}{L}}$$

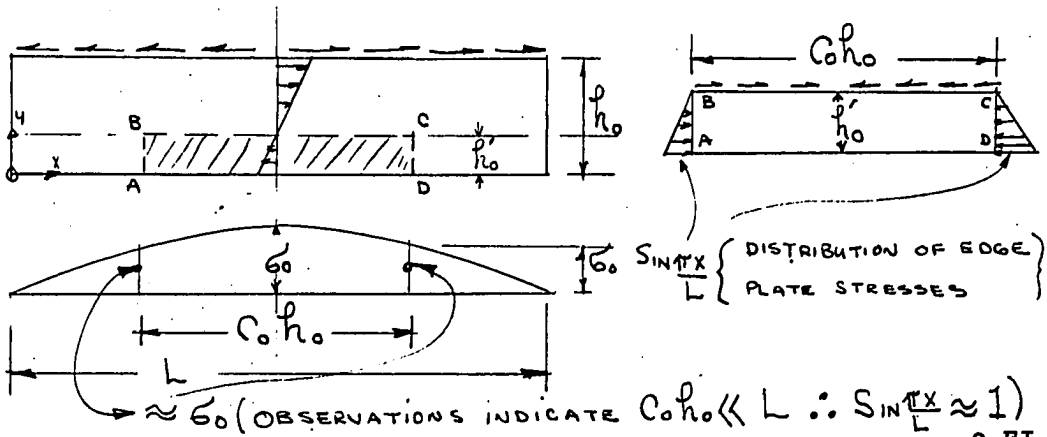
$$\underline{\tau_{xy} = \sigma_0 \left[ y + \frac{\alpha}{2} y^2 \right] \frac{\pi}{L} \cos \frac{\pi x}{L}}$$

Observation of these equations leads to the conclusion that  $\sigma_y$  and  $\tau_{xy}$  are of minor comparative magnitude. Therefore  $\sigma_x$  will be the predominating factor in the consideration of buckling.

Observation of the buckled configuration of a simulated edge plate model yields the following results:



In light of this configuration it is thought that a conservative estimate of the critical compressive edge stress can be made by isolating a strip of edge plate that is  $C_0 h_0$  long and has a width equal to the part in compression, i.e.



Now using an analogous Euler column condition i.e.  $P_{cr} = \pi^2 \frac{EI}{L^2}$ , the following analogy is realized:

$$0.5 \sigma_o' h_o t = \frac{\pi^2 E h_o t^3}{12(1-\mu^2) C_o^2 h_o^2}$$

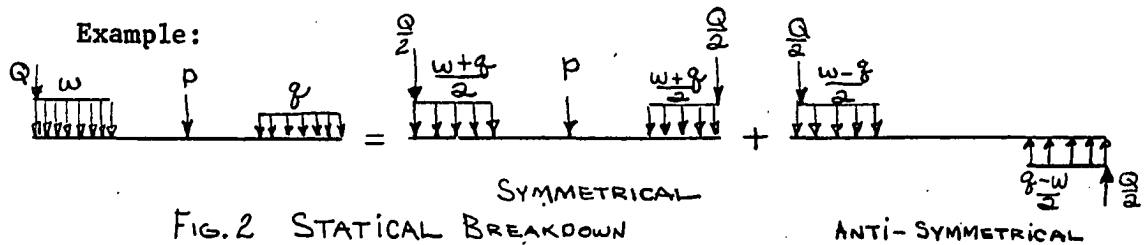
$$\sigma_o \text{ Critical} = \frac{\pi^2 E t^2}{6(1-\nu^2) C_o^2 h_o^2}$$

Investigation of several different conditions should bear out this trend and constant

G. Manipulative Techniques for Computations

The example shown in the development was not involved enough to warrant any short cut procedures but for a non-symmetric loading of a symmetric structural configuration consisting of many folds it behooves one to seek out all computational expediences. One of these expediences is familiar to all structural engineers and involved the concept of reduced stiffness factors when pinned-end conditions are known to exist. Another is the complete carry-over process before balancing moments or stresses. The third, which is most uniquely advantageous relative to the problem at hand is the resolution of the problem into symmetrical and anti-symmetrical parts (Fig. 2) each entailing the use of just one half of the structure.

This type of solution yields results for both symmetric and non-symmetric loading if needed and even though it requires two separate solutions involving one half of the structure the computations are much less in number than one solution involving the whole structure. This is the technique used to analyze the models used in conjunction with this dissertation.



## IV. THEORETICAL INVESTIGATION

## A. Criteria for Parameter Choice

In regards to the theoretical investigation the first problem to arise is - what model size and shape should be investigated. In the case of the writer this problem was resolved by asking the question - what are the parameters of structural configuration existing in practice? With this in mind, a definite configuration was chosen



This configuration was chosen because of its simplicity in form and its, nevertheless, inherent complexity in folded plate interaction. It was thought that this number of folds would be just enough to substantiate the trend from folded plate interaction at the edges, to beam action in the interior without such a large number of folds that computation and instrumentation would become an unnecessarily formidable task.

The construction periodicals were then combed to obtain a representative list of existing  $\frac{t}{h}$ ,  $\frac{H}{h}$  and  $\frac{L}{h}$  ratios. A careful study of this list influenced the choice of the following set of parameters as being the set encompassing the range of values most commonly encountered in the field.

Table 1. Model characteristics

Model No.	$\frac{L}{h}$	$\frac{H}{h}$	$\frac{t}{h}$	$t$	L	h
1	4	1/4	1/45	0.0888"	16"	4"
2	4	1/4	1/20.9	0.1915	16"	4"
3	4	5/8	1/45	0.0888	16"	4"
4	4	5/8	1/20.9	0.1915	16"	4"
5	8	1/4	1/45	0.0888	32"	4"
6	8	1/4	1/20.9	0.1915	32"	4"
7	8	5/8	1/45	0.0888	32"	4"
8	8	5/8	1/20.9	0.1915	32"	4"

## B. Pilot Model Considerations and The Analysis of a Typical Test Model

Before becoming too deeply involved in something that may prove to be a lost cause it behooves one to engage in a sort of preliminary test program in order to more or less obtain a preview of coming attractions. The function of these crude preliminaries is to establish prematurely whether our ideas are going to produce results that are in the realm of feasibility.

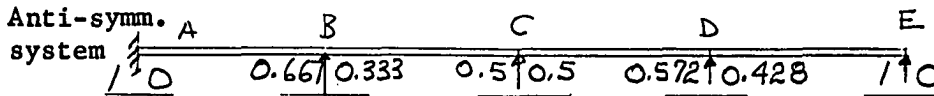
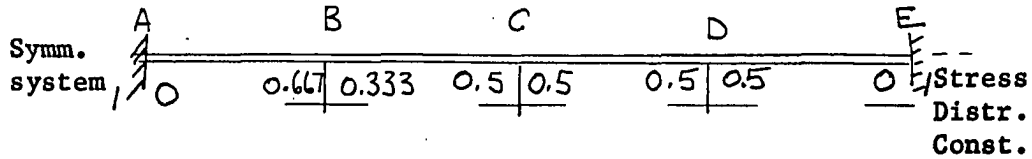
To accomplish this a pilot model was designed, built, theoretically analyzed and experimentally tested. The model was fabricated from a 0.050" thick sheet of aluminum which was subsequently folded into the chosen model configuration. The model was then loaded with a roving single concentrated load at the midspan of successive ridges and valleys and the resulting deflections were observed. By and large the agreement between the theoretical and experimental deflections was very good, with the consequence of a green light for pushing more deeply into the program. A typical set of pilot model calculations are given on the following pages. This set is based on the concentrated load being at point C.

The computed  $\delta^V$ -values could be slightly improved by iterative operation, i.e. load the structure with the reversed set of holding forces ( $R''$ -values). But insofar as very little would be gained by this additional step, the operations were terminated at this point. Theoretical and experimental data were obtained for loading at points other than C - in fact the experimental agreement is much better for loading at D but the C-case was presented because it reflects a folded plate characteristic that will be discussed later.





Determine plate stress distribution constants



Determine plate deflection factors

Uniform loading

$$\text{Plate}_{AB} \frac{L^2}{12Eh} = \frac{31.25^2}{(12)(10.1)(10^6)(2)} = 4.03 (10^{-6}) \text{ in/psi}$$

$$\text{Plate}_{BC} = \frac{31.25^2}{(12)(10.1)(10^6)(4)} = 2.015 (10^{-6}) \text{ in/psi}$$

}  $\delta$  factors

Sinusoidal loading

$$\text{Plate}_{AB} \frac{L^2}{9.87Eh} = \frac{31.25^2}{(9.87)(10.1)(10^6)(2)} = 4.89 (10^{-6}) \text{ in/psi}$$

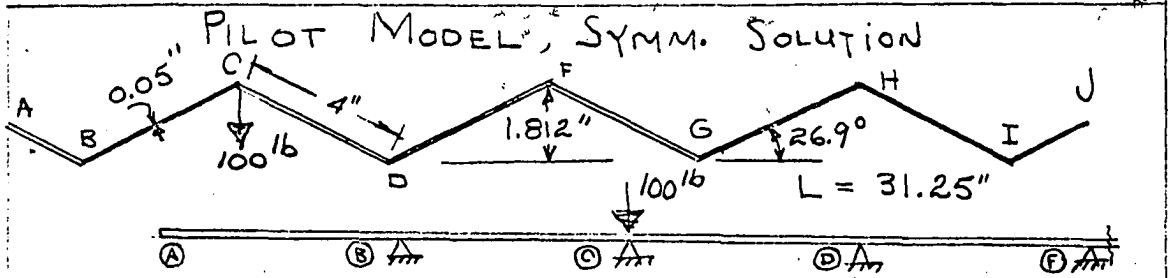
$$\text{Plate}_{BC} = \frac{31.25^2}{(9.87)(10.1)(10^6)(4)} = 2.44 (10^{-6}) \text{ in/psi}$$

Determine slab fixed end moment factors

$$\text{F.E.M.} = \frac{E't^3}{2hd} \times \Delta\delta^v = \frac{(10.1)(10^6)(0.05)^3}{(2)(4)(3.57)(8/9)} \Delta\delta^v$$

$$= \dots \dots \dots 49.7 \Delta\delta^v$$

← Slab  $\delta^v$  FEM



F' (lb)			+100							
C <sup>v</sup>		-1.105	+1.105	+1.105	-1.105	-1.105	+1.105			
P (lb)		0	0	+110.5	-110.5	0	0			
P (lb)	0		+110.5		-110.5		0			
M° (IN-lb)	0		+863		-863		0			
G° (PSI)	0		+6470		-6470		0			
D.F.	1 0	0.667	0.333	0.5	0.5	0.5	0.5	0 1		
C.O.F.		0.333	0.166	0.25	0.25	0.25	0.25	0		
		0	+6470	-6470	-6470	+6470	0			
	-2/57		+269	+1074		-269				
	-90		-376	+45	+1550	+376		-1550		
	+125		-39	-63	+94	+39		-94		
	+13		-4	-6	+10	+4		-10		
	+1			-1	+1			-1		
	-2/08		+6320	-5421	-4815	+6620	0	-1655		
	0		+4215	-2105	+303	-303	-3310	+3310		
G' (PSI)	-2108		+4215	+4215	-5118	-5118	+3310	+3310	-1655	
ΔG' (PSI)	-6323		+9333		-8428		+4965			
1/12EF	4.03		2.015		2.015		2.015		x 10 <sup>6</sup>	
S (IN)	-25.48		+18.81		-16.98		+10.00		x 10 <sup>3</sup>	
CS (IN)			+28.16	+20.79	+20.79	+18.76	+18.76	+11.05	+11.05	
S <sup>v</sup> (IN)			+48.95		+39.55		+29.81		+22.10	
ΔS <sup>v</sup> (IN)			+9.40		+9.74		+7.71			
F.E.M. (IN-lb)			+467		+484		+383		x 10 <sup>3</sup>	
D.F.		0 1		0.428	0.572		0.5	0.5		0 1
C.O.F.		0 0.5		0.214	0.286		0.25	0.25		0
			+467		-467	+484		-484	+383	-383
					+233					
					-166		+205			+166
					-12		-47			+12
					-1		-3			+1
					-234	+305	-329	+383		-204
					+231	-308	+256	-356		0
					-3	-3	+27	+27		-204 x 10 <sup>3</sup>
M'' (IN-lb/IN)					-0.003		+0.027			-0.204
R'' (lb/IN)					+0.0008	-0.0008	-0.0084	+0.0084	+0.0647	-0.0647
R'' (lb/IN)					+0.0008		-0.0092		+0.0731	-0.1294

PILOT MODEL, ANTI-SYMM. SOLUTION

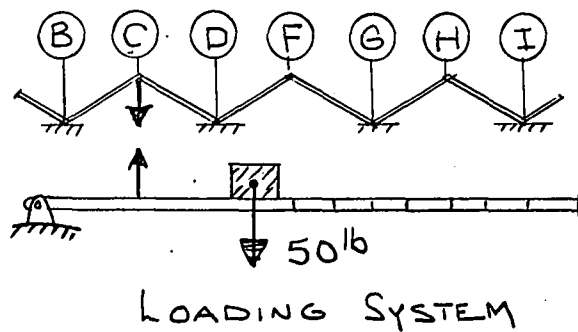
$F'$ (lb)		0	+100	0	0	0
$C^v$		-1.105 + 1.105	+1.105 - 1.105	-1.105 + 1.105	+1.105	
$P$ (lb)		0 0	+110.5 - 110.5	0 0	0	
$P$ (lb)	0		+110.5	-110.5	0	
$M^o$ (IN-lb)	0		+863	-863	0	
$G^o$ (PSI)	0		+6470	-6470	0	
D.F.	1 0	0.667 0.333	0.5 0.5	0.572 0.428	1 0	
C.O.F.		0.333 0.167	0.25 0.25	0.286 0.214		
		0 + 6470	-6470 - 6470	+6470 0	0	
	-2155		+1080			
	-90	+270		-270		
	+144	-432	+45 + 1773	+432		
	+16	-49	-72 + 124	+49		
	+2	-5	-8 + 14	+5		
			-1 + 1			
	-2083	0 + 6254	-5426 - 4558	+6686 0		
	0	+4171	+434 - 434	-3824 + 2862		
$G'$ (PSI)	-2083	+4171	-4992	+2862	0	
$\Delta G'$ (PSI)	-6254	+9163	-7854	+2862		
$L^2/12ER$	4.03	2.015	2.015	2.015	$\times 10^{-6}$	
$\int$ (IN)	+25.20	+18.46	+15.83	+5.77	$\times 10^{-3}$	
$CS$ (IN)	+27.85 + 20.40	+20.40 + 17.49	+17.49 + 6.38	+6.38 - 6.38		
$\Delta S^v$ (IN)	+48.25	+37.89	+23.87	0		
$\Delta S^v$ (IN)		+10.36	+14.02	+23.87		
F.E.M. ( $\frac{IN-lb}{IN}$ )		+515	+697	+1186	$\times 10^3$	
D.F.	0 1	0.128 0.572	0.572 0.428	1 0		
C.O.F.	0 0.5	0.214 0.286	0.286 0.214	0.5		
		+515	-515 + 697	-697 + 1186	-1186	
			+257			
				+273		
				-291		
				-83		
				-24		
				-7		
		+515	-258 + 380	-514 + 593	-1186	
		-515	+273 - 365	+634 - 473	+1186	
		0	+15 + 15	+120 + 120	0	$\times 10^{-3}$
$M''$ ( $\frac{IN-lb}{IN}$ )	0	+0.015	+0.120	0		
$R''_i$ (lb/IN)		-0.0042 + 0.0042	-0.029 + 0.029 + 0.033	-0.033 + 0.033		
$R''$ (lb/IN)		-0.0042	-0.0248	+0.062	0	

When the symmetrical and anti-symmetrical solutions are superimposed the resultant applied load becomes 200<sup>lb</sup>. It therefore becomes necessary to divide all results by 2. This could have been avoided by using 50<sup>lb</sup> for each loading to start with but 100 was used because of numerical simplicity.

Results:

	A	B	C	D	F	G	H	I	J
	-2108	+4215	-5118	+3310	-1655	+3310	-5118	+4215	-2108
$\sigma_{200}$	<u>-2083</u>	<u>+4171</u>	<u>-4992</u>	<u>+2862</u>	<u>0</u>	<u>-2862</u>	<u>+4992</u>	<u>-4171</u>	<u>+2083</u>
	-4191	+8386	-10,110	+6172	-1655	+448	-126	+44	-25
$\sigma_{100} \Rightarrow$	<u>-2095</u>	<u>+4193</u>	<u>-5055</u>	<u>+3086</u>	<u>-827</u>	<u>+224</u>	<u>-63</u>	<u>+22</u>	<u>-12 (psi)</u>
	48.95	39.55	29.81	22.10	29.81	39.55	48.95		
$\delta^v_{200}$	<u>48.24</u>	<u>37.89</u>	<u>23.87</u>	<u>0</u>	<u>-23.87</u>	<u>-37.89</u>	<u>-48.24</u>		
	97.20	77.44	53.68	22.10	5.94	1.66	0.70		
$\delta^v_{100} \Rightarrow$	<u>48.6</u>	<u>38.72</u>	<u>26.84</u>	<u>11.05</u>	<u>2.97</u>	<u>0.83</u>	<u>0.35</u>	<u>0.35</u>	<u>(in x 10<sup>-3</sup>)</u>

Following are the complete pilot model results:

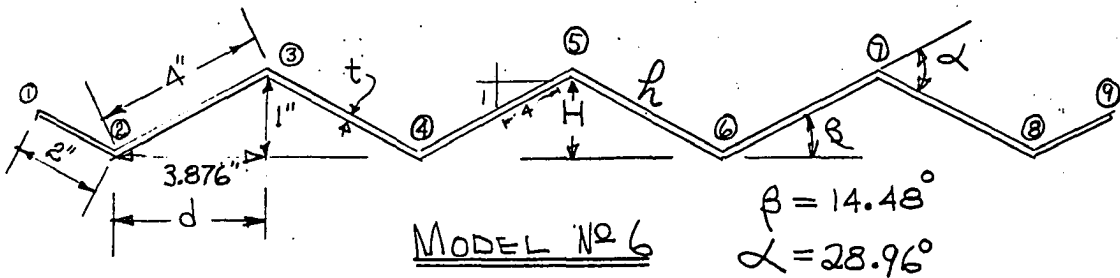


Load at	C		D		F		G		H	
Dial at	Test	Theo	Test	Theo	Test	Theo	Test	Theo	Test	Theo
B	37	49	16	16.7	5.2	4.5	2	1.2	1	0.4
C	35	39	25	26	11	11	4	2.9	2	0.8
D	25	27	33	34	25	26	12	10	4	3
F	9.5	11	25	25	37	35	27	25	10	11
G	3.8	3	11	10	24	26	37	34	24	27
H	1.4	0.8	4.2	2.9	11	11	27	26	38	39
I	0.7	0.4	2.7	1.2	6.5	4.5	18	17	42	49

Model Characteristics

$$\frac{L}{h} = 8, \quad \frac{H}{h} = \frac{1}{4}, \quad \frac{t}{h} = \frac{1}{21}$$

$$L = 32.00\text{in}, \quad h = 4.00\text{in}, \quad t = 0.19\text{in}$$



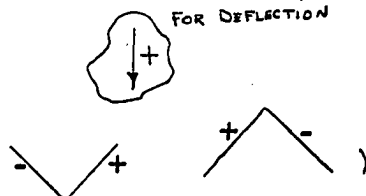
Compute Z values

$$z_{23} = \frac{th^2}{6} = \frac{0.19 \times 16}{6} = 0.506 \text{ in}^3$$

$$z_{12} = \frac{0.19 \times 4}{6} = 0.127 \text{ in}^3$$

Compute C<sup>v</sup> values

$$C_{21}^v = \frac{\cos \beta}{\sin \alpha} = -2.00 \text{ (all other } C^v = \pm 2)$$



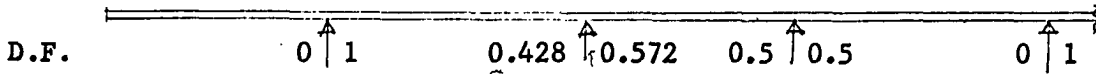
Compute  $C^H$  values

$$C^H = \frac{\sin \beta}{\sin \alpha} = -0.517 \text{ (all other } C^H = -0.517)$$

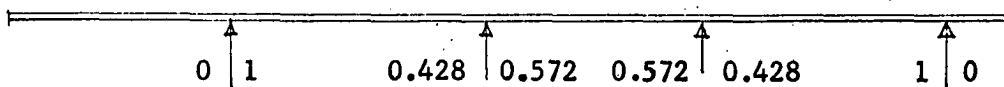


Determine slab moment distribution constants

Symmetrical system:

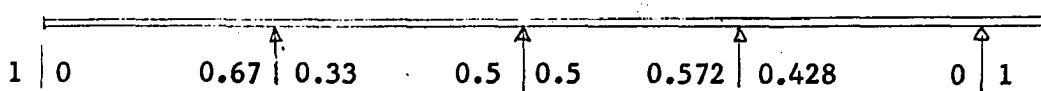


Anti-symmetrical system:

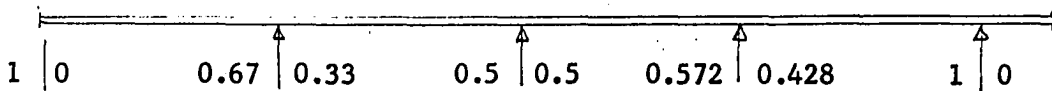


Determine plate stress distribution constants

Symmetrical system:



Anti-symmetrical system:



Determine plate deflection factors

Factors for uniform loading:

$$\text{Plate 12, } \frac{L^2}{9.6Eh} = \frac{32^2}{9.6 \times 10^7 \times 2} = 5.33 \times 10^{-6} \text{ in}^3/\text{lb}$$

$$\text{Plate 23, } \frac{32^2}{9.6 \times 10^7 \times 4} = 2.67 \times 10^{-6} \text{ in}^3/\text{lb}$$

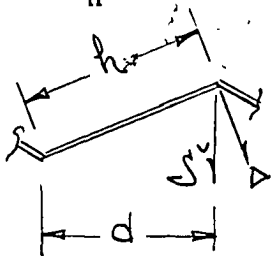
Factors for sinusoidal loading

$$\text{Plate 12, } \frac{L^2}{9.87Eh} = \frac{32^2}{9.87 \times 10^7 \times 2} = 5.18 \times 10^{-6} \text{ in}^3/\text{lb}$$

$$\text{Plate 23, } = \frac{32^2}{9.87 \times 10^7 \times 4} = 2.60 \times 10^{-6} \text{ in}^3/\text{lb}$$

Determine slab fixed end moment factors

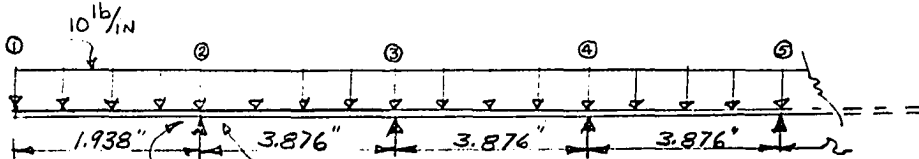
$$\text{F.E.M.} = \frac{6E'I}{h^2} \Delta = \frac{6EI}{h} \times \left( \frac{\Delta}{h} \text{ or } \frac{\Delta \delta^v}{d} \right) = \frac{6E't^3}{12h} \cdot \frac{1}{d} \times \Delta \delta^v$$



$$= \frac{10^7 \times 0.19^3}{2 \left(1 - \left(\frac{1}{3}\right)^2\right) (4) (3.876)} \Delta \delta^v$$

$$= \underline{\underline{2.49 \times 10^3}} \times \Delta \delta^v$$

Determine F.E.M. for symmetrical case



$$\text{FEM} = 10 \times \frac{1.938^2}{2} = \underline{\underline{-18.8}} \text{ in-lb}$$

$$\text{FEM} = \frac{10 \times 3.876^2}{12} = \underline{\underline{-12.5}} \text{ in-lb}$$

Determine F.E.M. for anti-symmetrical case

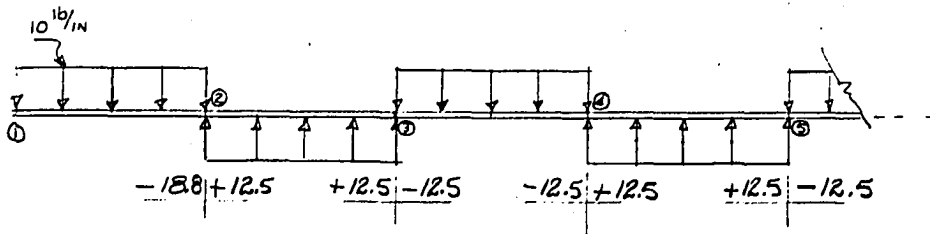
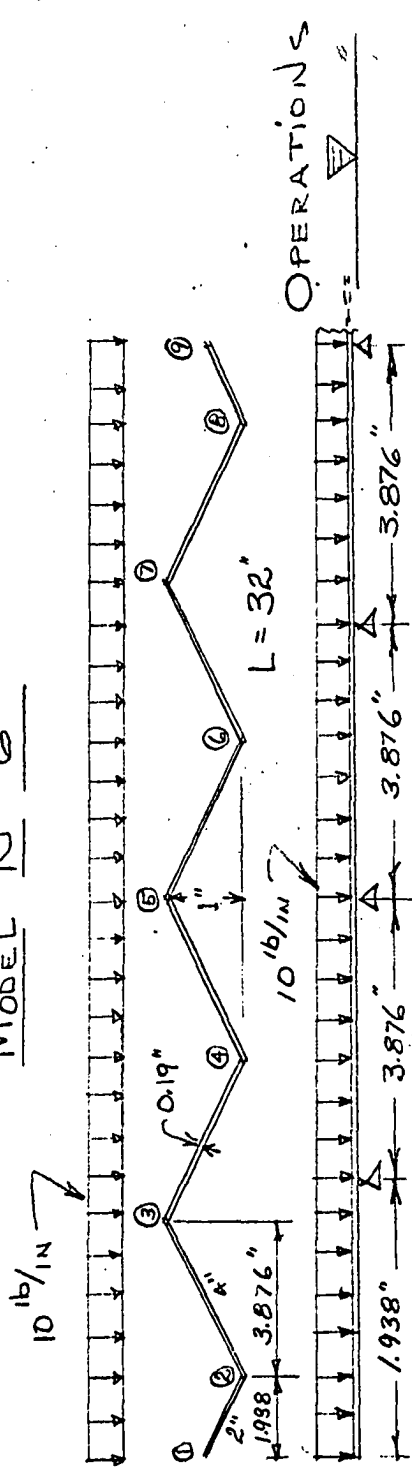


TABLE 2. OPERATION TABLE FOR MODEL NO 6 CALCULATIONS

MODEL NO 6



OPERATIONS

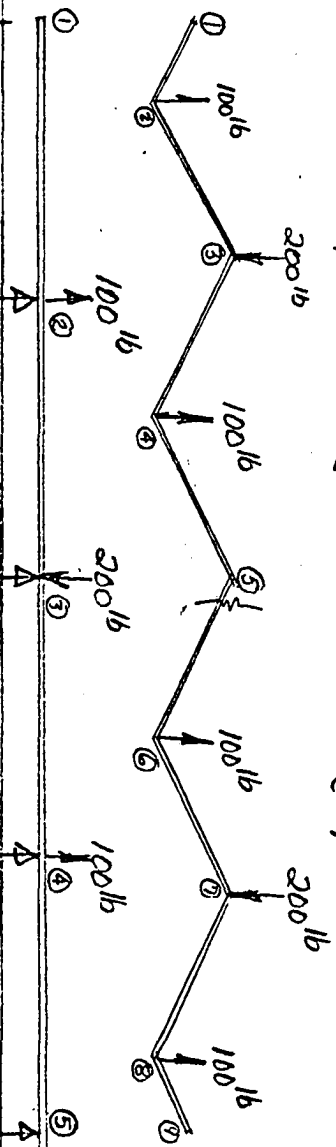
SLAB D.F.	0	1	0.428	0.572	0.5	0.5	0	1
C.O.F.	0.5	0.214	0.286	0.25	0.25	0	0	0
F.E.M. →	-18.8	-12.5	-12.5	-12.5	-12.5	-12.5	-12.5	-12.5
			+3.15		-0.90		+0.23	
					-0.01		+0.01	
	-18.8	-12.5	-9.35	-12.74	-13.46	-12.5	-12.26	
		-6.3	-1.45	+1.94	+0.48	-0.48	0	
$M'(in-lb)$	-18.8		-10.80		-12.98		-12.26	
$R'(lb)$ <small>REACT TO LOAD</small>	-38.76		-38.76		-38.76		-38.76	
$R'(lb)$ <small>REACT TO MOM.</small>	-2.06		+2.06	+0.56	-0.56	-0.19	+0.19	$\frac{M_1 - M_2}{L}$ , $\frac{M_2 - M_3}{L}$
$F'(lb)$	+40.82		+36.14		+39.51		+38.38	$-\sum R'$
$C^v$	-2	+2	+2	-2	-2	+2	+2	
$P'(lb)$	-81.64	+81.64	+72.28	-72.28	-79.02	+79.02	+76.76	$F' \cdot C^v$
$P'(lb)$	-81.64		+153.92		-151.30		+155.78	$P_{n_1, n_2, \dots} + P_{n+1, n}$
$M^o (in-lb)$	-10,440		+19,700		-19,370		+19,920	$PL^2/8$
$G^o (psi)$								$M^o/z$
PLATE D.F. 10	0.667	0.333	0.5	0.5	0.5	0.5	0.5	0



C.O.F.	0	0.333	0.167	0.25	0.25	0.25	0.25	0
F.E.S.	-82,200 -14,420 +655 +66 +7	+82,200 -1910 -199 -21	+39,000 -7210 -319 -33	-38,300 -275 +477 +50	+38,300 +1910 +199 +21	+39,400 +275 -477 -50 -5		-39,400 +275 -477 -50 -5
$\Delta G'$ (psi)	-67,072 0	+51,970	-42,303	+39,915	+39,915	-39,657		-39,657
$\Delta G'$	-119,042	+94,213	-82,216	+79,572	+79,572	$6n - 6n + 1$		
$L^2 / 96 E I$	$5.33 \times 10^{-6}$	$2.67 \times 10^{-6}$	$2.67 \times 10^{-6}$	$2.67 \times 10^{-6}$	$2.67 \times 10^{-6}$			
$\Delta$	-0.6350	+0.2520	-0.2196	+0.2196	+0.2196	-0.2126		$AG \cdot L^2 / 96 E I$
C'S	+1.2700	+0.5040	+0.5040	+0.4392	+0.4392	+0.4252		+0.4252
$\Delta S_V$	+1.7740	+0.9432	+0.8644	+0.8644	+0.8644	+0.8504		$\sum C'S$
$\Delta S_V$	+0.8308	+0.0788	+0.0788	+0.0140	+0.0140	$S_n - S_{n+1}$		
F.E.M.	+2068	-2068	+196	-196	+35	-35		$\Delta S_V \cdot (L^2 / 96 E I) = 2.49 \times 10^3$
SLAB D.F.	0.1	0.428	0.572	0.5	0.5	0.1		
C.O.F.	0.5	0.214	0.286	0.25	0.25	0		
F.E.M. $\rightarrow$	+2068	-2068	+196	-196	+35	-35		
		+1034						
			+352			-30		
				+30				
			+2			-2		
$\Delta M''$								
R''	+127.7	-127.7	+153.5	+153.5	+43.2	-43.2		
R''	+127.7	-281.2	+196.7	+196.7		-86.4		

TABLE 2. (CONTINUED)

PARTICULAR LOAD SYSTEM (a)



$F_1$	-100	+200	+200	-100	0	0
$C_v$	-2	+2	+2	-2	+2	+2
$P$	+200	-200	+200	-200	+200	-200
$M^o$	+20,750	+20,750	-20,750	-20,750	-20,750	-20,750
$G^o$	+163,600	+41,000	-41,000	-41,000	-41,000	-41,000
$D.F.$	0	0.667	0.333	0.5	0.5	0.5
$C.O.F.$	0	0.333	0.167	0.25	0.25	0.25
$F.E.S.$	+163,600	-163,600	+41,000	-41,000	-41,000	+41,000
	-68,200	+34,200	+34,200	+20,500	-34,200	-20,500
	-1,140	+356	+572	-856	-357	+856
	-119	+60	+60	-89	-357	+89
	-12	+37	+37	-10	-37	+10
	-2	+4	+4	-1	-4	+1

OPERATIONS  
AS BASIC

	+94,127	-163,600 + 44,817	-6,161 - 21,456	+37,182 - 41,000	
		+139,000 - 24,600	-69,397 - 13,809	-39,091 + 39,091	
G'	+94,127	-24,600	-13,809	-1,909	+21,456
ΔG'	+118,727	-10,791	-11,900	-23,365	
E <sup>1/2</sup> EPH	5.18 x 10 <sup>-6</sup>	2.60 x 10 <sup>-6</sup>	2.60 x 10 <sup>-6</sup>	2.60 x 10 <sup>-6</sup>	
S <sup>v</sup>	+0.6150	-0.0284	-0.0309	-0.0607	
C <sup>v</sup>	-2	+2	-2	+2	
C <sup>v</sup> S <sup>v</sup>	-1.2300	-0.0567	-0.0567 + 0.0617	+0.0617 - 0.1213	-0.1213 - 0.1213
S <sup>v</sup> S <sup>v</sup>	-1.2867	+0.0050	-0.0050	-0.0596	-0.2426
ΔS <sup>v</sup>		-1.2917	+0.0646	+0.1830	
F.E.M.		-3220	+3220 + 161	-161 + 456	-456
SLAB D.F.	0.1	0.428	0.572	0.505	0
C.O.F.	0.5	0.214	0.286	0.25	0
F.E.M.		-3220 + 3220 + 161	-161 + 456	-456	
		-1610 - 155	-458	+155	
		-114	-114	+114	
		-8	-32	+8	
		-1	-2	+1	
		-3220	+1610 - 117	-653 + 456	-178
		+3220	-738 + 989	+555 - 555	0
M''		0	+872	-99	-178
R <sup>1</sup>		-225	+225 + 251	-251 + 20	-20.3
R <sup>2</sup>		-225	+476	-230	-40.5
F		-325	+676	-330	-40.5



			-2		+2		
	+1	-					
	-7650	0	+22,877	-32,166	+35,263	-22,877	0
	0	+15,259		+36,215	-36,215	+11,439	-11,439
A	-7650	+15,259		-952		-11,439	+5737
	-27,909		+16,211		+10,487		-17,176
	5.18 x 10 <sup>-6</sup>		2.6 x 10 <sup>-6</sup>		2.6 x 10 <sup>-6</sup>		2.6 x 10 <sup>-6</sup>
	-0.1190		+0.0422		+0.0273		-0.0448
		-2 + 2		+2 - 2		-2 + 2	+2
	+0.2380	+0.0843	+0.0843	-0.0547	-0.0547	-0.0895	-0.0895
A	+0.3223		+0.0297		-0.1440		-0.1790
		+0.2926		+0.1737		+0.0350	
	+728		-728	+433		-433	+87
	0		0.428	0.572		0.5	0.5
	0.5		0.214	0.286		0.25	0.25
	+728		-728	+433		-433	+87
			+364	-130			+130
			+48		+191		-48
			-3		+14		-3
					+1		
	+728		-364	+354		-227	+87
	-728		+307	-412		+157	-157
	0		-57		-70		-8
M	+14.7		-14.7	+3.56		-3.56	-16.12
R	+14.7		-11.11			-19.67	+38.24
F	+14.7		+88.89			-219.67	+232.24



	+ 1909	0	- 5720	- 954 + 2,1930	- 35397 + 41,000	- 2,1966	
	0	- 3820 + 1910	+ 11,456 - 11,450	+ 38,206 - 38,200	0	0	
D 2'	+ 1909	- 3820	+ 10,486	+ 2800	- 2,1960		
AG'	+ 5,730	- 14,300	+ 7680	+ 24,180			
$\frac{L^2}{4} \frac{w}{Eh}$	$5.16 \times 10^{-6}$	$2.60 \times 10^{-6}$	$2.60 \times 10^{-6}$	$2.60 \times 10^{-6}$			
$\frac{w}{h}$	+ 0.0297	- 0.0372	+ 0.0198	+ 0.0644			
$\frac{w}{h}$	- 2 + 2	+ 2 - 2	- 2 + 2	+ 2			
$\frac{w}{h}$	- 0.0594 - 0.0743	- 0.0743 - 0.0396	- 0.0396 + 0.1288	+ 0.1288 + 0.1288			
$\frac{w}{h}$	- 0.1336	- 0.1138	+ 0.0892	+ 0.2576			
$\frac{w}{h}$	- 0.0198	- 0.2030	- 0.1684				
ASV	- 50	+ 50 - 505	+ 505 - 419	+ 419			
F.E.M.	0	0.4280.52	0.50.5	0			
SLAB D=	0	0.2140.286	0.250.25	0			
C.O.F.	- 50	+ 50 - 505	+ 505 - 419	+ 419			
F.E.M.		- 25 + 231	- 86	- 231			
		- 21	- 6	+ 21			
		- 1		+ 1			
	- 50	+ 25 - 296	+ 413 - 419	+ 210			
D M''	+ 50	- 139 + 184	- 416 + 416	0			
R''	0	- 1/2	- 3	+ 2/10			
R''	+ 28.9	- 28.9 - 28.0	+ 28.0 - 55.1	+ 55.1 + 55.1			
R''	+ 28.9	- 56.9	- 270	+ 110.2			
F	+ 28.9	- 56.9	- 127	+ 310			

Indicial equations for model No. 6

$$aF_{3a} + bF_{3b} + cF_{3c} + R''_{3 \text{ basic}} = 0$$

$$aF_{4a} + bF_{4b} + cF_{4c} + R''_{4 \text{ basic}} = 0$$

$$aF_{5a} + bF_{5b} + cF_{5c} + R''_{5 \text{ basic}} = 0$$

Substituting values from operation tables gives:

$$676a + 88.89b - 56.9c - 281.2 = 0$$

$$-330a - 219.67b - 127c + 196.7 = 0$$

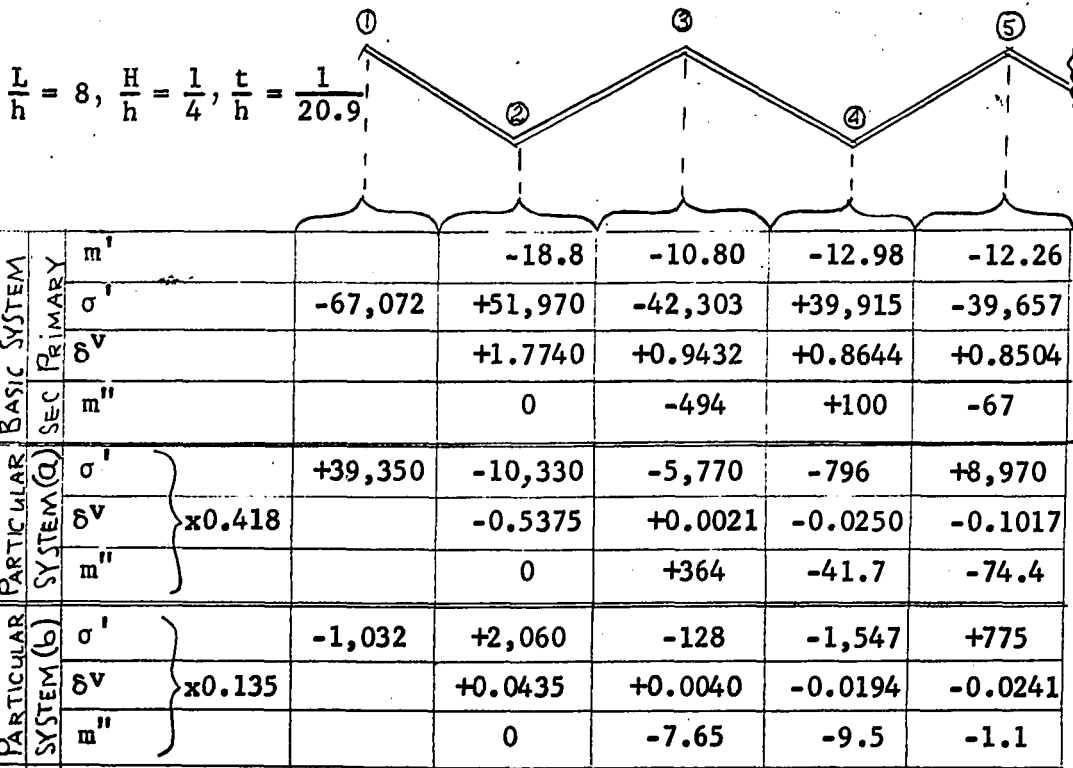
$$-40.5a + 232.23b + 310c - 86.4 = 0$$

The solution of which is:

$$a = 0.418, \quad b = 0.135, \quad c = 0.232$$

Compilation of Results:

$$\lambda = \underline{157.5}$$





PARTICULAR SYSTEM (C)	$\sigma'$	+442	-885	+2,434	+663	-5,090
	$\delta v$	} x0.232	-0.0310	-0.0264	+0.0207	+0.0597
	$m''$		0	-26	-0.75	+48.7
FINAL	$\sigma$	-28,312	+42,815	-45,767	+38,235	-35,000
	$\delta v$		+1.249	+0.9229	+0.8407	+0.7843
	$m$		-18.8	-174	+35.	-106

58% Corr.  $\frac{R''}{F'} = 315\%$   
to basic system

### C. Dimensionless Parameter - $\lambda$

There could conceivably be times when it would be desirable to carry out the folded plate solution to some predetermined degree of accuracy. In fact it could be that the basic solution alone would give answers to the desired degree of precision. In order to obtain a measure of the importance of the particular solution corrections the dimensionless parameter  $\lambda$  was developed. It was developed by making a step by step check of the operation table and thereby establishing the proportionality existing between  $R''$  and the system parameters (L, t, h and H) - also between  $F'$  and the system parameters and then dividing the  $R''$  - proportionality by the  $F'$  - proportionality. The result of this operation was

$$\lambda = \frac{\left(\frac{L}{h}\right)^4 \cdot \left(\frac{t}{h}\right)^2}{\left(\frac{H}{h}\right)^2 \left[1 - \left(\frac{H}{h}\right)^2\right]}$$

From this it is seen that  $\lambda$  is a measure of the ratio of superfluous  $R''$  to the activating force  $F'$ . It was therefore thought that  $\lambda$  would also be a measure of the correction to the basic system afforded by the particular solutions.

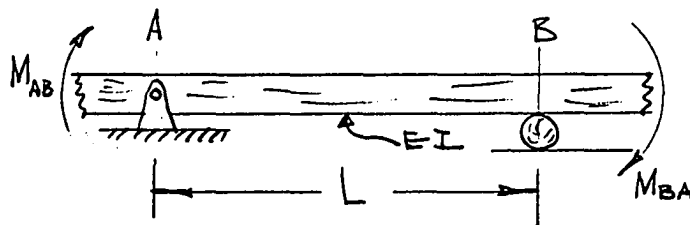
To confirm this reasoning a plot (Fig. 3) was made showing the relationship existing between  $\lambda$  and  $\frac{R''}{F}$  { at first valley } and between  $\lambda$  and the percentage correction to the basic edge beam at point A. As seen from the plot,  $\lambda$  vs.  $\frac{R''}{F}$  is linear as anticipated and the percentage correction to the basic system increases at a decreasing rate as  $\lambda$  increases. In fact the trend is toward a percentage correction that is asymptotic to some limiting correction value. The significance of all of this is that in knowing  $\lambda$  for this particular configuration we also have an idea of the magnitude of particular corrections to the basic system and therefore can predetermine their importance.

#### D. Check System for Theoretical Calculations

After the execution of a complete set of model calculations it is comforting to have a check system to insure the correctness of our manipulative operations. No check will tell us that we have used the wrong geometry, loads, or material properties but once we have selected these quantities, the operational correctness will be reflected in the degree to which the statics and geometry of the problem have been simultaneously satisfied. With this in mind a system based on slope deflection was devised for checking the compatibility of the  $m$  and  $\delta$  values.

Starting with the well known slope deflection equation

$$M_{AB} = \frac{2EI}{L} \left[ 2\theta_A + \theta_B - 3\frac{\Delta}{L} \right] + C_{AB} \text{ where:}$$



NOTE:  $M$  is  
ANALOGOUS  
TO  $m$

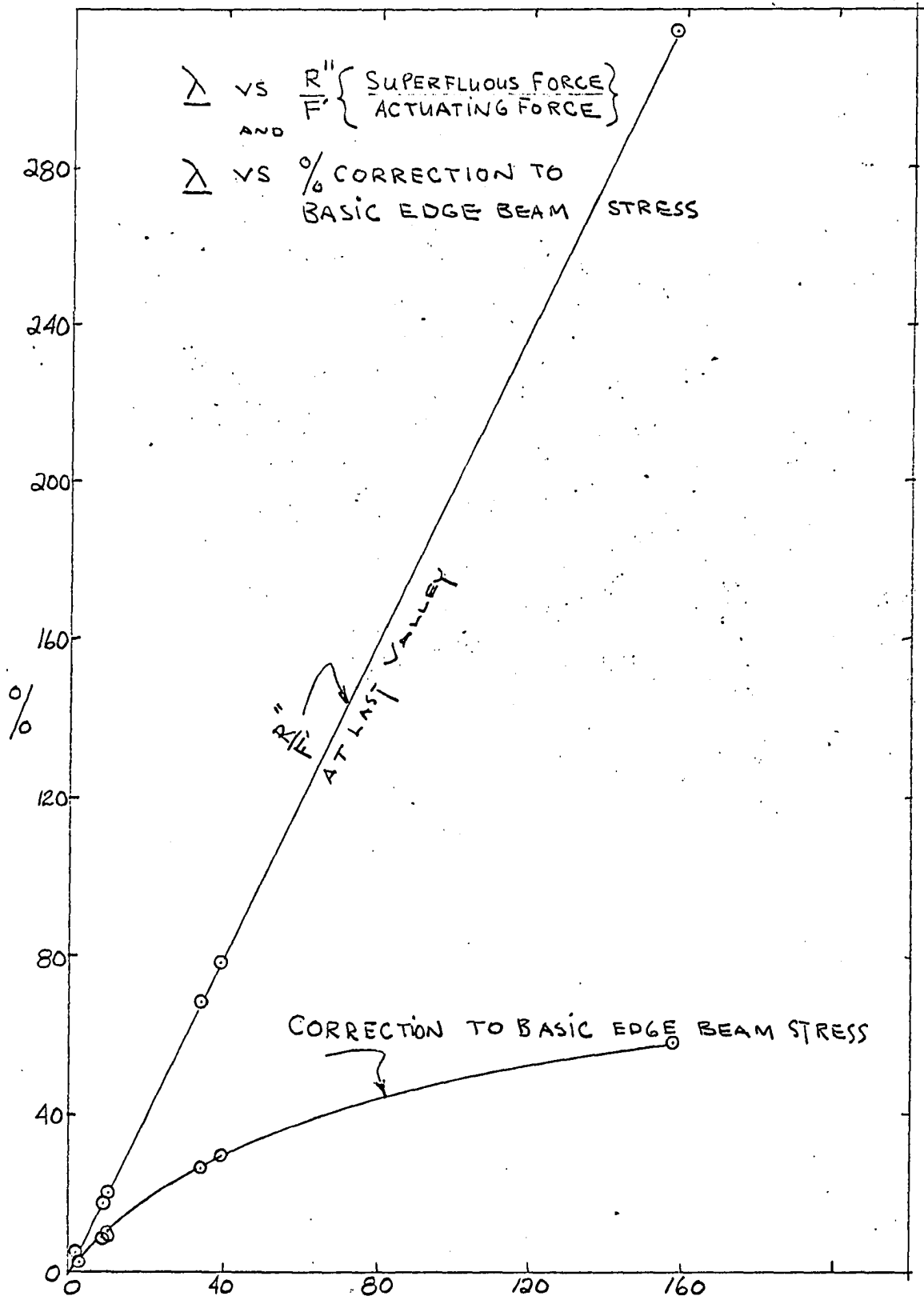
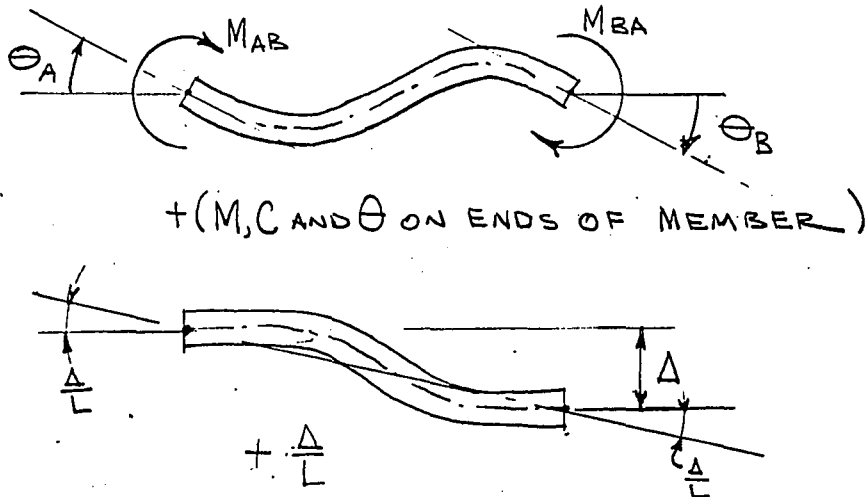


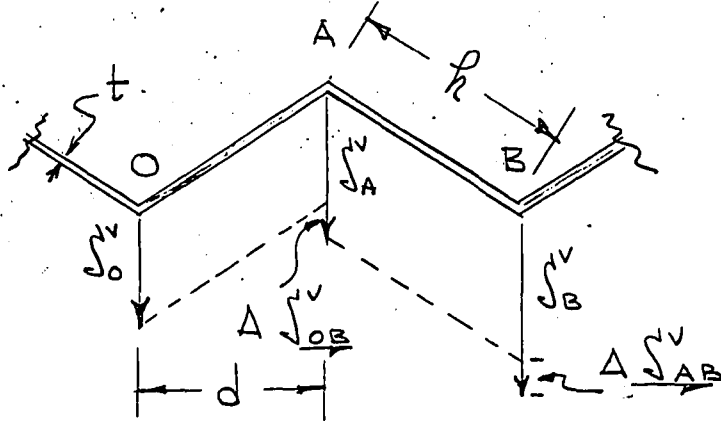
FIG.3 SYSTEM BEHAVIOR AS A FUNCTION OF  $\lambda$



The following relationship was derived:

$$M_{AB} = \frac{M_{BA} - M_{OA}}{4} + \left[ \frac{(2C_{AB} - C_{BA}) - (2C_{AO} - C_{OA})}{4} \right] - \frac{3EI}{2hd} \left[ \frac{\Delta \delta^v}{AB} - \frac{\Delta \delta^v}{OA} \right]$$

This has direct application to the following real situation:

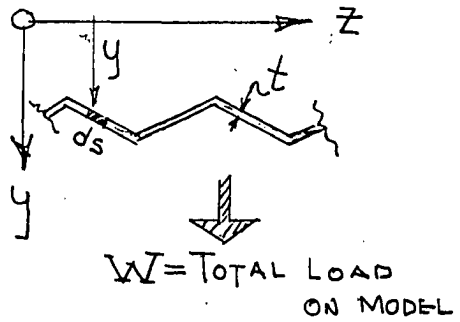


Comparing the final  $M_{ij}$  values obtained in the folded plate solution to those determined by using this equation gives assurance that the manipulations involving M - values and  $\delta$ -values stand a good chance of being correct.

Another check to make is based on the longitudinal stresses and is carried out by the following operation:

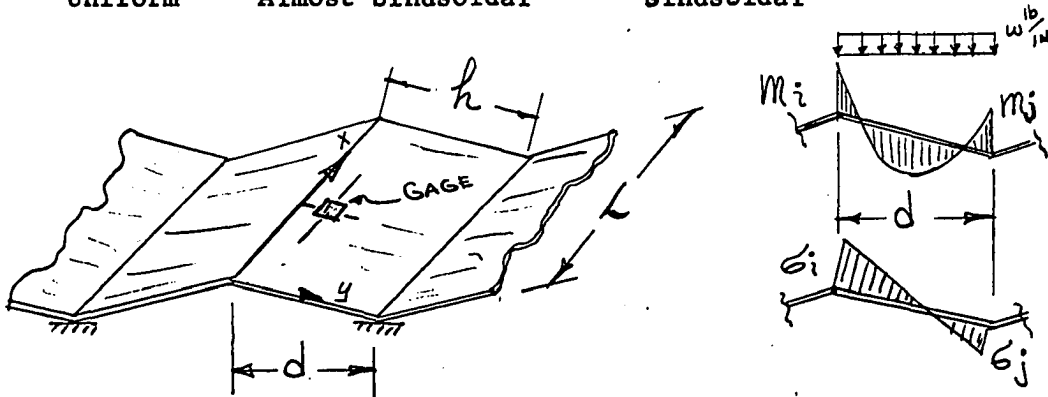
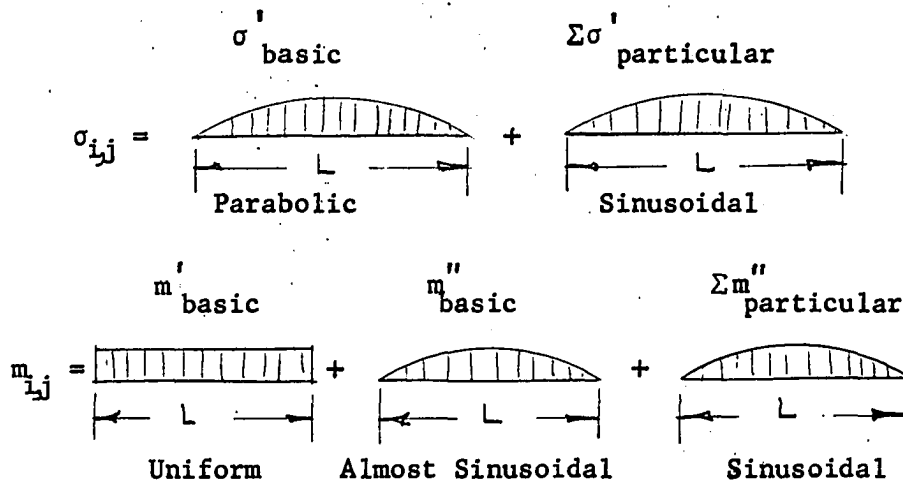
$$\int_0^s \sigma_x t ds = 0$$

and 
$$\int_0^s \sigma_x t y ds = \frac{1}{8} WL$$



**E. Stress and Moment Determination at Gage Location**

Inasmuch as it was thought to be unwise to place gages directly in the sharp folds of the structure the need arises for the computation of the theoretical stress and moment at the point of experimental measurement because the folded plate theory gives the stresses and moments at the ridges. The following reduction formulas are based on the already stated stress and moment patterns.



$$m_{\text{at any gage}} = \underbrace{m'_{i\text{basic}} + \sin \frac{\pi x}{L} \Sigma m''}_{m_i} \pm \frac{y}{h} \Delta m_{i \rightarrow j} - \left[ 1 - \left( \frac{\frac{h}{2} - y}{\frac{h}{2}} \right)^2 \right] \frac{1}{8} w d^2$$

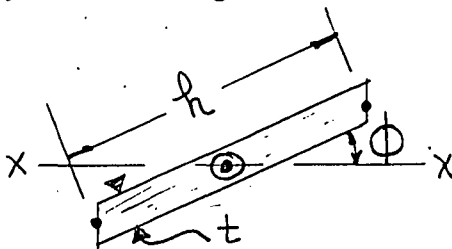
$$m_{\text{at mid-span gage}} = m_i \pm \frac{y}{h} \Delta m_{i \rightarrow j} - \left[ 1 - \left( \frac{\frac{h}{2} - y}{\frac{h}{2}} \right)^2 \right] \frac{1}{8} w d^2$$

$$\sigma_{\text{at any gage}} = \underbrace{\left[ 1 - \left( \frac{\frac{L}{2} - x}{\frac{L}{2}} \right)^2 \right] \sigma'_{i\text{basic}} + \sin \frac{\pi x}{L} \Sigma \sigma'_{\text{part.}}}_{\sigma_i} \pm \frac{y}{h} \Delta \sigma_{i \rightarrow j}$$

$$\sigma_{\text{at mid-span gage}} = \sigma_i \pm \frac{y}{h} \Delta \sigma_{i \rightarrow j}$$

#### F. Beam Analysis

For comparison purposes the folded plate system was assumed to behave as one huge simple beam and stresses were thereby determined. The most important phase of this endeavor was probably the moment of inertia computation technique which hinges upon the following chosen element of plate system as being basic to the complete solution.



$$I_{xx} = \frac{1}{12} \frac{t^3 h}{\cos^2 \phi} + \frac{1}{12} t h^3 \sin^2 \phi$$

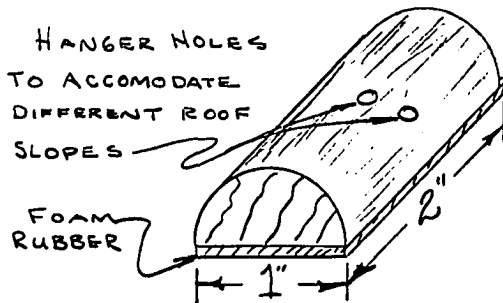
The remaining operations in determining the moment of inertia and locating the neutral axis of the whole system are quite involved from a manipulative standpoint but follow from routine statics. The final step in the solution involved the application of the flexure formula.

## V. EXPERIMENTAL INVESTIGATION

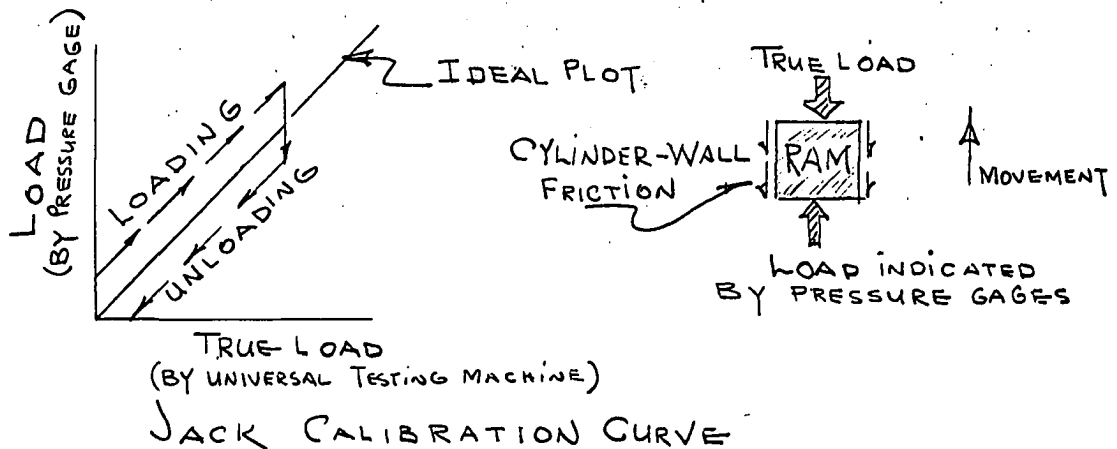
### A. Loading System

Before the design of the experimental set up could be initiated the question of what type of loading was to be administered and what quantities were to be measured, had to be answered. The design was strongly influenced by the pilot test observations, wherein the rather thin model was subjected to a concentrated ridge load. The question was - were these realistic conditions? Even with this rather crude setup the correlation was excellent, but the outcome was probably influenced by the favorable conditions of thin plates having smaller secondary effects and the load, being applied at the ridge, not having to undergo the physical process of finding its way to a ridge as would a uniform surface load. In other words when we apply the forces at the ridges, they are already "there" - but when we apply the loads on the surface we have to "assume" that they get to the ridges. Therefore the former case is circumventing a part of the assumptions and thereby stands a better chance of producing effects that are closer to those theoretically predicted.

With this background thinking, the decision was made to use a uniform surface load which was simulated by a pattern of discrete loading pads. The pads were fabricated by splitting 1 in. wood dowel stock in half, gluing a layer of form rubber on the flat side, and then drilling holes for the wire load hangers as shown:



The pads were uniformly distributed on the surface in a pattern such that a pad was centered on every 2-in. x 4-in. area. The load hangers then formed the upper part of a whiffle-tree mechanism, Fig. 4, that served as the transition between the concentrated applied load and the simulated uniform surface load. The load application mechanism consisted of a 12-ton hydraulic jack, enclosed in a frame designed for transmitting a vertical load to the structure, Fig. 5. The load measuring system originally consisted of a 3-range (low, medium, high) system composed of 3 pressure gages that were tapped into the fluid reservoirs of the jack, Fig. 6. As a consequence of the internal ram friction, difficulty was encountered with this measuring system and calibration of the system yielded plots with the following characteristics:

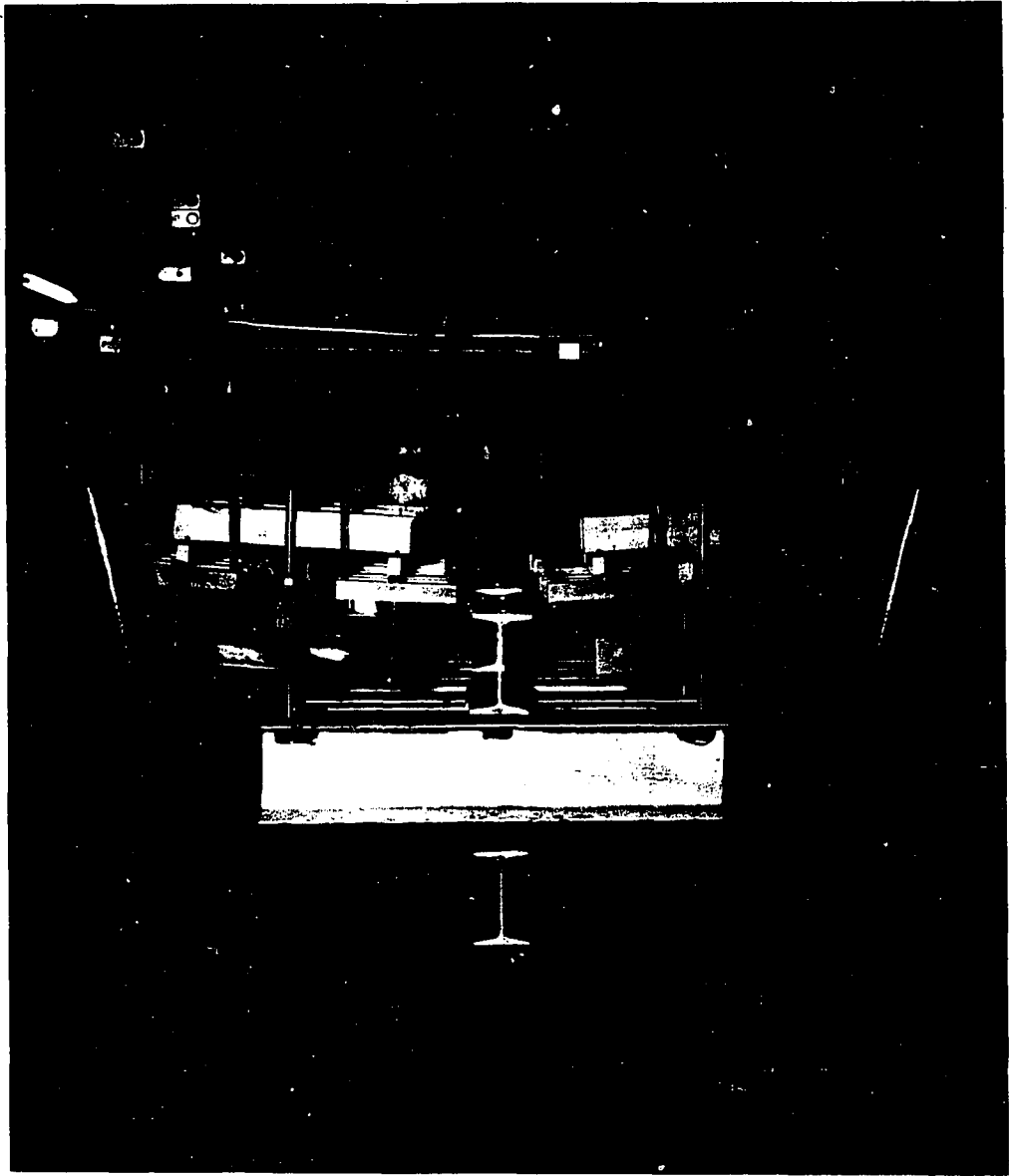


Judicious use of these calibration curves could conceivably have resulted in reliable load determinations were it not for the fact that the nature of the test procedure dictates that the load be sustained at each increment for a substantial period of time. During the actual model testing operation there would be an element of uncertainty as to where on the calibration curve we would find our true load.

With this outcome the decision was made to use the pressure gages as approximate load indicators and incorporate a more dependable load



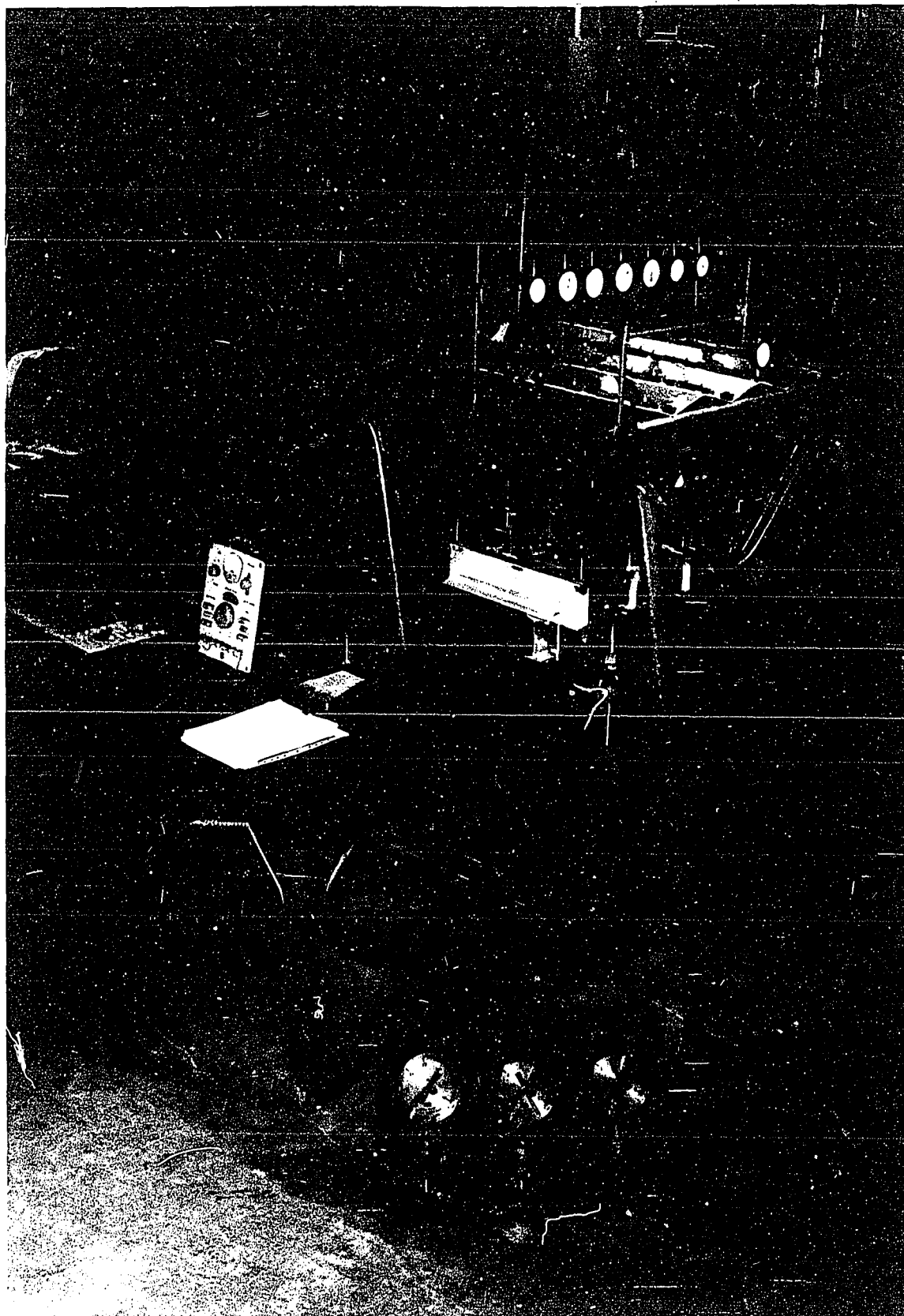
**Fig. 4. Whiffle-Tree Mechanism**



**Fig. 5. Jack Assembly**



**Fig. 6. Experimental Set-up Showing  
Pressure Gages as Load-Measuring  
Device**



measuring device in series with the jack system. Subsequently two SR-4 strain gage load cells (low range 0  $\rightarrow$  5000<sup>lb</sup>, high range 0  $\rightarrow$  20,000<sup>lb</sup>) were designed by mounting SR-4 gages on high strength aluminum rods. Swivel end-connectors were designed for the rods to eliminate as much load eccentricity as possible. Four gages were used per load cell - 2 diametrically opposite longitudinal gages and 2 diametrically opposite transverse gages. This arrangement corrected for eccentricity, compensated for temperature and increased the sensitivity approximately 30%, Fig. 7. This high capacity loading system was designed to enable plastic behavior observations to be made.

#### B. Deflection Measurement

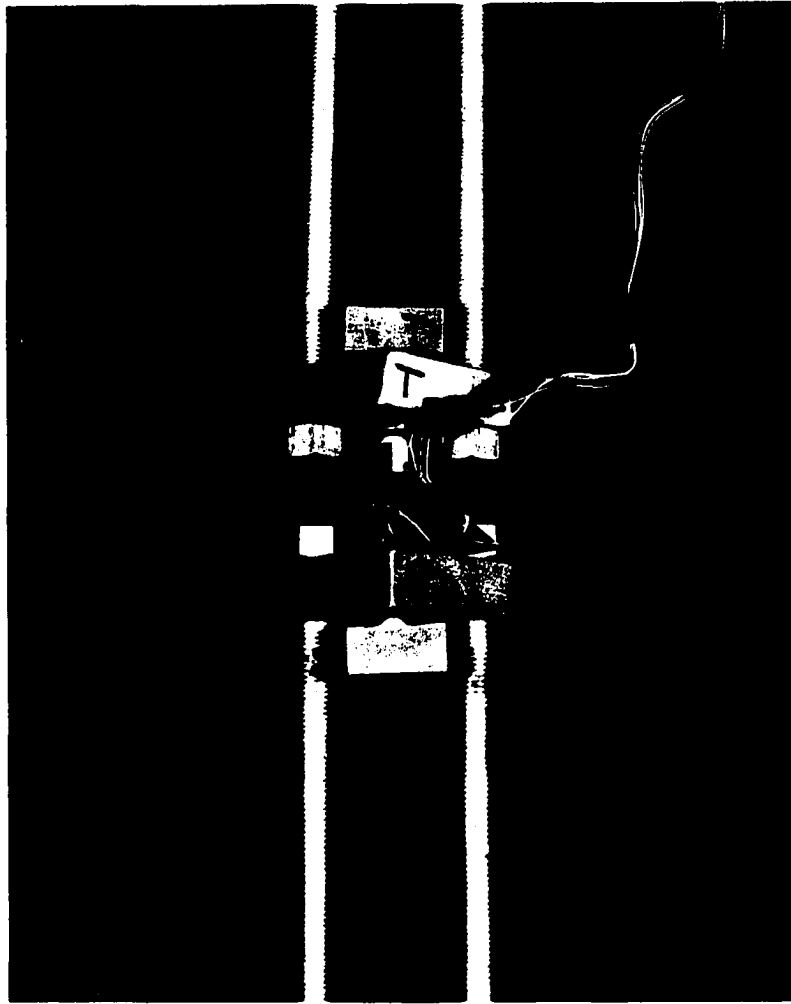
For deflection measurement,  $\frac{1}{1000}$ " dial indicators were pulled with fine wire to alleviate transverse contact effects that sometimes arise when the structure has a deflection component that is perpendicular to the axis of the dial indicator stem. The fact that there is no measurable error induced by this pulling system was confirmed by placing two indicators in series - with a 12-in. spacing, and observing any differential dial movement between them.

#### C. Stress and Moment Measurement

The next step in the experimental program involves the measurement of stresses and moments. Care was taken to select strategic gage locations what would reflect a representative behavior of the whole structure without employing an excessive number of SR-4 gages. As it was, each of the 8 models used a total of eighteen 90°-rosettes which required 36 gage

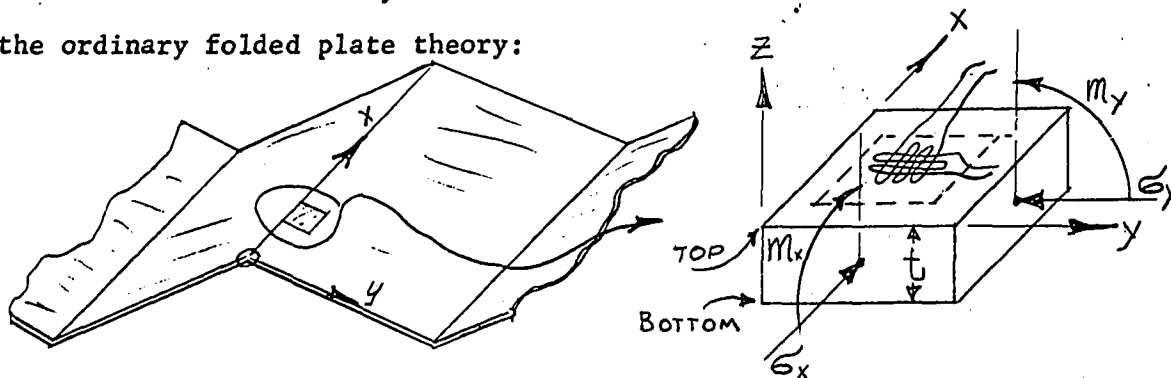
Fig. 7. Small Load Cell (0→5000<sup>lb</sup>)



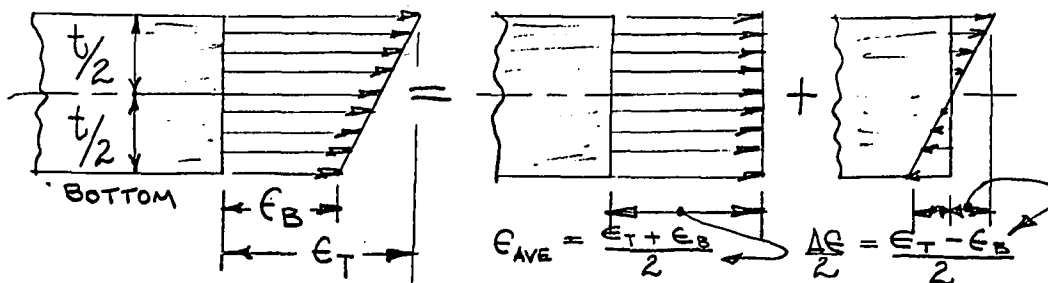


readings per load interval. It was thought that the gages would reflect a truer strain picture if they were not placed right in the sharp folds of the plates, so the location in the majority of cases was 0.25-in. from the folds. The gages used (AX-5-1) had a 7/16-in. gage length which obviously caused them to still be awfully close to the folds. There were essentially 4 gages at each location (90°-rosettes, top and bottom) purposely placed to facilitate the determination of membrane stresses and slab moments, Figs. 8 to 15.

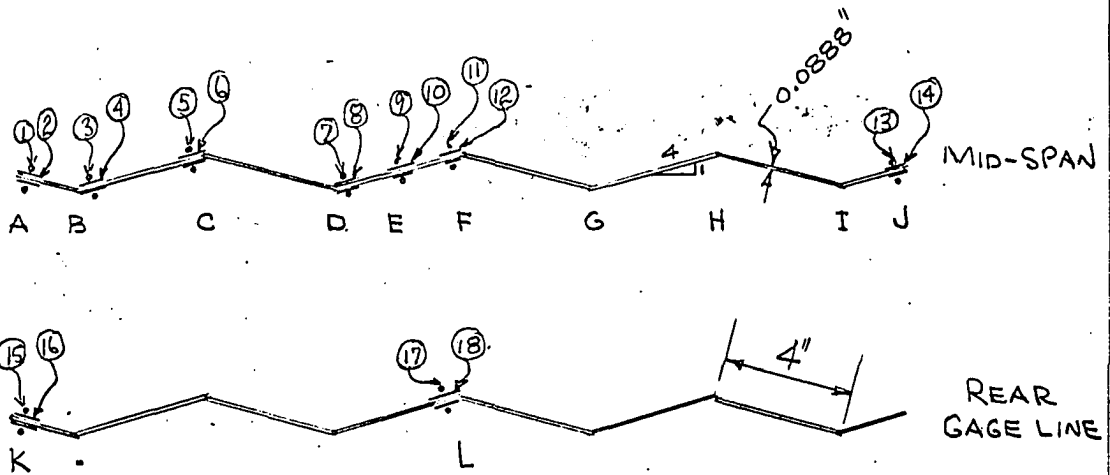
The desired quantities in these tests were plate membrane stresses ( $\sigma_x$ ) and slab moments ( $m_y$ ) which are the primary quantities predicted by the ordinary folded plate theory:



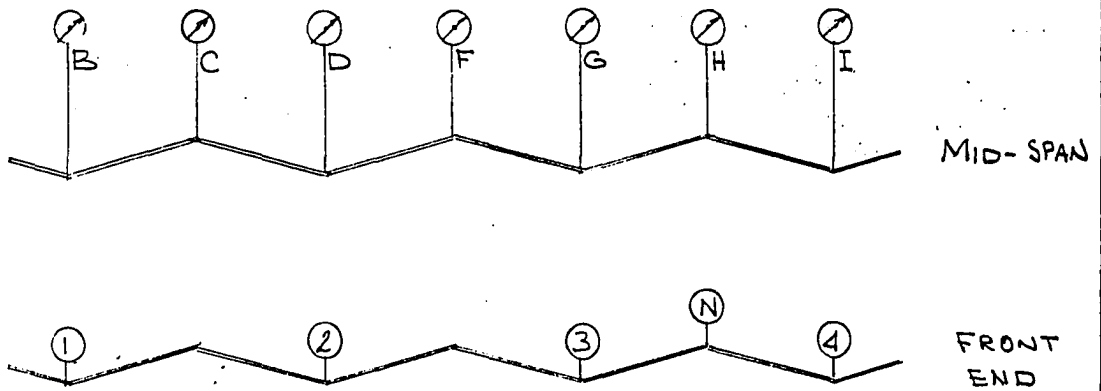
The other quantities ( $m_x$  and  $\sigma_y$ ) are assumed by the theory to be insignificant, which is an assumption requiring experimental confirmation or refutation. Since any linear strain pattern occurring across the plate thickness can be resolved into a membrane strain (average strain, or strain at mid-plane of the plate) and a moment strain ( $\Delta\epsilon$  from top to bottom of plate) as shown in the following illustration -



GAGES: — TRANSVERSE • LONGITUDINAL



DIALS:



TOP VIEW: (DIMENSIONS ARE NOT HORZ. PROJ.)

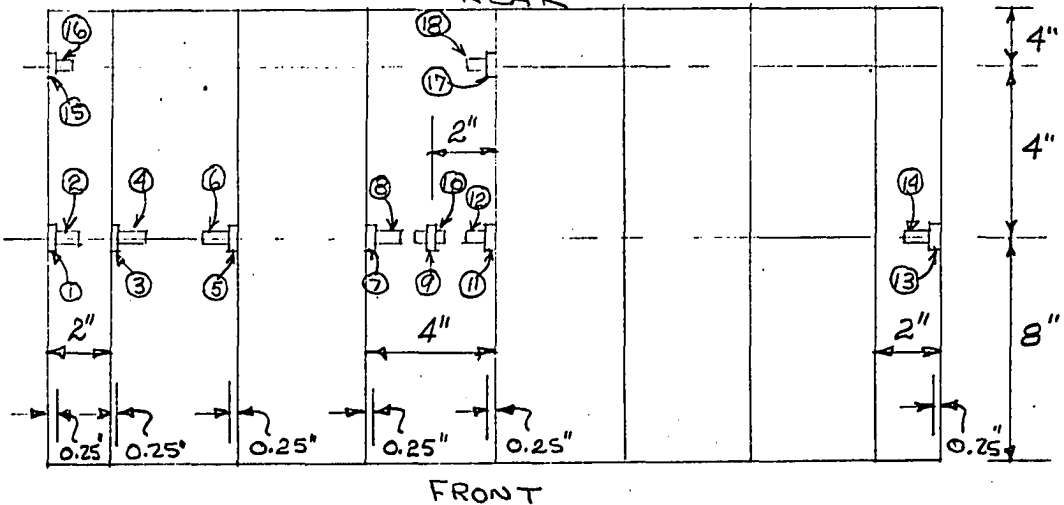


FIG. 8 GAGE AND DIAL PLACEMENT (MODEL 1)

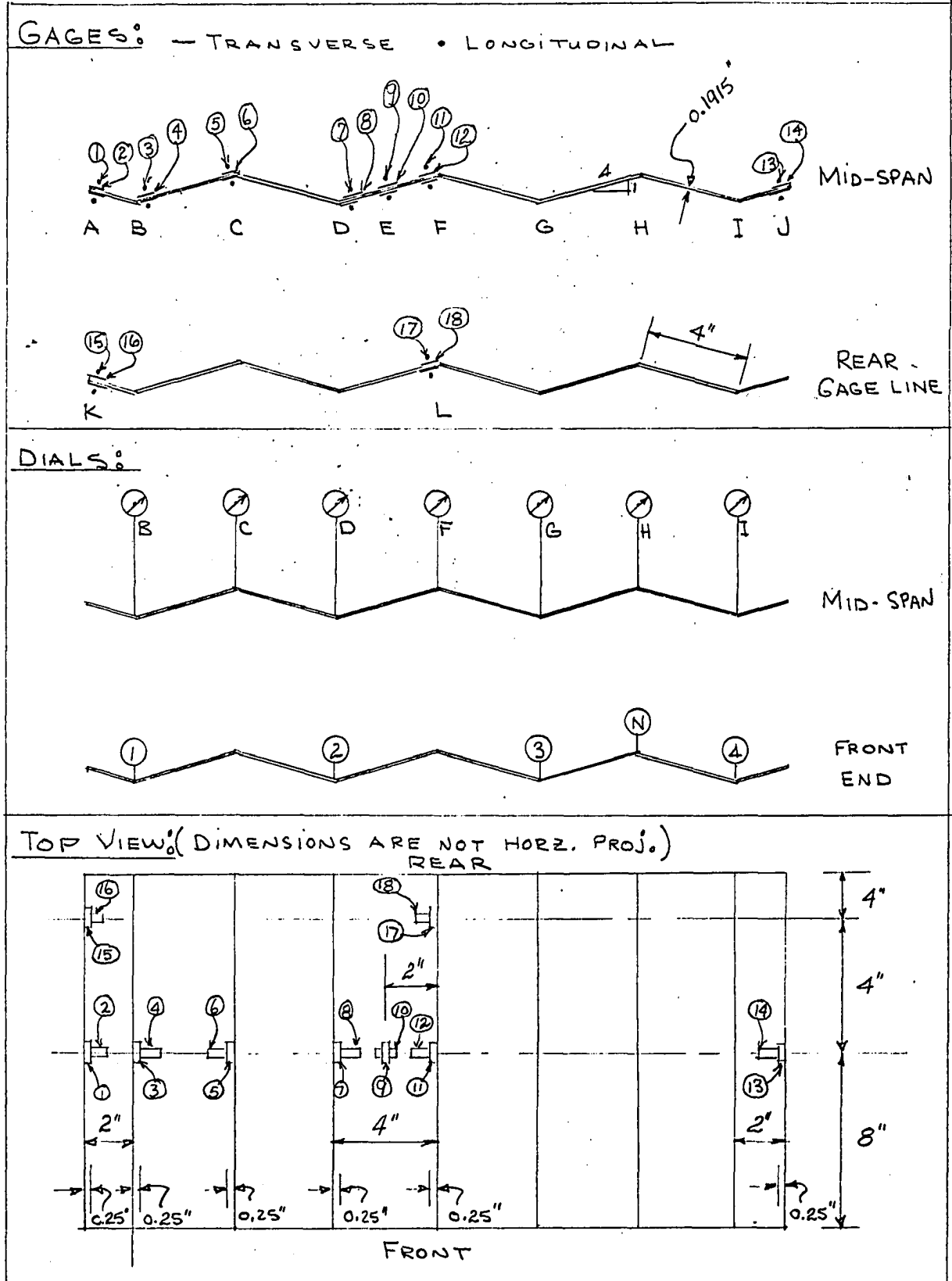


FIG. 9 GAGE AND DIAL PLACEMENT (MODEL 2)

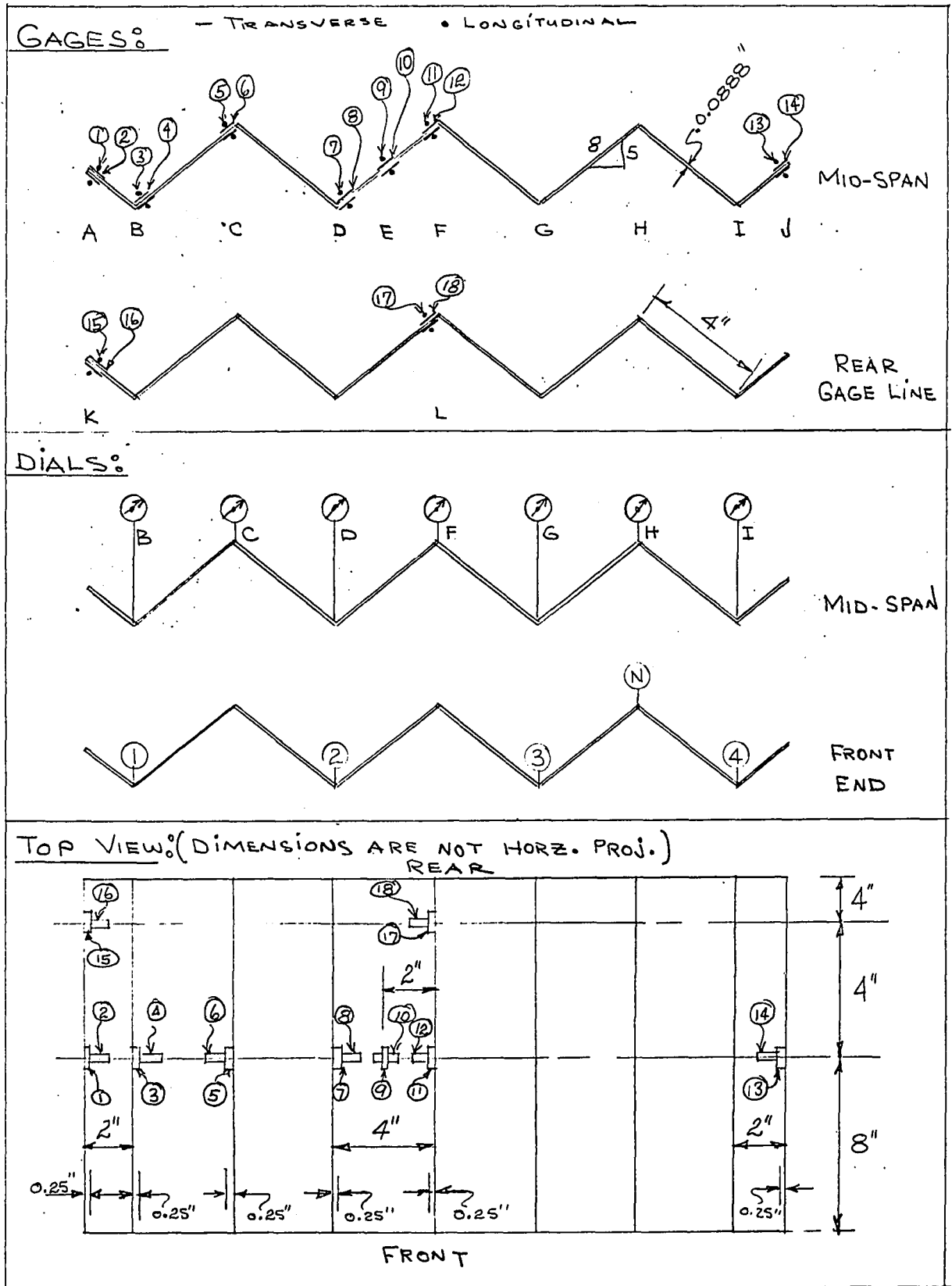


FIG. 10 GAGE AND DIAL PLACEMENT (MODEL 3)

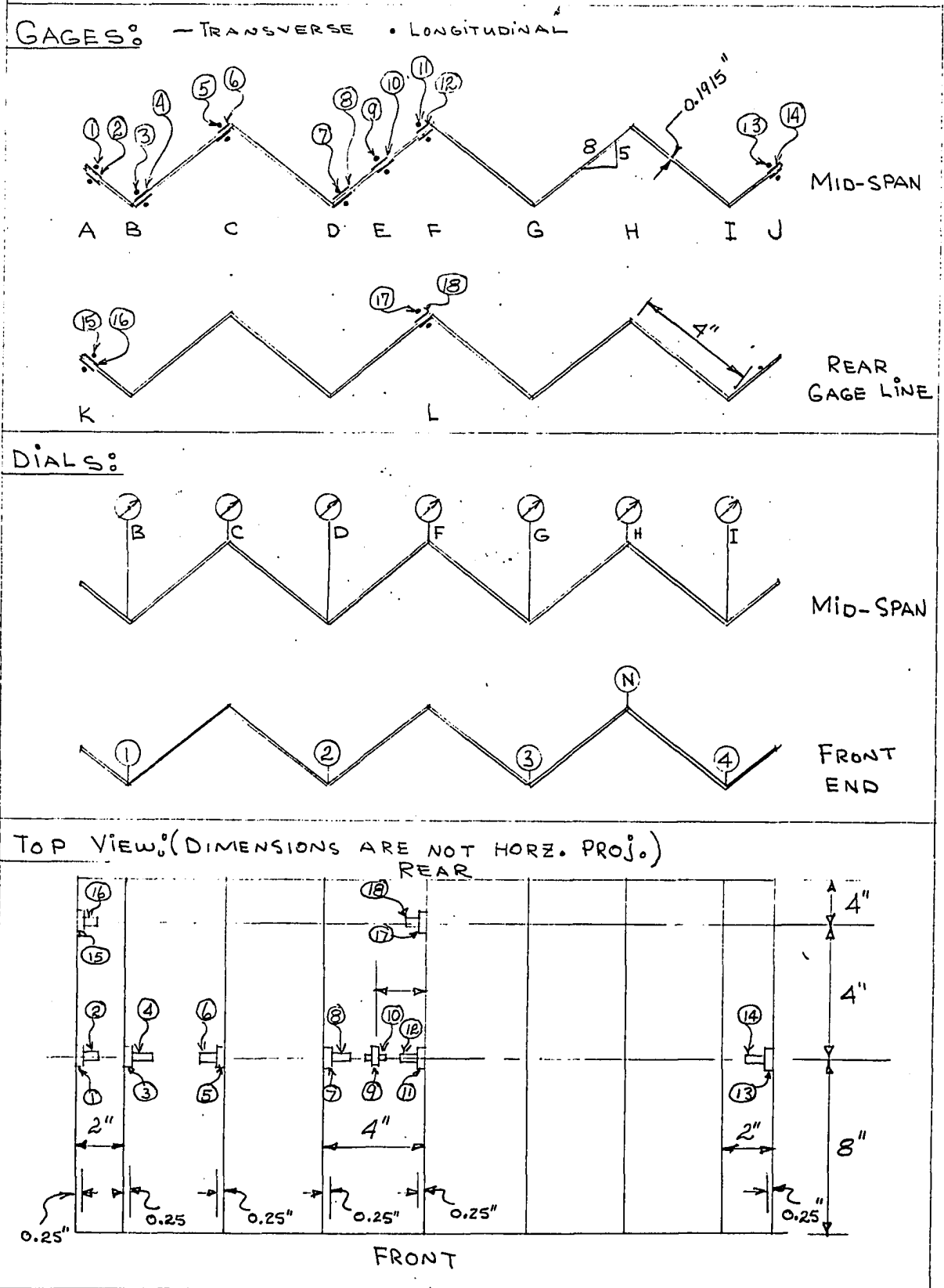


FIG. 11 GAGE AND DIAL PLACEMENT (MODEL 4)

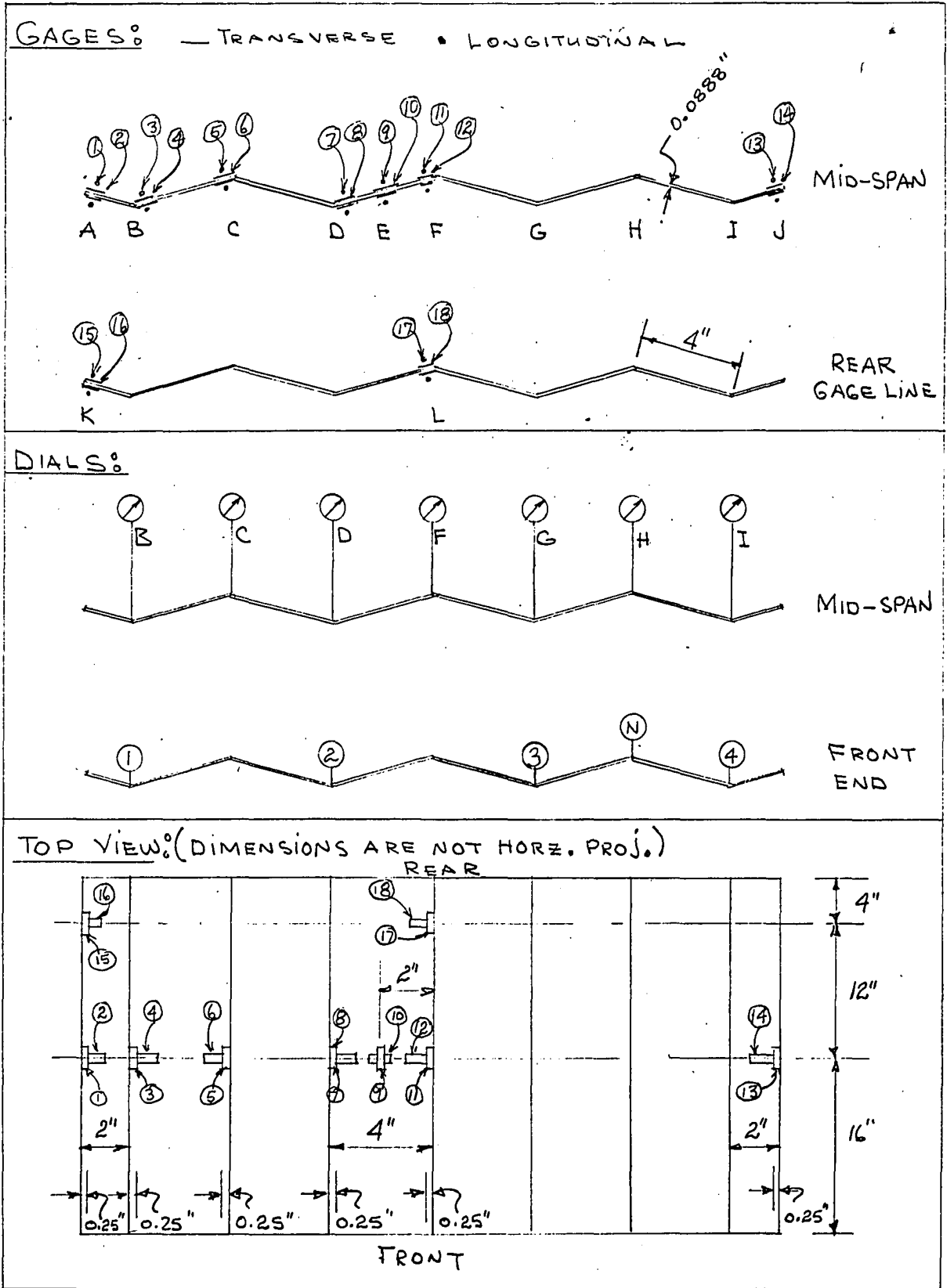


FIG. 12 GAGE AND DIAL PLACEMENT (MODEL 5)

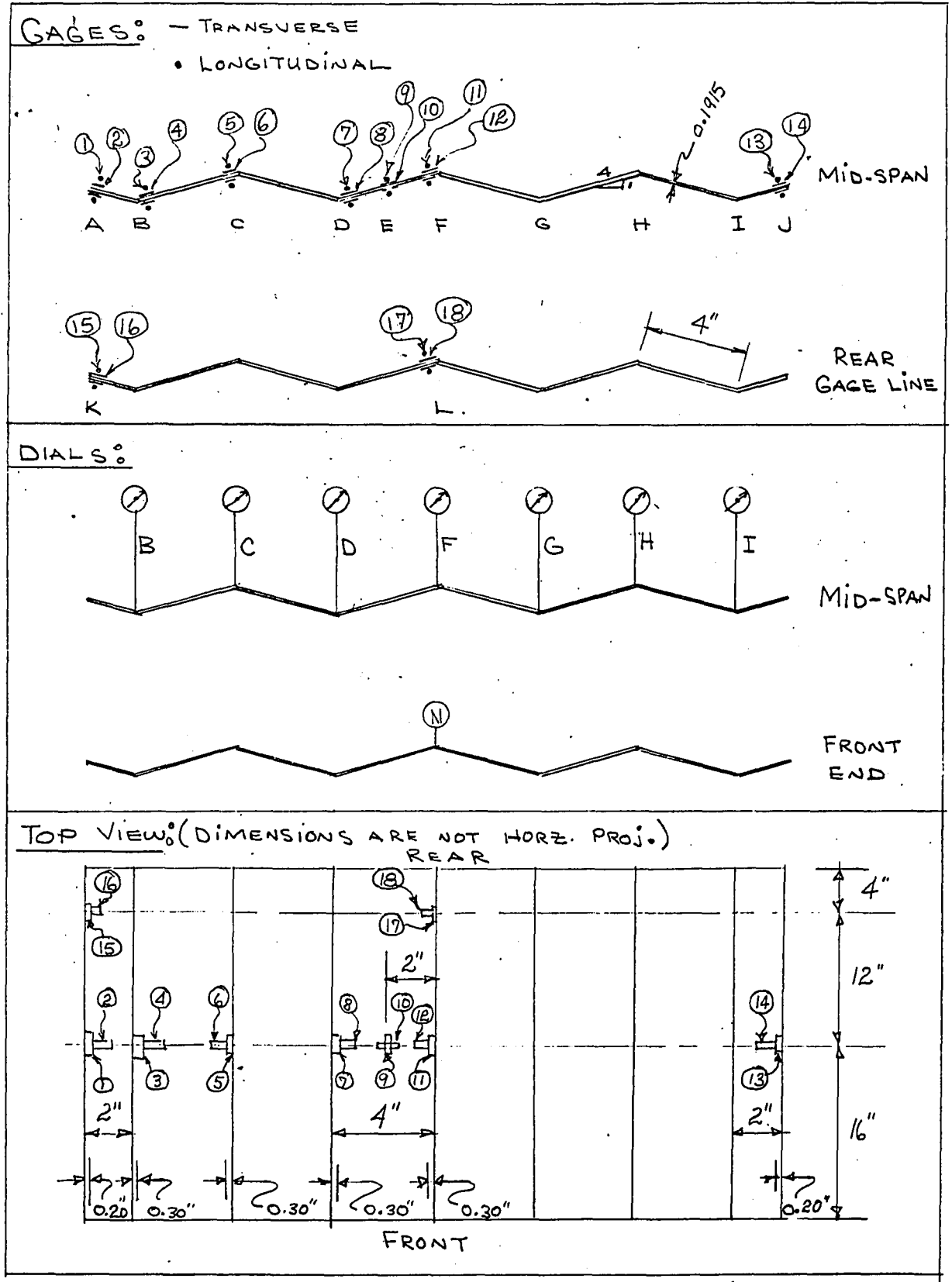


FIG. 13 GAGE AND DIAL PLACEMENT (MODEL 6)



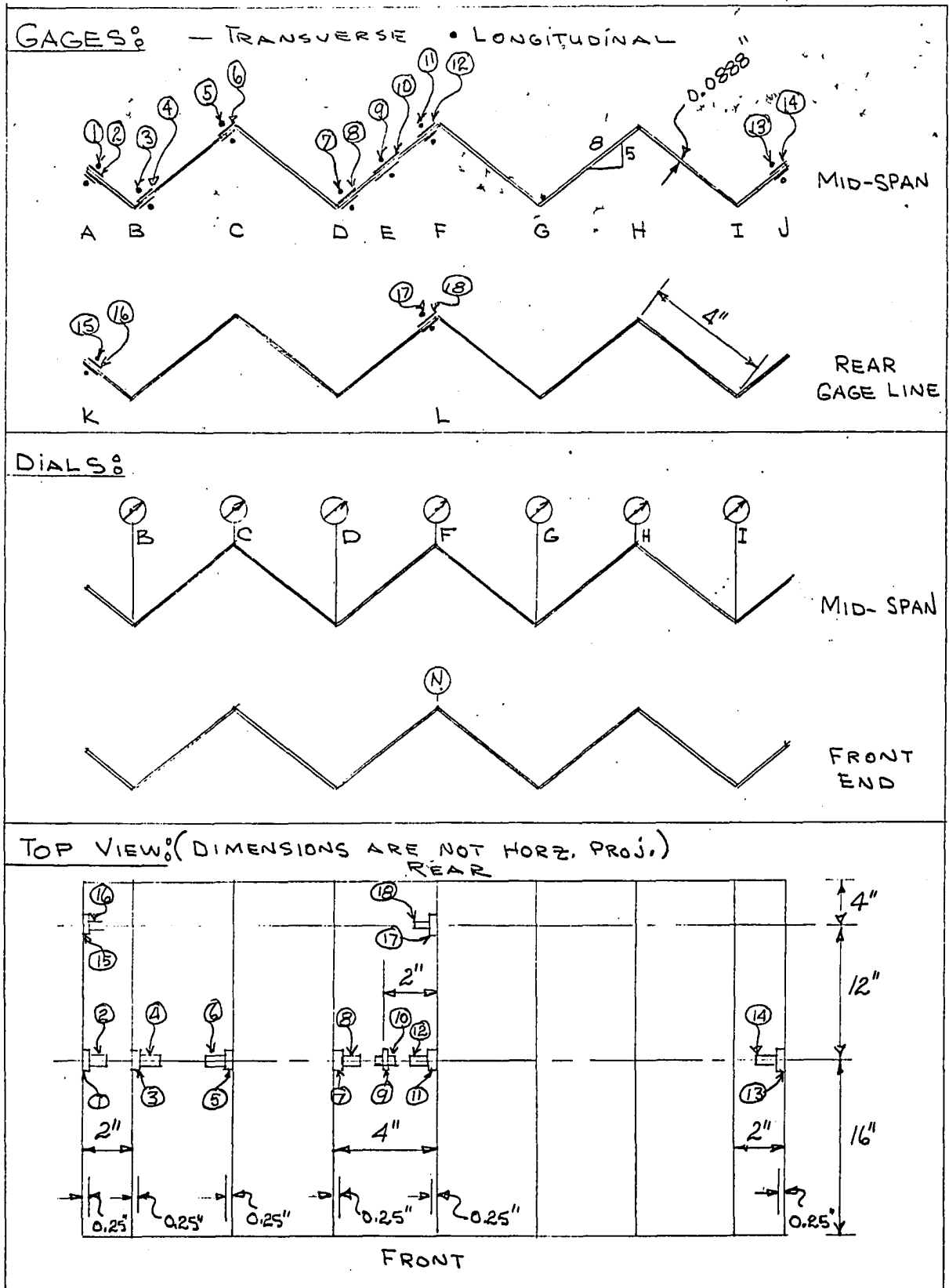


FIG. 14 GAGE AND DIAL PLACEMENT (MODEL 7)

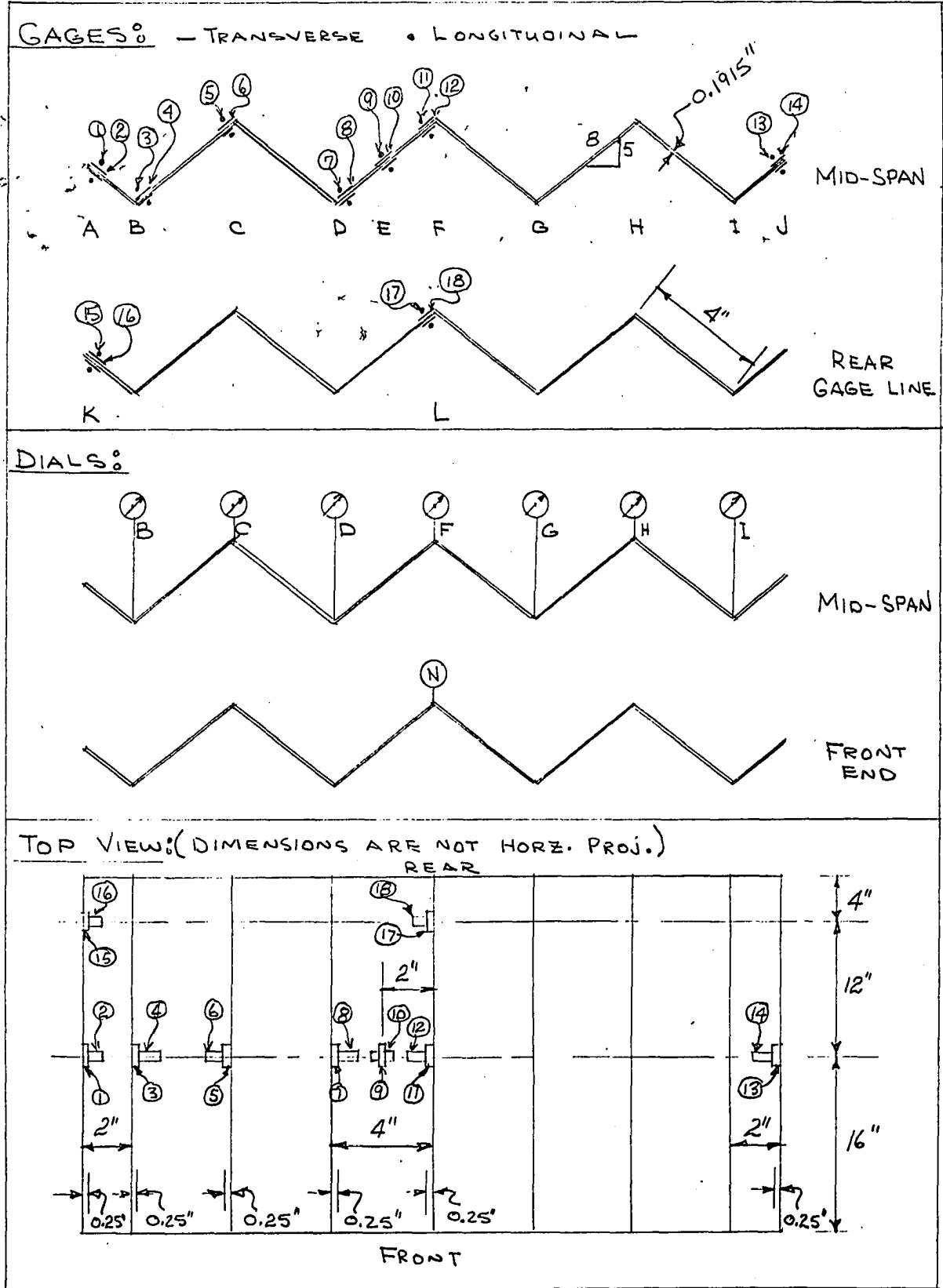


FIG.15 GAGE AND DIAL PLACEMENT (MODEL 8)

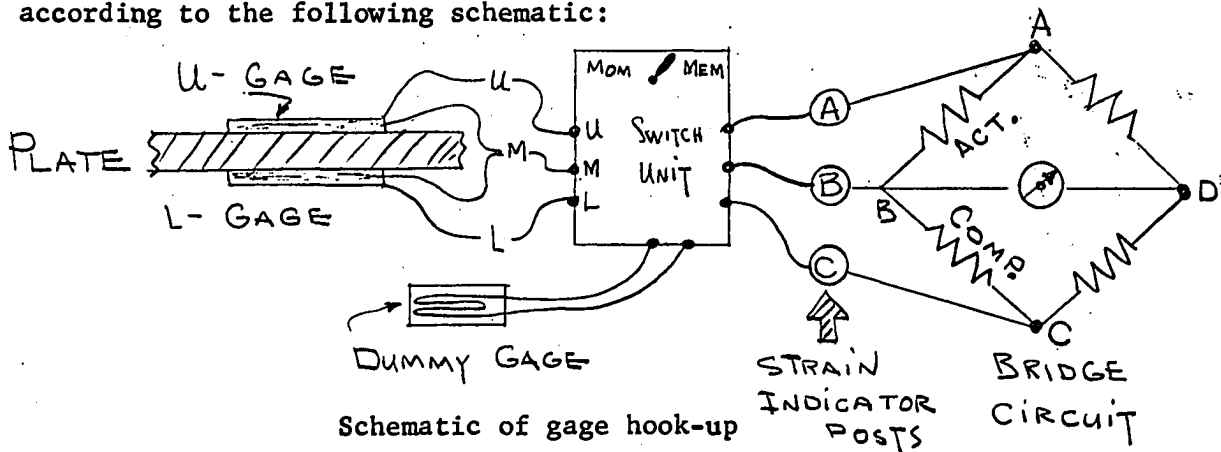
It follows that the membrane-stress equation

$$\sigma_x = \frac{E}{1-\mu^2} [\epsilon_x + \mu \epsilon_y] \quad \text{resolves itself into } \sigma_{x\text{ave}} = \frac{E}{1-\mu^2} [\epsilon_{x\text{ave}} + \mu \epsilon_{y\text{ave}}]$$

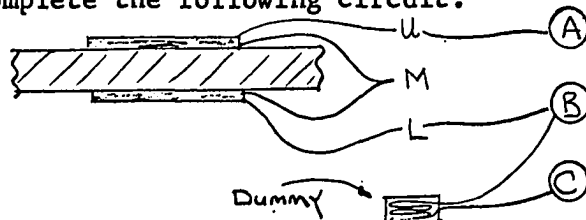
It also follows that the slab moment equation

$$m_y = D \left[ \frac{\partial^2 z}{\partial y^2} + \mu \frac{\partial^2 z}{\partial x^2} \right] \approx \frac{Et^3}{12(1-\mu^2)} \left[ \frac{\Delta \epsilon_y}{t} + \mu \frac{\Delta \epsilon_x}{t} \right]$$

The solution of these experimental equations for stresses and moments would have necessitated the employment of a multiplicity of arithmetic operations were it not for the switching unit that was conceived and designed expressly for this operation. This unit was designed to be used in conjunction with a regular SR-4 strain indicator, Fig. 16, and operates according to the following schematic:



For membrane readings the switch is flipped to membrane to automatically complete the following circuit:

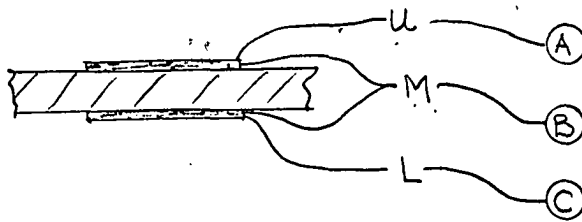


Schematic for membrane stress

Fig. 16. Switching Unit



For moment readings the switch is flipped to moment to automatically complete the following circuit:



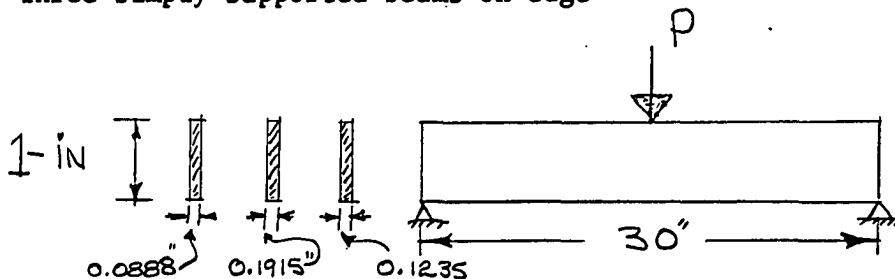
Schematic for moment reading

This technique reduces the strain readings to a form directly applicable to the membrane and moment equations and with several thousand readings to make any reduction in tedium is a labor economy.

#### D. Property Tests of Model Material (Aluminum 1100-H-14)

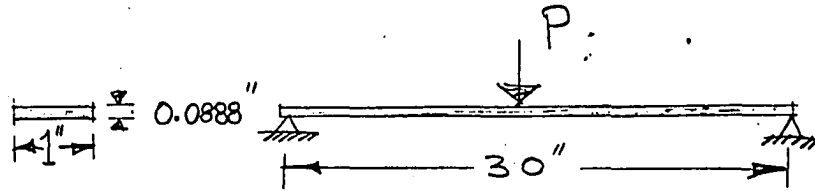
The experimental stresses and moments are accurate only to the degree of our knowledge of the material properties. The 2 obviously significant properties are  $E$  and  $\mu$ , as seen from inspection of the experimental equations. In order to discern these characteristics, the 3 following basic approaches were used on strips taken from the actual plates that were to later be formed into the test models:

- (1) Three simply supported beams on edge



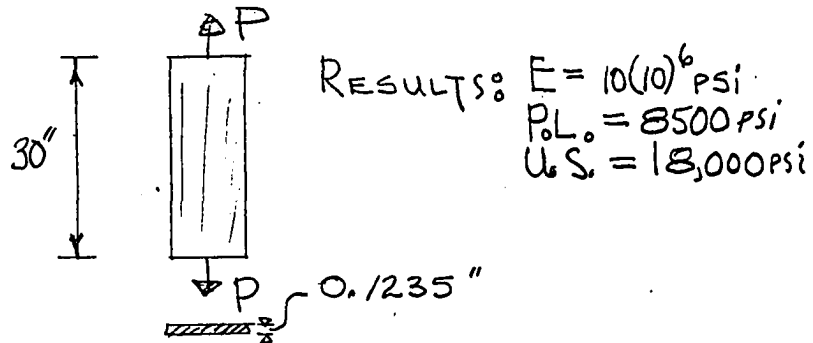
Result:  $E = 10(10)^6$  psi

- (2) One simply supported beam - flat



Result:  $E'$  was  $11.0(10)^6$  psi, which indicates that Poisson's Ratio is closer to 0.30 than 0.33 or possibly that the strip wasn't wide enough to develop complete plate behavior.

- (3) Two axial tension tests



When models are loaded into the plastic zone this knowledge of the proportional limit makes it possible to distinguish between non-linear relationships caused by material properties and those caused by secondary geometry effects.

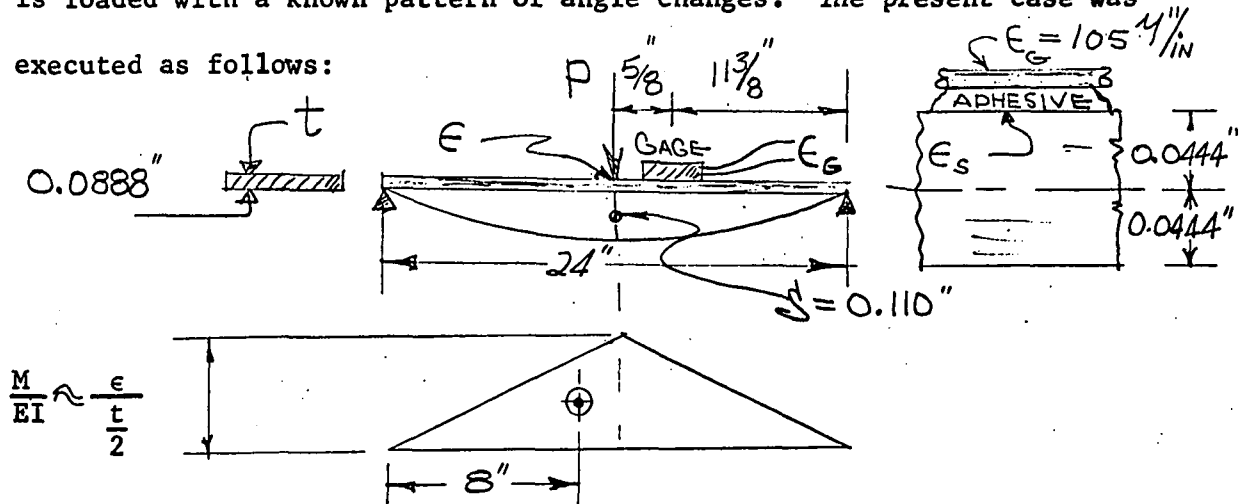
#### E. Effect of Gage and Adhesive Thickness

##### On Moment Determination

It was thought wise, in light of the rather thin plates, that a check be made to ascertain the relative importance of correcting for any error that might be introduced due to the gage wires not being on the surface, but at a distance from the surface equal to the thickness of the adhesive layer plus approximately  $\frac{1}{2}$  the gage thickness. The scheme for making this

check is based on the fact that deflections are just manifestations of strains. Consequently if we know the deflection, and the strain pattern, an expression can be derived in the form  $\epsilon = f(\delta)$ , which enables one to predict strain without using the modulus of elasticity.

The procedure was essentially the conjugate beam method whereby a beam is loaded with a known pattern of angle changes. The present case was executed as follows:



$$\delta = \left(\frac{L}{2}\right) \left(\frac{2\epsilon}{t}\right) \left(\frac{1}{2}\right) \left(\frac{2}{3}\right) \left(\frac{L}{2}\right) = \frac{\epsilon L^2}{6t} \Rightarrow \epsilon = \frac{6t\delta}{L^2}$$

$$\text{Then: } \epsilon_s = \left(\frac{11.375}{12}\right) \frac{(6)(0.0888)(0.110)}{(24)^2} = \underline{96.5(10)^{-6}} \text{ } \mu\text{"/in}$$

$$\text{But } \epsilon_G = 105 \mu\text{"/in} \quad \text{Error} = 8.8\%$$

The implication of these results is that the gage wires are probably located a distance from the surface equal to 8.8% of  $t/2$ , i.e.

$$\frac{8.8}{100} (0.044) = \underline{0.00392\text{'}}$$

a value very closely approximated by taking the micrometer thickness of the gage alone and adding  $1/1000\text{'}$  for adhesive thickness. Actually in



order to arrive at this adhesive thickness the gage was measured before attaching it to the member - the member thickness was measured before, and the combined thickness of gage plus member was measured after. It follows that the experimental stress formula must include an adjustment in the measured curvature, i.e.  $t'$  rather than  $t$  must be used for  $\frac{\partial^2 z}{\partial x^2} \approx \frac{\Delta \epsilon_x}{t'}$  and  $\frac{\partial^2 z}{\partial y^2} \approx \frac{\Delta \epsilon_y}{t'}$ . Obviously when the plate thickness increases, this correlation rapidly becomes insignificant but when the thickness is decreased the error can easily become 10% or 20% depending on the gage type and adhesive.

#### F. Testing Procedure

The actual testing procedure consisted of applying approximately 10 to 15 load increments with the jack and simultaneously recording the strain and deflection readings at all the designated locations. All of the models were loaded into the plastic zone, usually to the limit of the model's capacity or in the case of excessive deflections, to the limit of the allowable distortion in the whiffle tree mechanism.

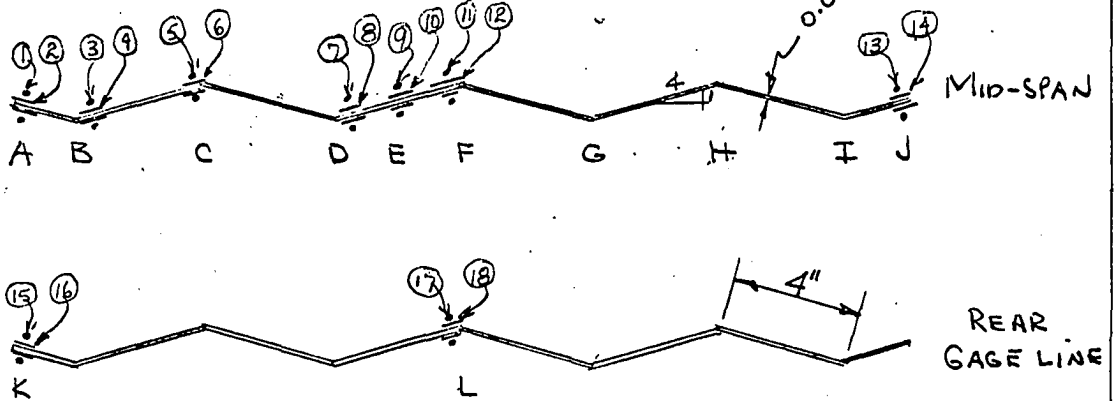
#### G. Typical Set of Model Data and Data Reduction

Insofar as model No. 5 exhibits some rather interesting behavioral patterns it has herein been chosen for sample presentation. The compiled results from this model and all of the remaining models are found in Table 3. (Page 108-115)

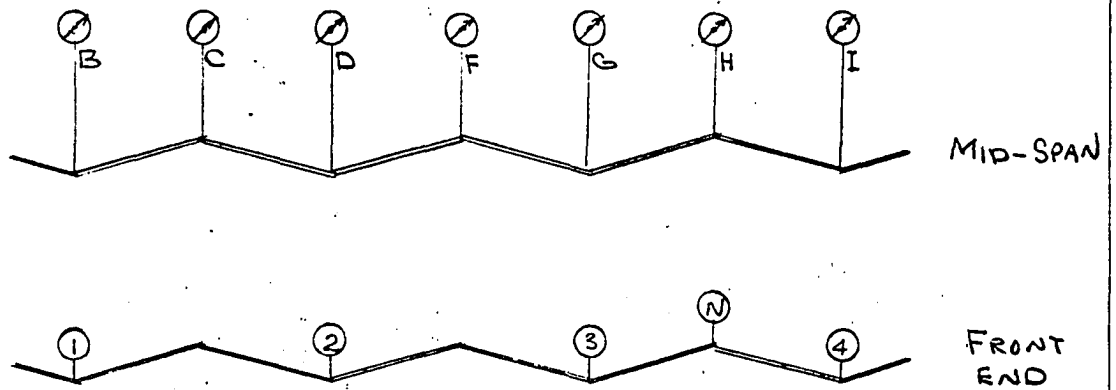
TYPICAL SET OF MODEL DATA AND REDUCTION

MODEL N<sup>o</sup> 5

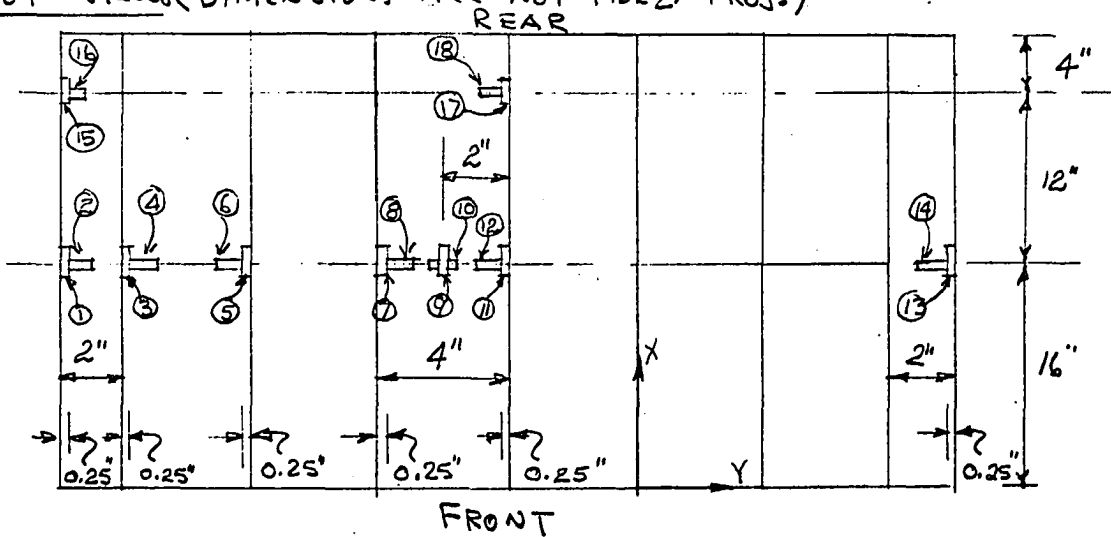
GAGES:




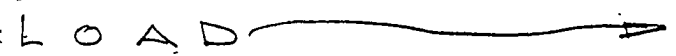
DIALS:

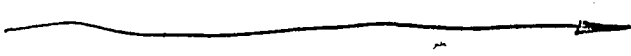


TOP VIEW: (DIMENSIONS ARE NOT HORIZ. PROJ.)

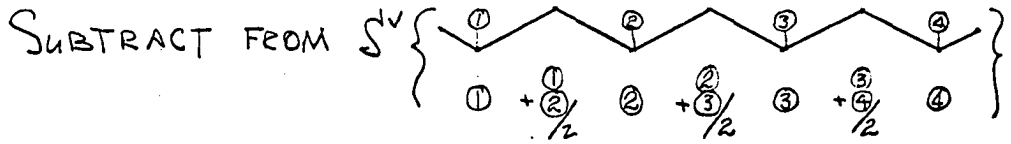


POSITION	GAGE NO	DIRECTION	STRAIN CHARACTER	LOAD 									
				ZERO READ	100	300	500	700	1000	1500	2000		0
A	1	X	MOM	12570	12550	12500	12455	12420	12355	12245	12120	10965	12300
			MEM	0	+20	+70	115	150	215	325	450	1605	270
	2	Y	MOM	10275	10290	10300	10315	10330	10350	10395	10450	10525	10370
			MEM	0	-5	-25	4	55	75	120	175	250	95
B	3	X	MOM	11355	11330	11300	11265	11240	11195	11120	11030	10915	11200
			MEM	0	+25	+55	90	115	160	235	325	440	155
	4	Y	MOM	7995	8096	8250	8400	8520	8725	9075	9530	10180	8780
			MEM	0	+95	+255	405	525	730	1080	1535	2185	785
C	5	X	MOM	11095	11140	11235	11320	11400	11550	11920	12470	12255	12285
			MEM	0	-45	-140	225	305	455	825	1375	1160	1190
	6	Y	MOM	10330	10360	10310	10265	10230	10170	10090	9860	9590	10020
			MEM	0	-20	-70	115	150	210	340	520	790	360
D	7	X	MOM	8690	8680	8650	8630	8610	8580	8520	8435	8280	8520
			MEM	0	+10	+40	60	80	110	170	255	410	170
	8	Y	MOM	7895	7805	7640	7485	7355	7150	6780	6270	5965	7110
			MEM	0	-90	-255	410	540	745	1115	1625	2430	785
D	7	X	MOM	9845	9930	10080	10220	10340	10490	10630	10880	11045	9940
			MEM	0	-85	-235	375	495	645	835	1035	1200	95
	8	Y	MOM	10930	10950	10995	11030	11065	11120	11220	11370	11610	11190
			MEM	0	+20	+65	100	135	190	290	440	680	260
D	7	X	MOM	11375	11360	11330	11300	11280	11245	11180	11100	10975	11270
			MEM	0	+15	+45	75	95	130	195	275	400	105
	8	Y	MOM	9185	9270	9430	9575	9695	9900	10270	10805	11790	10110
			MEM	0	+85	+245	390	510	715	1085	1620	2555	925
D	7	X	MOM	13470	13445	13400	13350	13310	13290	13230	13410	13500	13990
			MEM	0	+25	70	120	160	180	140	60	-30	-520
	8	Y	MOM	10340	10315	10270	10220	10180	10120	9980	9770	9360	9880
			MEM	0	-25	-70	120	160	220	360	570	980	460

POSITION	GAGE NO	DIRECTION	STRAIN CHARACTER	LOAD 											
				ZERO READ	100	300	500	700	1000	1500	2000		0		
M	9	X	MOM	8250	8240	8220	8200	8190	8165	8120	8045	7900	8160		
			MEM	0	+10	+30	50	60	85	130	215	350	150		
		MOM	8355	8360	8360	8365	8370	8375	8380	8380	8340	8330			
		MEM	0	+5	+5	10	15	20	25	25	-15	-25			
	10	Y	MOM	10945	10935	10920	10900	10890	10880	10860	10830	10650	10860		
			MEM	0	+10	+25	45	55	65	85	115	295	85		
N	11	X	MOM	11710	11695	11670	11650	11630	11600	11540	11455	11315	11580		
			MEM	0	+15	+40	60	80	110	170	255	395	130		
		MOM	7850	7765	7620	7475	7360	7165	6800	6230	5180	6870			
		MEM	0	-85	-230	375	440	685	1050	1620	2670	980			
	12	Y	MOM	11620	11665	11750	11825	11890	11990	12150	12390	12710	11830		
			MEM	0	-45	-130	205	270	370	530	770	1690	210		
O	13	X	MOM	9550	9520	9460	9410	9370	9310	9195	9075	8960	9240		
			MEM	0	+30	+90	140	180	240	355	475	590	310		
		MOM	9420	9340	9215	9120	9050	8950	8790	8700	8720	8960			
		MEM	0	-80	-205	300	370	470	630	726	700	460			
	14	Y	MOM	11670	11680	11700	11720	11730	11765	11825	11880	11940	11800		
			MEM	0	-10	-30	50	60	95	155	210	270	130		
R	15	X	MOM	9520	9515	9500	9490	9480	9470	9450	9430	9410	9510		
			MEM	0	+5	+20	30	40	50	70	90	110	10		
		MOM	9615	9590	9540	9495	9460	9380	9270	9160	9080	9510			
		MEM	0	-25	-75	120	155	235	345	455	535	105			
	16	Y	MOM	11440	11440	11450	11455	11460	11470	11485	11500	11520	11450		
			MEM	0	0	-10	15	20	30	45	60	80	10		
			MOM	10000	10010	10025	10035	10050	10070	10100	10130	10150	10035		
			MEM	0	+10	+25	35	50	70	100	130	150	35		

POSITION	GAGE NO	DIRECTION	STRAIN CHARACTER	LOAD 											
				ZERO READ	100	300	500	700	1000	1500	2000		0		
2	17	X	MOM	12085	12080	12070	12065	12055	12045	12030	12010	11980	12080		
			MEM	0	+5	+15	20	30	40	55	75	105	5		
	18	Y	MOM	11650	11070	11110	11150	11185	11220	11245	11265	11250	10900		
			MEM	0	-20	-60	100	135	170	195	215	200	+150		
DIAL B				355	385	438	487	527	596	715	860	826	342		
				0	30	83	132	172	241	360	505	697	213		
" C				192	214	253	289	319	370	466	592	786	385		
				0	22	61	97	127	178	274	400	594	193		
" D				268	290	329	366	397	447	537	658	857	440		
				0	22	61	98	129	179	269	390	589	172		
" F				519	540	578	614	643	691	779	896	989	485		
				0	21	59	95	124	172	260	377	589	180		
" G				289	313	353	390	421	473	566	691	963	475		
				0	24	64	101	132	184	277	402	614	186		
" H				559	583	625	662	694	748	849	986	1604	579		
				0	24	66	103	135	189	290	421	631	206		
" I				239	276	338	394	440	515	645	793	765	256		
				0	37	99	155	201	276	406	554	749	240		
" N				0	1	1	2	2	4 1/2	15	28	45	25		
				0	1	1	1	1	1 1/2	1 1/2	1 1/2	1	1		
" 2				0	1	2	2 1/2	2 3/4	3	3 1/2	3	2 1/2	1 (40)		
				0	1	2 1/2	3 1/2	4	4 1/2	5 1/2	6	5 1/2	1 1/2 (40)		
" 4				0	1/2	1 1/2	2	2 1/2	3	3	2	2	1/2		
				12870	12940	13065	13190	13290	13455	13710	14000	14280	12860		
LOAD CELL			MOM	0	70	195	320	420	585	840	1130	1410			
				0	111	310	510	668	930	1336	1800	2280	0		

CORRECTION TECHNIQUE :



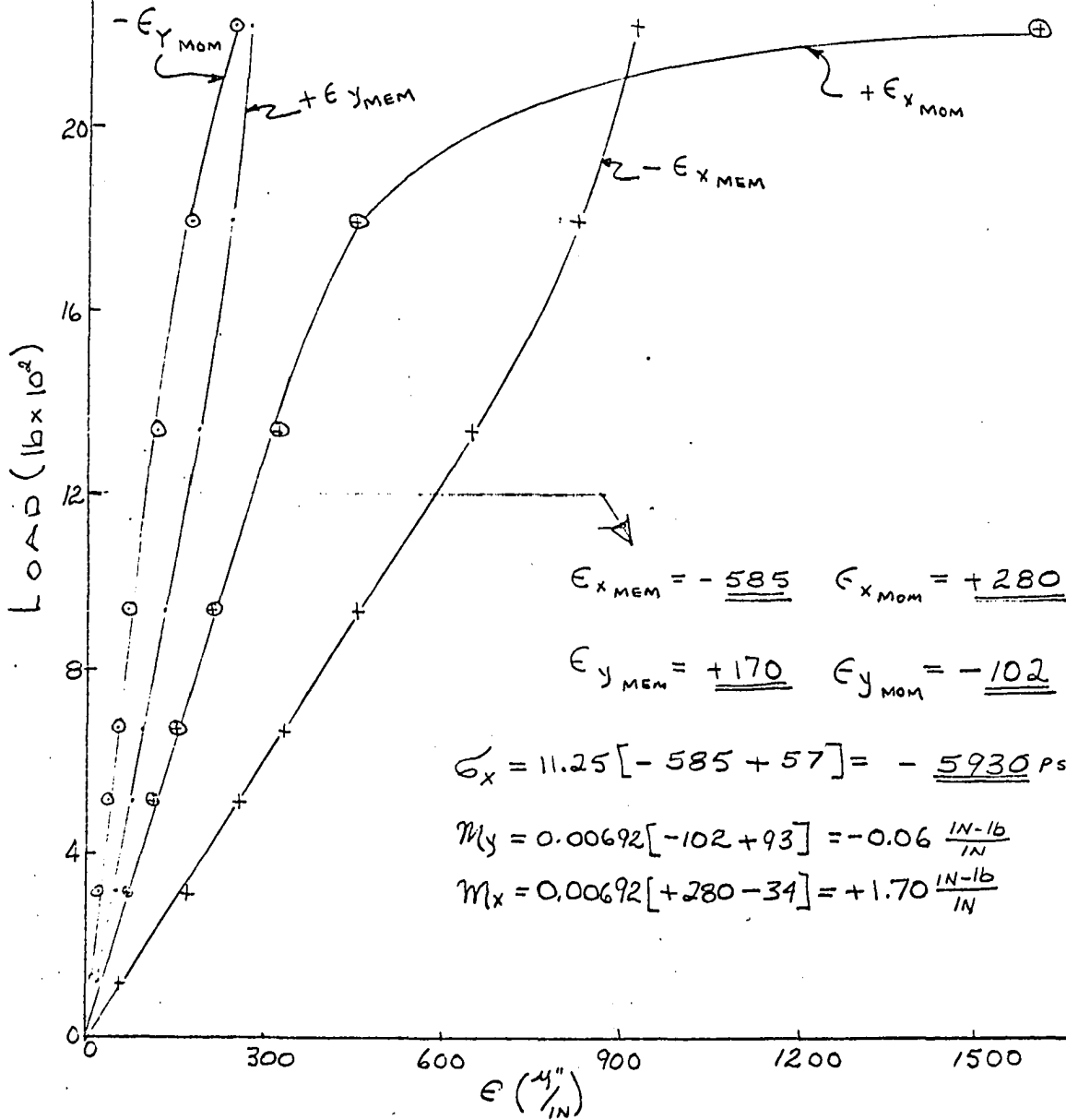
CORRECTED  $\sum V$  - VALUE

B	0	29	82	131	171	239	358	503	696
C	0	21	59½	95½	125	176	271½	398	592
D	0	21	59	95½	126	176	265½	387	586½
F	0	20	57	92	120½	168	255½	372½	580
G	0	23	61½	97½	128	179½	271½	396	608½
H	0	23	64	100½	132	185	286	417	627
I	0	36½	97½	153	193½	273	403	552	747
TRUE LOAD	0	111	310	668	936	1336	1800	2240	0 lbs

MODEL No 5

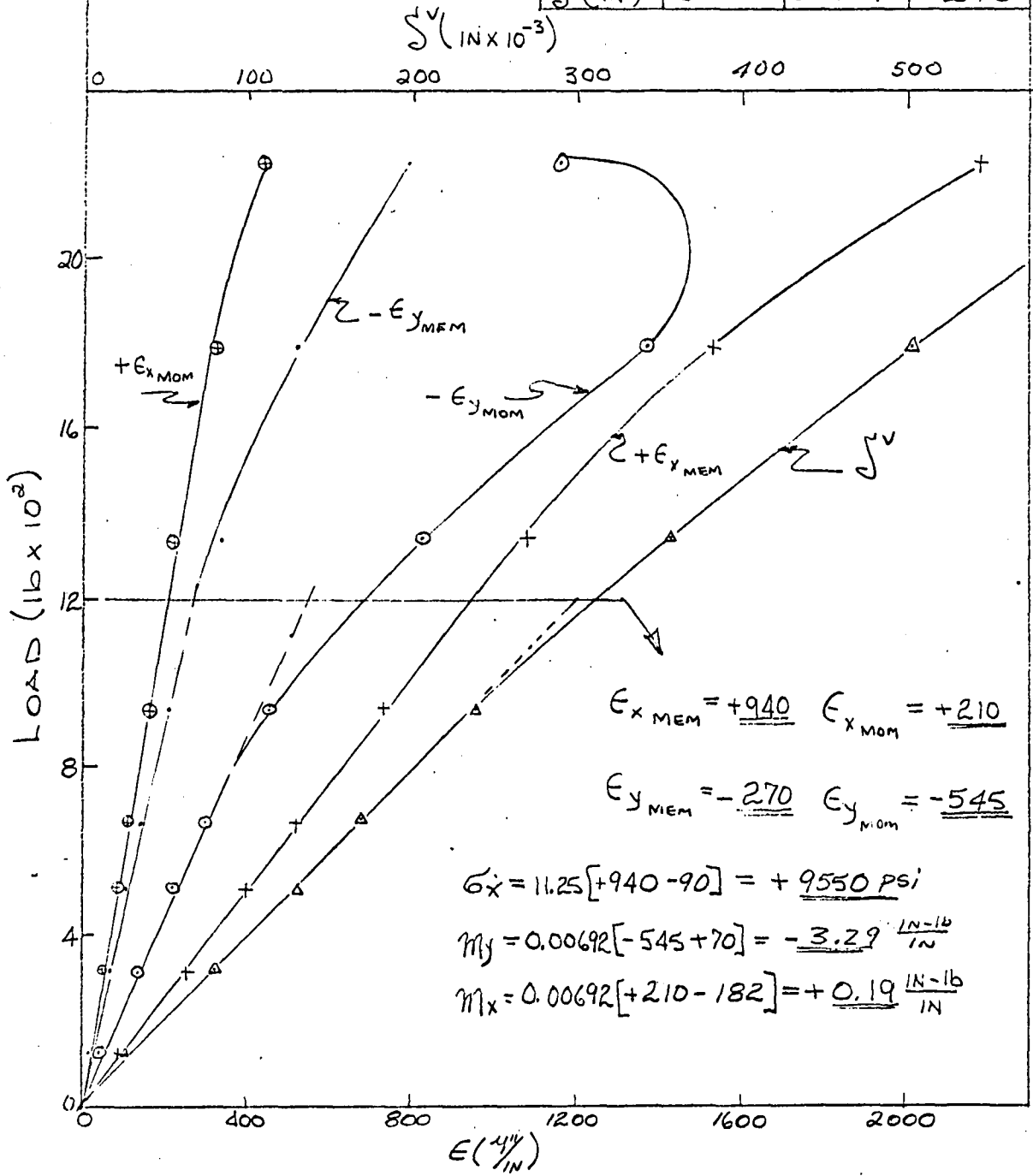
LOCATION A

	EXPR.	THEO.	BEAM
$\sigma_x$ (P's I)	-5,930.	-11,120	+626
$M_y$ ( $\frac{IN-lb}{IN}$ )	0	—	—
$M_x$ ( $\frac{IN-lb}{IN}$ )	+1.70	—	—
$S_y$ (IN)	—	—	—



MODEL NO 5  
LOCATION B

	EXPR.	THEO.	BEAM
$\sigma_x$ (Psi)	+9,550	+12,500	+9,360
$M_y$ ( $\frac{IN-lb}{IN}$ )	-3.29	-2.57	—
$M_x$ ( $\frac{IN-lb}{IN}$ )	+0.19	---	—
$\delta^v$ (IN)	0.300	0.457	0.248

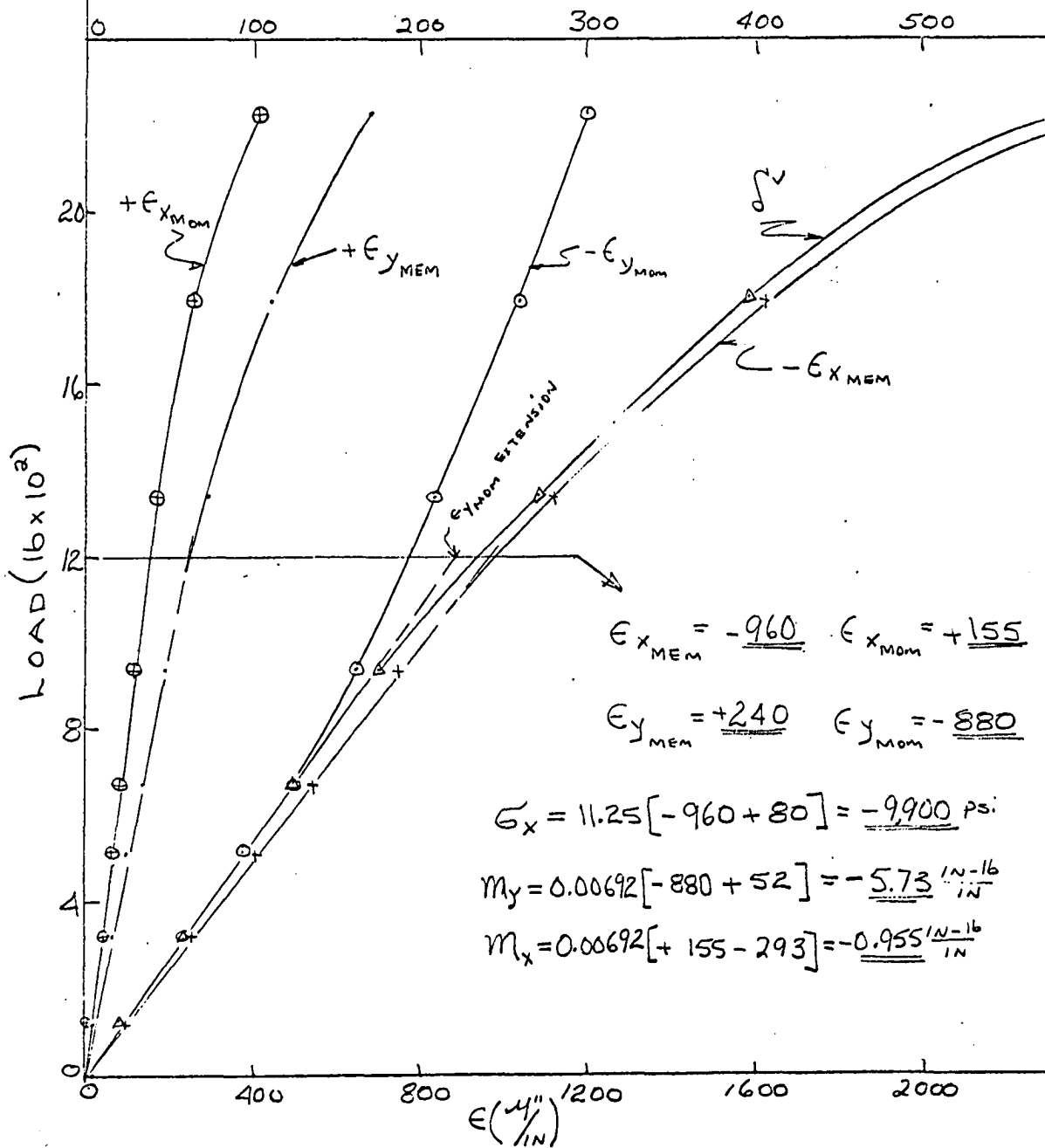




MODEL NO 5  
LOCATION C

	EXPR.	THEO.	BEAM
$\epsilon_x$ (PSI)	-9,900	-11,470	-11,000
$M_y$ ( $\frac{IN-16}{IN}$ )	-5.73	-10.56	—
$M_x$ ( $\frac{IN-16}{IN}$ )	-0.96	—	—
$\delta^y$ (IN)	0.221	0.278	0.248

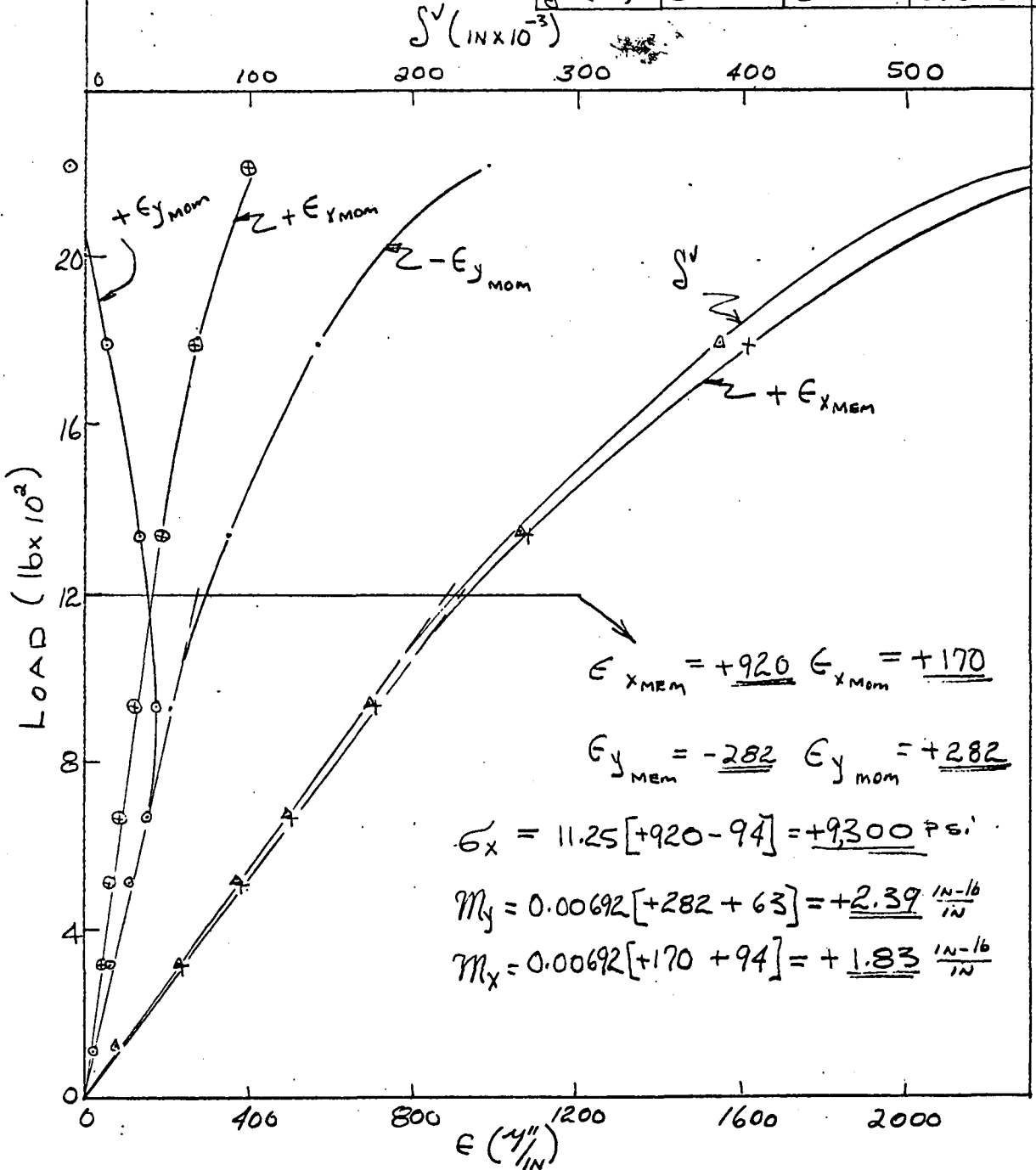
$\delta^y$  ( $IN \times 10^3$ )



MODEL NO 5

LOCATION D

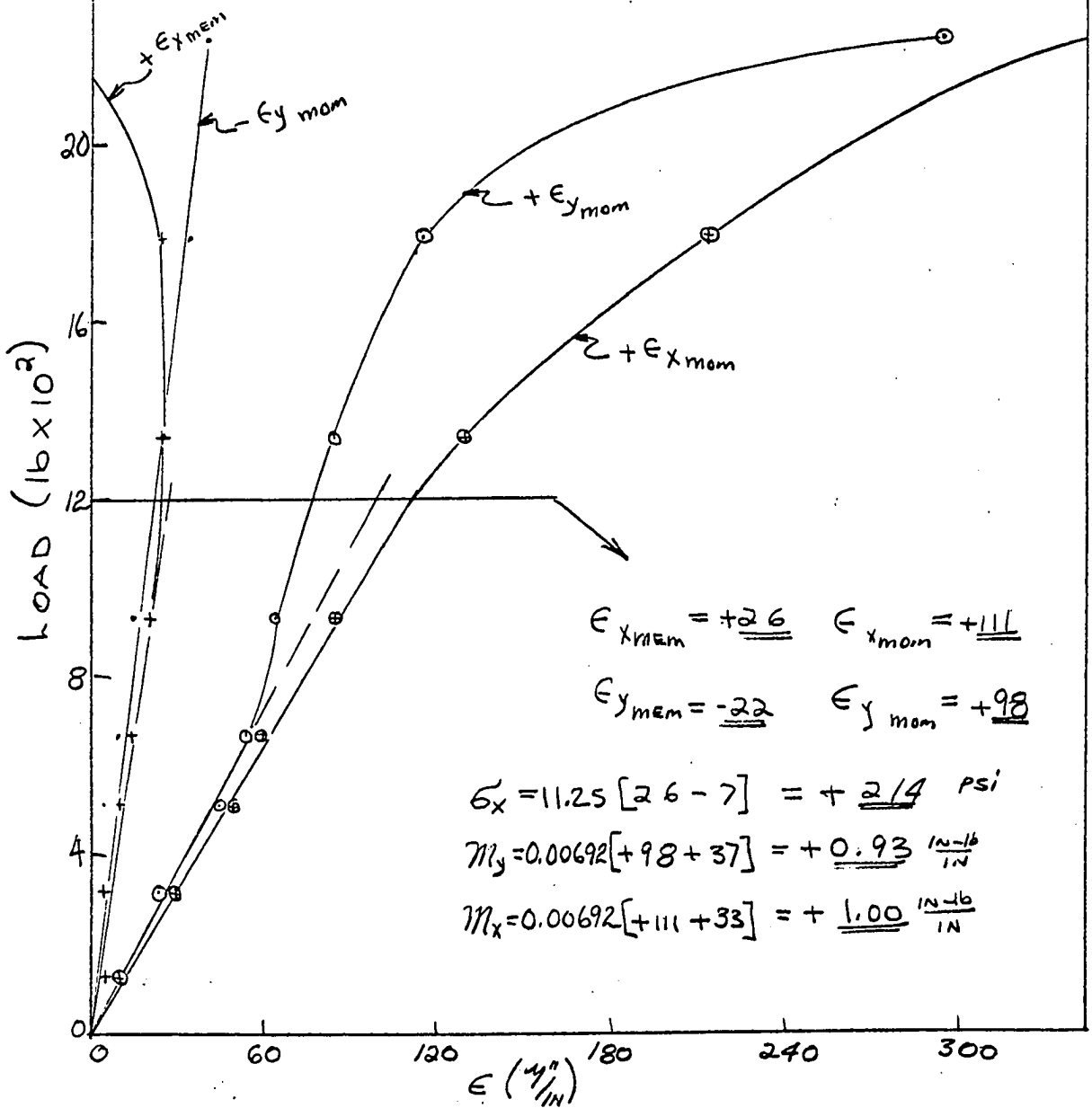
	EXPR.	THEO.	BEAM
$\sigma_x$ (Psi)	+9,300	+10,200	+9,360
$M_y$ ( $\frac{IN-lb}{IN}$ )	+2.39	+0.848	—
$M_x$ ( $\frac{IN-lb}{IN}$ )	+1.83	—	—
$\int v$ (IN)	0.221	0.252	0.248



MODEL No 5

LOCATION E

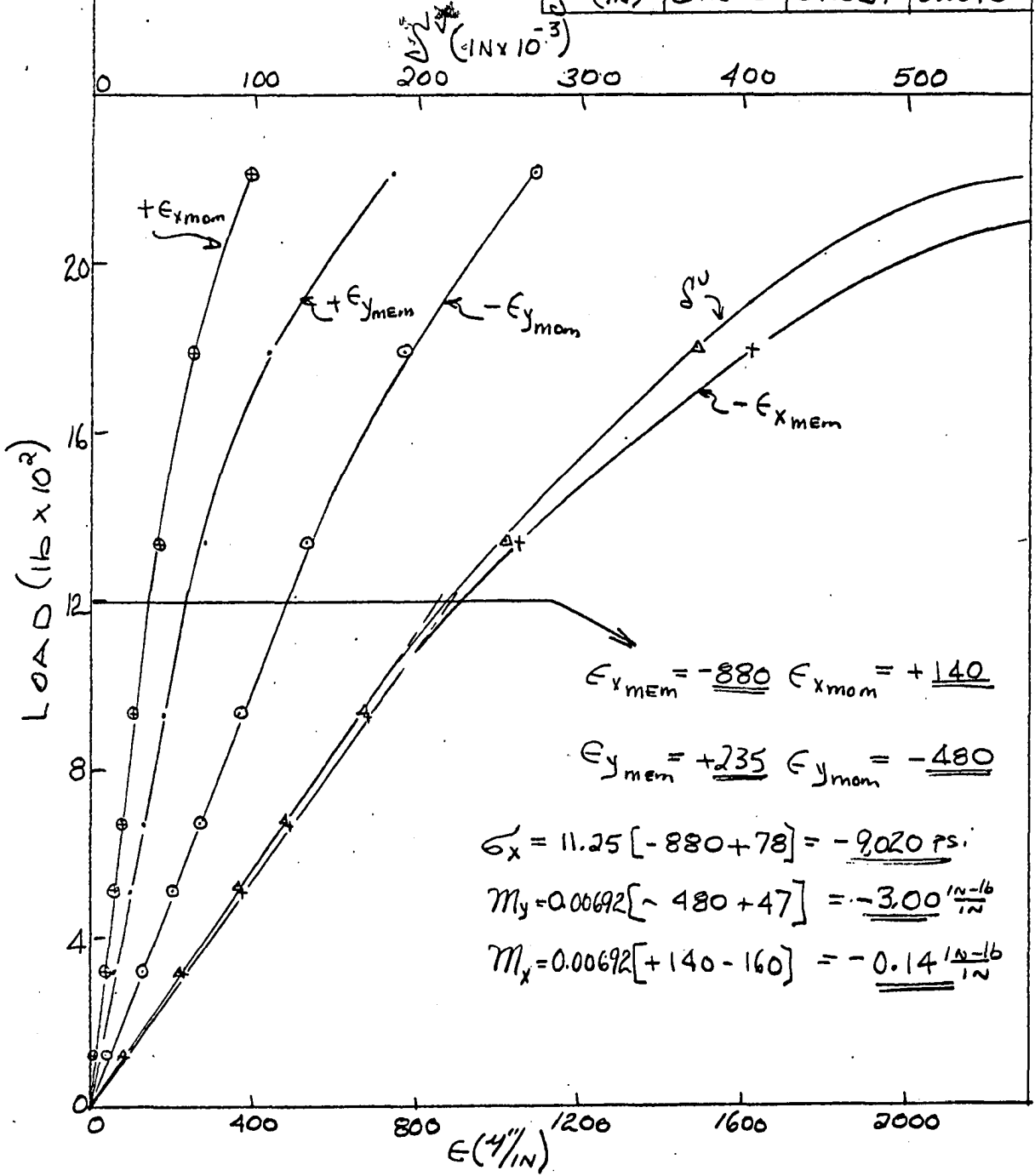
	EXPR.	THEO.	BEAM
$\epsilon_x$ (Psi)	+214	+418	-832
$M_y$ ( $\frac{IN-lb}{IN}$ )	+0.93	+0.65	—
$M_x$ ( $\frac{IN-lb}{IN}$ )	1.00	—	—
$\delta^u$ (IN)	—	—	—



MODEL No 5

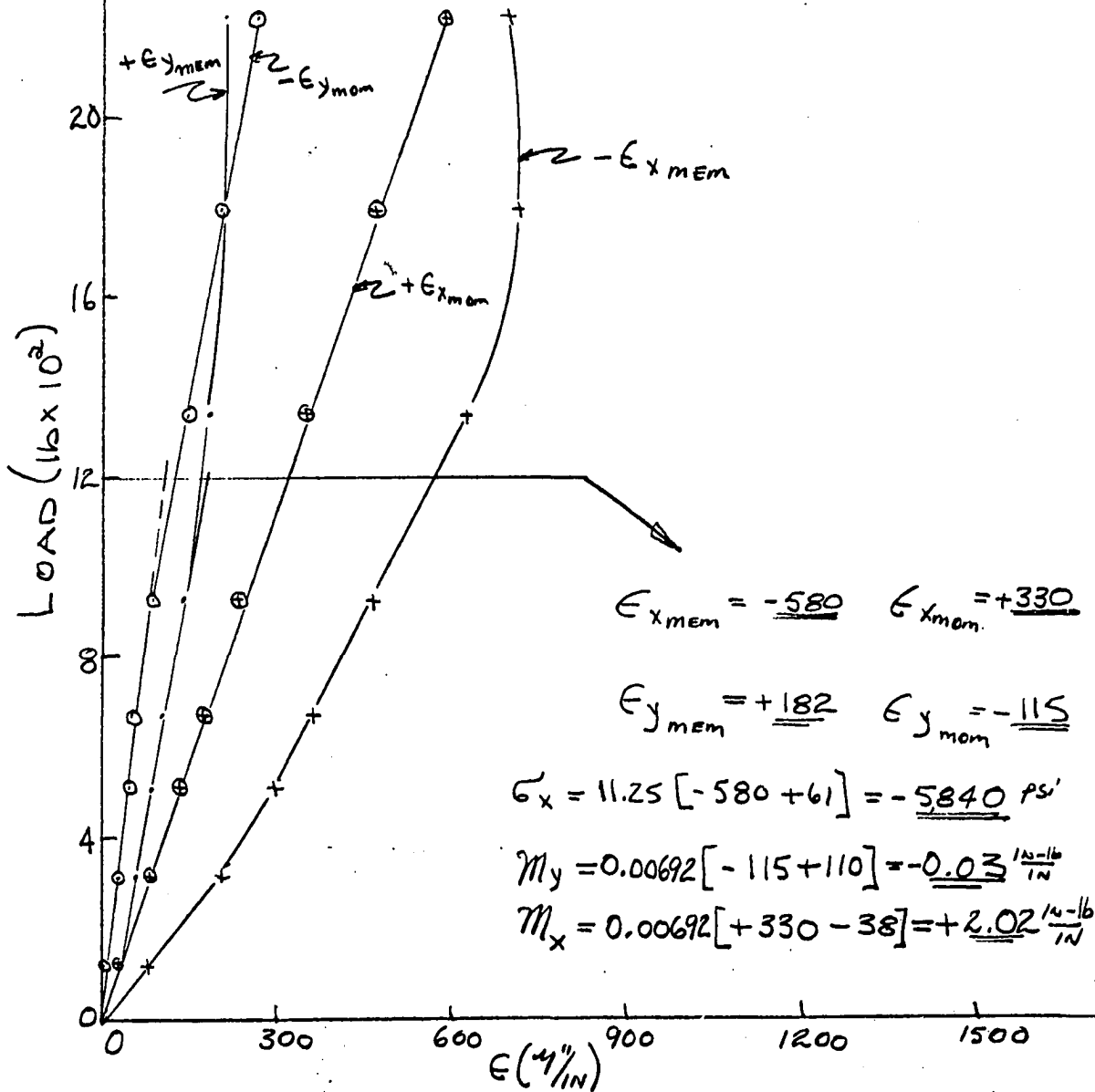
LOCATION F

	EXPR.	THEO.	BEAM
$\sigma_x$ (Psi)	-9020	-9330	-11,000
$M_y$ ( $\frac{IN-lb}{IN}$ )	-3.00	-3.56	—
$M_x$ ( $\frac{IN-lb}{IN}$ )	-0.14	—	—
$\int v$ (IN)	0.215	0.239	0.248



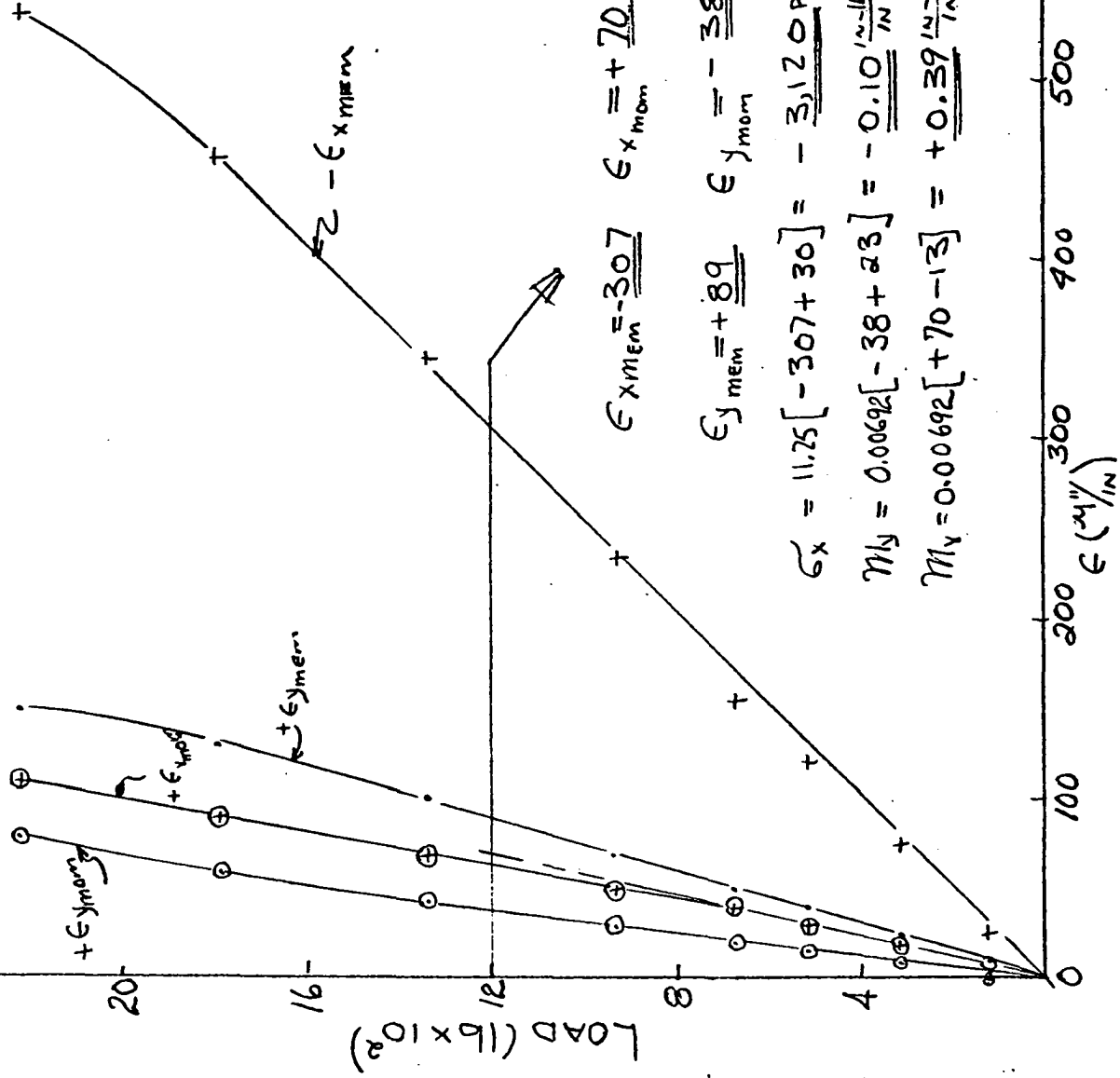
MODEL N<sup>o</sup> 5LOCATION J

	EXPR.	THEO.	BEAM
$\epsilon_x$ (psi)	-5840	-11,120	+626
$M_y$ ( $\frac{IN-lb}{IN}$ )	0	—	—
$M_x$ ( $\frac{IN-lb}{IN}$ )	+2.02	—	—
$\int v$ (IN)	—	—	—



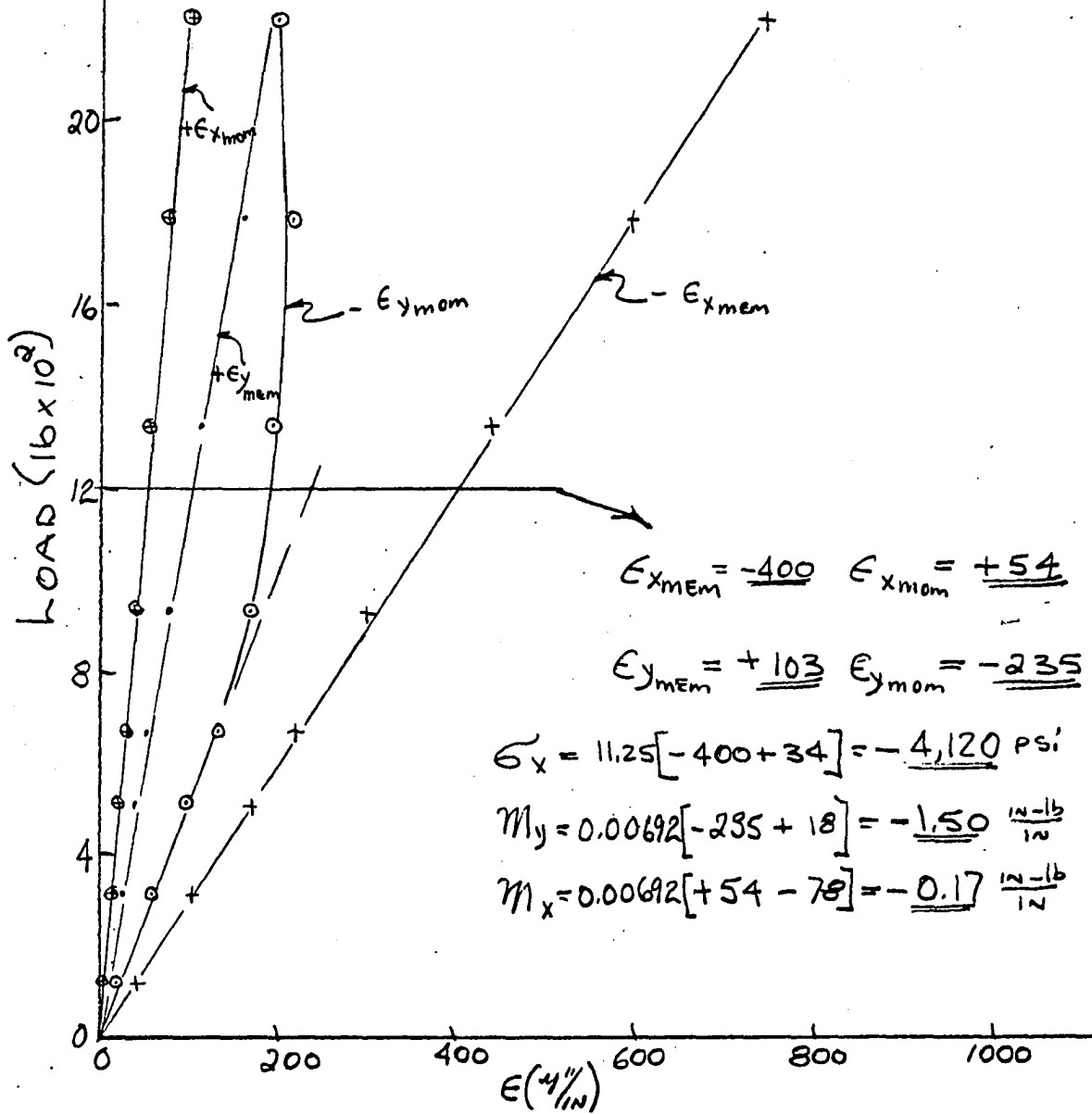
MODEL NO 5  
LOCATION K

	EXPR.	THEO.	BEAM
$\bar{G}_x$ (PSI)	-3,120	-5,100	+274
$M_y$ ( $\frac{IN^2}{IN}$ )	-0.10	-	-
$M_x$ ( $\frac{IN^2}{IN}$ )	+0.39	-	-
$g_y$ (IN)	-	-	-



MODEL NO 5  
LOCATION L

	EXPR.	THEO.	BEAM
$\sigma_x$ (PSI)	-4,120	-4,150	-4,810
$M_y$ ( $\frac{IN-lb}{IN}$ )	-1.50	-2.04	—
$M_x$ ( $\frac{IN-lb}{IN}$ )	-0.17	—	—
$\delta_y$ (IN)	—	—	—



MODEL N<sup>o</sup>5

LOCATION G, H, I

	EXPR.	THEO.	BEAM.
$\sum G^V$ (IN)	0.228	0.252	0.248
$\sum H^V$ (IN)	0.239	0.278	0.248
$\sum I^V$ (IN)	0.342	0.457	0.248

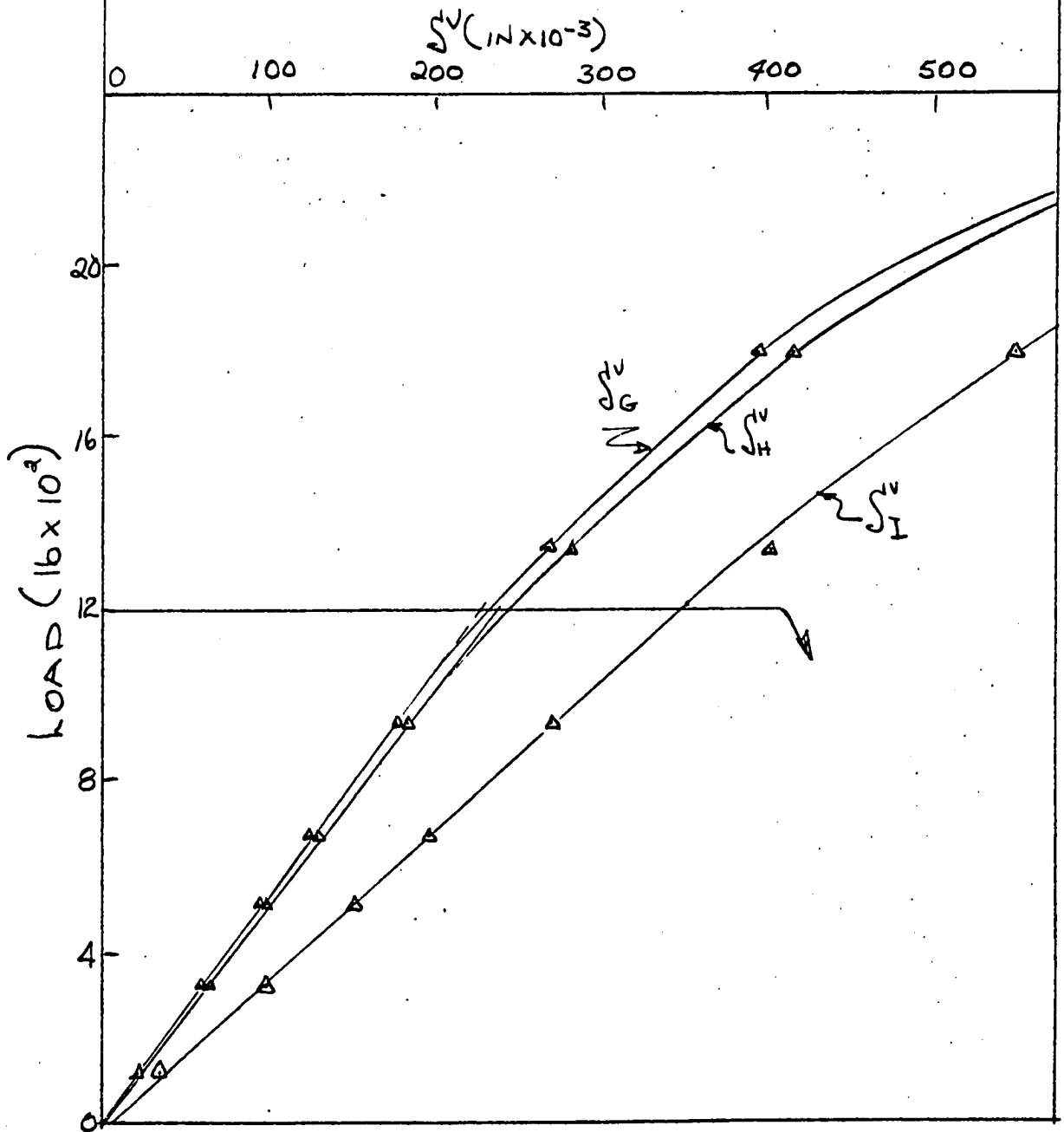




Table 3 Compilation of experimental and theoretical results

Model No. 1 1,200 lb		A	B	C	D	E	F
Expr.		-5,540	+5,430	-4,590	+4,920	-34	-5,150
Theor.	( $\sigma_x$ )	-7,550	+6,780	-5,440	+5,174	+42	-5,080
Beam		+313	+4,680	-5,500	+4,680	-416	-5,500
%E		+36	+25	+19	+5	XX	-1
Expr.		-0.24	-4.59	-1.84	-1.56	+1.34	-1.85
Theor.	( $m_y$ )	. . .	-3.96	-3.62	-2.03	+1.75	-2.41
%E		. . .	-14	+97	+30	+30	+30
Expr.	( $m_x$ )	-0.08	-0.84	-0.33	-0.06	+0.51	-0.19
Expr.		. . .	0.046	0.032	0.031	. . .	0.036
Theor.	( $\delta^v$ )	. . .	0.065	0.035	0.032	. . .	0.031
Beam		. . .	0.031	0.031	0.031	. . .	0.031
%E		. . .	+41	+9	+3	. . .	-14

Model No. 2  
4,000 lb

Expr.		-8,000	+7,760	-7,020	+7,370	+191	-7,080
Theor.	( $\sigma_x$ )	-10,700	+10,220	-8,550	+7,950	+150	-7,650
Beam		+464	+7,020	-8,260	+7,020	-623	-8,260
%E		+34	+32	+22	+8	-22	+8
Expr.		+0.33	-14.60	-15.85	+3.68	+9.38	-5.58
Theor.	( $m_y$ )	. . .	-14.44	-30.30	-3.12	+6.08	-11.22
%E		. . .	-1	+91	XX	-35	+100
Expr.	( $m_x$ )	+14.38	+7.92	+2.74	+9.25	+10.34	+5.58
Expr.		. . .	0.068	0.042	0.041	. . .	0.043
Theor.	( $\delta^v$ )	. . .	0.096	0.053	0.049	. . .	0.048
Beam		. . .	0.047	0.047	0.047	. . .	0.047
%E		. . .	+41	+26	+20	. . .	+12

$\sigma_x$ (psi),  $m_y$  ( $\frac{\text{in-lb}}{\text{in}}$ ),  $m_x$  ( $\frac{\text{in-lb}}{\text{in}}$ ),  $\delta^v$ (in), Number under Model No. is load at which tabular values are evaluated.

All errors to nearest 1%

+ Error signifies that absolute value of Theor. > absolute value of Expr.

XX Indicates the data obtained was erratic

G	H	I	J	K	L
• • •	• • •	• • •	-6,000	-4,060	-3,700
• • •	• • •	• • •	-7,550	-5,660	-3,820
• • •	• • •	• • •	+313	+235	-4,120
• • •	• • •	• • •	+26	+40	+3
• • •	• • •	• • •	-0.84	-0.11	-1.67
• • •	• • •	• • •	• • •	• • •	-2.34
• • •	• • •	• • •	• • •	• • •	+40
• • •	• • •	• • •	-0.59	+0.28	-0.29
0.039	0.041	0.055	• • •	• • •	• • •
0.032	0.035	0.065	• • •	• • •	• • •
0.031	0.031	0.031	• • •	• • •	• • •
-18	-15	+18	• • •	• • •	• • •
• • •	• • •	• • •	-8,030	-5,660	-5,250
• • •	• • •	• • •	-10,700	-8,080	-5,760
• • •	• • •	• • •	+464	+348	-6,200
• • •	• • •	• • •	+33	+43	+10
• • •	• • •	• • •	+1.14	+0.57	-4.45
• • •	• • •	• • •	• • •	• • •	-10.08
• • •	• • •	• • •	• • •	• • •	+127
• • •	• • •	• • •	+17.60	+9.68	+4.45
0.045	0.046	0.078	• • •	• • •	• • •
0.049	0.053	0.096	• • •	• • •	• • •
0.047	0.047	0.047	• • •	• • •	• • •
+9	+15	+23	• • •	• • •	• • •

Table 3 Continued

Model No. 3 2000 lb		A	B	C	D	E	F
Expr.		-6,170	+5,325	-3,580	+3,470	+90	-3,330
Theor.		-5,150	+4,530	-3,580	+3,430	+20	-3,405
Beam	( $\sigma_x$ )	+334	+3,146	-3,710	+3,146	-279	-3,710
%E		-17	-15	0	-1	-78	+2
Expr.		-0.62	-9.20	-1.83	-2.64	+1.16	-2.08
Theor.		. . .	-5.18	-3.14	-3.06	+2.30	-3.01
%E	( $m_y$ )	. . .	-44	+72	+16	+98	+45
Expr.	( $m_x$ )	-1.87	-3.07	-0.70	-0.88	-0.27	-0.89
Expr.		. . .	0.023	0.011	0.012	. . .	0.011
Theor.		. . .	0.017	0.009	0.008	. . .	0.008
Beam	( $\delta v$ )	. . .	0.008	0.008	0.008	. . .	0.008
%E		. . .	-26	-18	-33	. . .	-27
<hr/>							
Model No. 4 12,000 lb							
Expr.		-14,300	+12,720	-10,180	+9,600	+382	-8,850
Theor.		-13,900	+12,500	-10,040	+9,550	+75	-9,400
Beam	( $\sigma_x$ )	+576	+8,675	-10,220	+8,675	-770	-10,220
%E		-3	-2	-1	-1	-83	+6
Expr.		-0.90	-34.80	-23.53	-9.85	+10.50	-13.80
Theor.		. . .	-31.90	-30.90	-15.92	+14.25	-19.62
%E	( $m_y$ )	. . .	-8	+31	+61	+36	+42
Expr.	( $m_x$ )	+3.57	-5.61	-5.61	-1.07	+2.60	-2.68
Expr.		. . .	0.054	0.033	0.028	. . .	0.024
Theor.		. . .	0.048	0.026	0.024	. . .	0.023
Beam	( $\delta v$ )	. . .	0.023	0.023	0.023	. . .	0.023
%E		. . .	-11	-21	-14	. . .	-4

G	H	I	J	K	L
. . .	. . .	. . .	-5,510	-4,370	-2,460
. . .	. . .	. . .	-5,150	-3,860	-2,555
. . .	. . .	. . .	+334	+250	-2,780
. . .	. . .	. . .	-6	-12	+4
. . .	. . .	. . .	-0.37	-0.42	-2.10
. . .	. . .	. . .	. . .	. . .	-2.99
. . .	. . .	. . .	. . .	. . .	+42
. . .	. . .	. . .	-1.11	-1.25	-0.85
0.011	0.012	0.019	. . .	. . .	. . .
0.008	0.009	0.017	. . .	. . .	. . .
0.008	0.008	0.008	. . .	. . .	. . .
-27	-25	-10	. . .	. . .	. . .
. . .	. . .	. . .	-14,250	-10,660	-6,910
. . .	. . .	. . .	-13,900	-10,400	-7,050
. . .	. . .	. . .	+576	+432	-7,660
. . .	. . .	. . .	-2	-2	+2
. . .	. . .	. . .	0	0	-14.03
. . .	. . .	. . .	. . .	. . .	-19.00
. . .	. . .	. . .	. . .	. . .	+35
. . .	. . .	. . .	0	0	-3.77
0.025	0.028	0.051	. . .	. . .	. . .
0.024	0.026	0.048	. . .	. . .	. . .
0.023	0.023	0.023	. . .	. . .	. . .
-4	-7	-6	. . .	. . .	. . .

Table 3 Continued

Model No. 5 1200 lb		A	B	C	D	E	F
Expr.		-5,930	+9,550	-9,900	+9,300	+214	-9,020
Theor.	$(\sigma_x)$	-11,120	+12,500	-11,470	+10,200	+418	-9,330
Beam		+626	+9,360	-11,000	+9,360	-832	-11,000
%E		+87	+31	+16	+10	+95	+3
Expr.		0	-3.29	-5.73	+2.39	+0.93	-3.00
Theor.	$(m_y)$	. . .	-2.57	-10.56	+0.85	+0.64	-3.56
%E		. . .	-22	+84	-64	-31	+19
Expr.	$(m_x)$	+1.70	+0.19	-0.96	+1.83	+1.00	-0.14
Expr.		. . .	0.300	0.221	0.221	. . .	0.215
Theor.	$(\delta^v)$	. . .	0.457	0.278	0.252	. . .	0.239
Beam		. . .	0.248	0.248	0.248	. . .	0.248
%E		. . .	+52	+26	+14	. . .	+11
<hr/>							
Model No. 6 2000 lb							
Expr.		-2,620	+6,230	-7,170	+6,520	+236	-6,460
Theor.	$(\sigma_x)$	-4,880	+8,340	-9,030	+7,560	+374	-6,810
Beam		+250	+6,800	-8,050	+6,800	-623	-8,050
%E		+87	+34	+26	+16	+58	+5
Expr.		. . .	-3.66	-18.80	+9.68	-0.17	-12.40
Theor.	$(m_y)$	. . .	-5.82	-36.20	+6.83	-3.87	-20.80
%E		. . .	+59	+93	-29	XX	+68
Expr.	$(m_x)$	+10.26	+8.60	+1.75	+11.45	+7.20	+3.13
Expr.		. . .	0.193	0.155	0.146	. . .	0.143
Theor.	$(\delta^v)$	. . .	0.286	0.213	0.194	. . .	0.181
Beam		. . .	0.186	0.186	0.186	. . .	0.186
%E		. . .	+48	+37	+33	. . .	+27

G	H	I	J	K	L
. . .	. . .	. . .	-5,840	-3,120	-4,120
. . .	. . .	. . .	-11,120	-5,100	-4,150
. . .	. . .	. . .	+626	+274	-4,810
. . .	. . .	. . .	+90	+63	+1
. . .	. . .	. . .	0	-0.10	-1.50
. . .	. . .	. . .	. . .	. . .	-2.04
. . .	. . .	. . .	. . .	. . .	+36
. . .	. . .	. . .	+2.02	+0.39	-0.17
0.228	0.239	0.342	. . .	. . .	. . .
0.252	0.278	0.457	. . .	. . .	. . .
0.248	0.248	0.248	. . .	. . .	. . .
+10	+16	+34	. . .	. . .	. . .
. . .	. . .	. . .	-2,860	-1,700	-3,250
. . .	. . .	. . .	-4,880	-2,580	-3,040
. . .	. . .	. . .	+250	+103	-3,530
. . .	. . .	. . .	+71	+52	-7
. . .	. . .	. . .	. . .	0	-3.96
. . .	. . .	. . .	. . .	. . .	-9.00
. . .	. . .	. . .	. . .	. . .	+127
. . .	. . .	. . .	+11.20	+4.99	+2.44
0.159	0.170	0.206	. . .	. . .	. . .
0.194	0.213	0.286	. . .	. . .	. . .
0.186	0.186	0.186	. . .	. . .	. . .
+22	+25	+39	. . .	. . .	. . .

Table 3 Continued

Model No. 7 2000 lb		A	B	C	D	E	F
Expr.		-8,020	+8,130	-7,000	+7,000	+75	-6,520
Theor.	( $\sigma_x$ )	-9,280	+8,780	-7,310	+6,860	+108	-6,640
Beam		+668	+6,292	-7,420	+6,292	-558	-7,420
%E		+16	+8	+4	-2	+44	+2
Expr.		-0.22	-3.38	-4.29	-0.37	+0.69	-1.82
Theor.	( $m_y$ )	. . .	-2.85	-5.42	-0.76	+1.24	-2.10
%E		. . .	-16	+26	+106	+80	+15
Expr.	( $m_x$ )	0	-0.76	-1.43	-0.09	0	-0.67
Expr.		. . .	0.120	0.075	0.073	. . .	0.071
Theor.	( $\delta v$ )	. . .	0.134	0.075	0.068	. . .	0.066
Beam		. . .	0.067	0.067	0.067	. . .	0.067
%E		. . .	+12	0	-7	. . .	-7
<hr/>							
Model No. 8 6000 lb							
Expr.		-9,980	+10,900	-9,850	+8,970	+372	-8,250
Theor.	( $\sigma_x$ )	-9,810	+11,440	-10,700	+9,450	+396	-8,650
Beam		+576	+8,675	-10,220	+8,675	-770	-10,220
%E		-2	+5	+9	+5	+6	+5
Expr.		+0.22	-8.75	-28.4	+3.74	-1.30	-16.15
Theor.	( $m_y$ )	. . .	-10.57	-46.00	+4.33	+2.28	-15.80
%E		. . .	+21	+62	+16	XX	-2
Expr.	( $m_x$ )	+6.00	+3.61	-6.78	+4.51	+2.10	-3.00
Expr.		. . .	0.155	0.108	0.094	. . .	0.085
Theor.	( $\delta v$ )	. . .	0.166	0.103	0.093	. . .	0.088
Beam		. . .	0.092	0.092	0.092	. . .	0.092
%E		. . .	+7	-5	-1	. . .	+4

G	H	I	J	K	L
...	...	...	-7,420	-2,980	-2,970
...	...	...	-9,280	-4,120	-2,910
...	...	...	+668	+292	-3,250
...	...	...	+25	+38	-2
...	...	...	-0.17	-0.22	-1.28
...	...	...	...	...	-1.71
...	...	...	...	...	+33
...	...	...	-0.06	-0.38	-0.43
0.075	0.077	0.117	...	...	...
0.068	0.075	0.134	...	...	...
0.067	0.067	0.067	...	...	...
-9	-3	+15	...	...	...
...	...	...		-4,530	-3,610
...	...	...	Faulty	-4,560	-3,880
...	...	...	Gage	+252	-4,480
...	...	...		+1	+7
...	...	...	...	...	-11.96
...	...	...	...	...	-8.75
...	...	...	...	...	-27
...	...	...	...	0	-3.10
0.088	0.104	0.157	...	...	...
0.093	0.103	0.166	...	...	...
0.092	0.092	0.092	...	...	...
+6	-1	+6	...	...	...



## VI. TEST RESULTS - INTERPRETATIONS AND OBSERVATIONS

A.  $\sigma_x$  - values

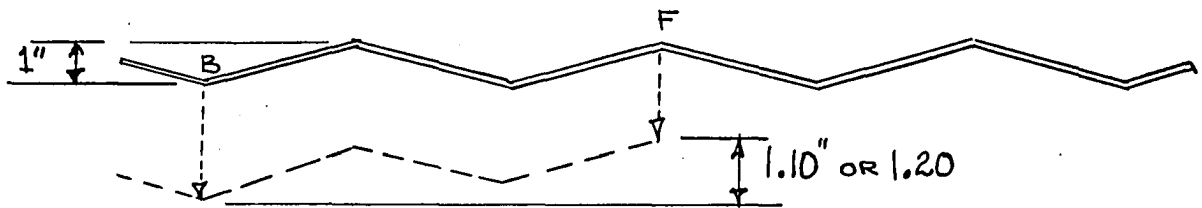
After a critical inspection of Table 3 it is seen that the theoretical correlation of the  $\sigma_x$ -values is in general, best for the steep-pitched configurations and worst for the shallow. The length and thickness have a less pronounced effect on the accuracy of stress prediction but still proved to be influential. The shorter model configurations tended to have better correlation than the longer ones and the thicker configurations tend to have better overall correlation than the thinner ones.

As was stated before, this model configuration in general has proved to be an extremely interesting one because of its extreme sensitivity to subtle parameter changes and secondary effects due to the changes in geometry caused by deflections. There even seems to be a hidden thrust type of interaction between the valley folds that doesn't show up in the theory because the theory presupposes all loads to be transferred to the end supports through the action of shear in the plane of the plates.

The deceiving aspect of this general configuration lies in the seemingly innocent form of repeated ridges and valleys with its anticipated simple behavior. First of all, in regards to shallow models the plate thickness is a significant % of the total model depth, whereas our theory assumes the model material to be concentrated on a working line represented by the mid-thickness of the plates. In essence we are saying, as in the case of models 1, 2, 5 and 6, that the model has a total depth of 1-in. when in reality the model is 1.0888-in. or 1.1915-in. in total depth. This fact helps to explain why, when we get away from the outside edge of the

model, the beam method is at times even closer to the experimental than the folded plate theory. This is because the beam method utilizes a moment of inertia that includes the entire model depth. However, the beam method is dangerous to use because of the gross errors in predicted stress at the boundaries.

Conceivably another deterrent to good correlation lies in the fact that in the shallow, long cases the difference between  $\delta_B^V$  and  $\delta_F^V$  can very easily create an increased effective depth of the overall configuration in the magnitude of 10 to 20 per cent, i.e.

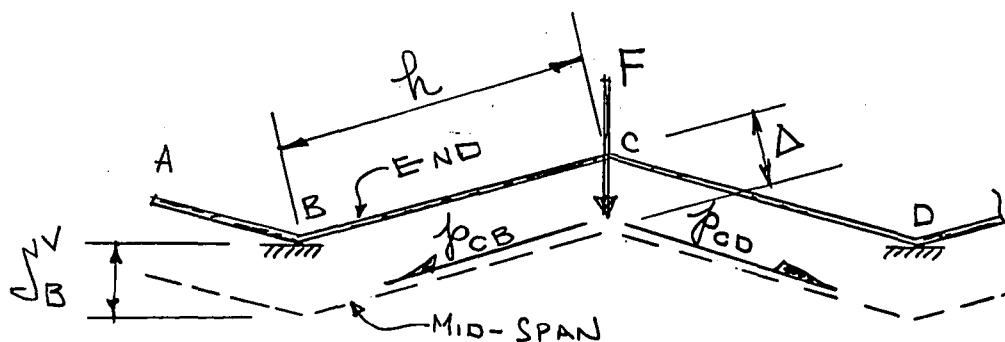


Increase in effective depth

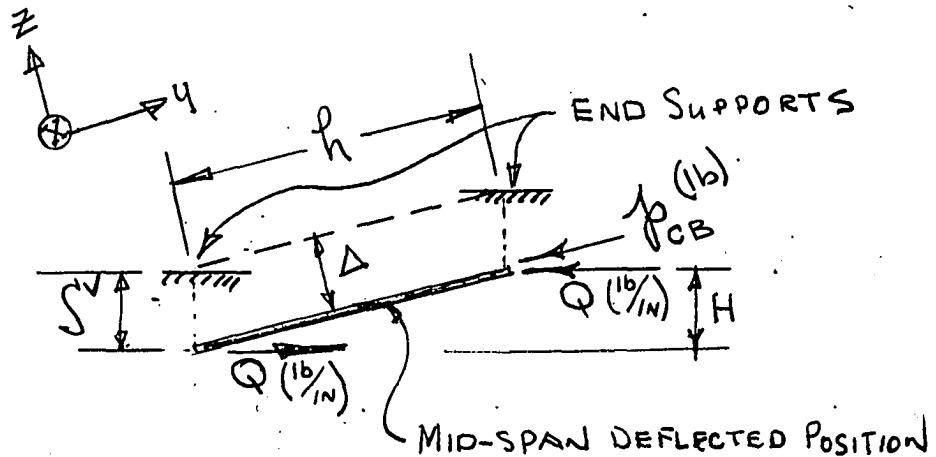
This effect, coupled with the foregoing thickness effect, probably accounts for the fact that with shallow configurations all of the experimental  $\sigma_x$ -values tend to be considerably less than the theory predicts - whereas one would logically assume that some values would be greater than and some less than predicted due to the fact that both the  $\sigma_{x\text{expr}}$ -values and the  $\sigma_{x\text{theo}}$ -values must form the same magnitude of internal resisting moment.

Another very elusive effect which seems to have entered into the picture is what could be called a side thrust phenomenon due to deflection geometry. The behavior of the pilot model first gave clue to the existence of this behaviorism. If a comparison is made of the correlation of  $\delta_B^V$  due to a concentrated load at the fold C and  $\delta_B^V$  due to a concentrated load at

fold D, it will immediately be seen that when the load is at D the correlation is much closer than when the load is at C. For both loading conditions the  $\Delta\delta^V$  between B and C is approximately the same, which dispels any notion that the transverse slab effects could be the explanation. Careful consideration uncovered the fact that the basic difference between the two loading conditions, in reference to their effect on  $\delta_B^V$  is that when the load is at C, plate BC is being deflected by a system of forces having a very large resultant in the plane of the plate, i.e.



When the load is at D, there is no resultant force in the plate BC in the direction of  $p_{CB}$  other than those that will be induced by lateral slab action. The plate BC is hereby bent in its plane by the effect of stresses being fed into it at its edge at C. The question is - what is the significance of this? If we observe that after loading,  $p_{CB}$  can be thought of as acting on a beam that has been deflected normal to the plane of loading, it will immediately be seen that for the plate BC to be in equilibrium there must be an additional set of edge forces (Q) distributed along the edges B and C, e.g.

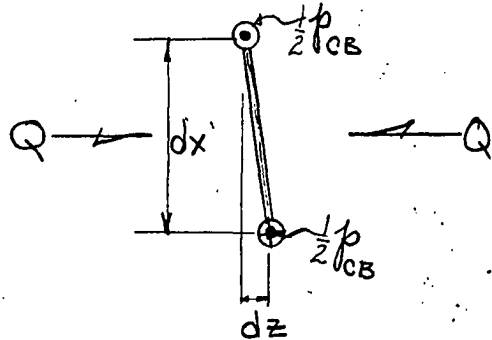


For the concentrated load case these edge forces will tend to be distributed in such a manner as to nullify the torsion that would tend to exist at each section along the plate, i.e.

$$QdxH = \frac{1}{2} p_{CB} dz, \text{ where } z \approx \Delta \sin \frac{\pi x}{L}$$

$$\therefore QdxH = \frac{1}{2} p_{CB} \frac{\pi}{L} \Delta \cos \frac{\pi x}{L} dx$$

$$\text{and } Q = \frac{1}{2} p_{CB} \frac{\pi \Delta}{LH} \cos \frac{\pi x}{L}$$



As shown above these  $Q$ -values are holding forces, so their effect on the structure is reversed, thereby creating the so-called side thrust phenomenon. If instead of a concentrated force in the plane of the plate we had a distributed force  $p = p_{CB} \sin \frac{\pi x}{L}$ , then the shearing force at any longitudinal section would equal  $p_{CB} \frac{L}{\pi} \cos \frac{\pi x}{L}$ , and from the foregoing analysis,  $QdxH = p_{CB} \frac{L}{\pi} \cos \frac{\pi x}{L} \cdot \frac{\Delta \pi}{L} \cos \frac{\pi x}{L} dx$  or  $Q = p_{CB} \frac{\Delta}{H} \cos^2 \frac{\pi x}{L}$

It is believed that this kick-out or side-thrust force is partially responsible for the greatly reduced edge beam stresses in the shallow configurations and by consequence the reduction of  $\delta_B^V$ -values. Of course there are other factors that contribute to the error in stress prediction but

they are readily mentioned in the literature and have already been mentioned in a previous section of this dissertation.

#### B. $\delta^V$ - values

All of the aforementioned items in regards to the  $\sigma_x$  - values are also applicable to the correlation of  $\delta^V$  - values because deflections are just manifestations of the stresses and strains. There is however a very important additional consideration to be made, especially in regards to the short models. This involves the significance of the shear deflection. Models 3 and 4 are glaring examples of this phenomenon because in these models, the aforementioned elements that have in other models produced conservative results, have here, been overpowered by shear effects that cause experimental  $\delta^V$  - values to actually exceed the theoretical. In the case of the short, shallow models (1 and 2) the shear effect is present but is not predominant over the other deflection-reducing effects.

With the interaction of all of these effects it is seen that even though we get the best  $\sigma_x$  correlation with the short, steep models we get the best  $\delta^V$  correlation with the long, steep models.

#### C. $m_y$ - values

The correlation of  $m_y$  - values has proven to be a rather unpredictable affair. As was originally anticipated, the surface loading with its allied difficulties has introduced some perplexing but nevertheless interesting problems. If ridge loading had been used, all  $m_y$  moments would have been a manifestation of the  $\Delta\delta^V$  - values and consequently would have yielded correlations of the same order as  $\delta^V$ , but with the surface loading the  $m_y$  - values become a function of the manner in which the loads are distributed

on the surface as well as  $\Delta\delta^V$ . In other words the discrete loading system here used, is seen by the total structure as a continuous and uniform loading system, with the consequence that the  $\sigma_x$  - values and the  $\delta^V$  - values respond correspondingly to the system. On the other hand the  $m_y$  moments are localized functions of this discrete loading system and correspondingly proved to be very sensitive to their location relative to the actual loading pad.

This conclusion was reached after a lengthy search for the cause of the discrepancy in the moment correlation and was confirmed by what the writer has chosen to call a post mortem on model No. 3. The purpose of the post mortem was to establish the variation of  $m_y$  - values as a function of their position relative to the actual load application pad. This operation was accomplished by cutting a representative sample from model No. 3 in such a way as to form a very basic folded plate structure with a span short enough to preclude longitudinal action and thereby accentuate lateral slab bending. The test section, Fig. 17, consisted of 1 fold plus 2 edge plates and had a span of 8-in. A variety of loadings were initiated to establish the effect of the load being on the plate where  $m_y$  - values were being measured and the effect of the load being on the plate adjacent to the one in which  $m_y$  - values are being measured.

The reason for this was to discern the Saint-Venant effect of the moment being transferred across a ridge. It was thought that the chosen structural element, by being stripped of the usual folded plate interaction would yield a direct insight on the relationship between the experimental and theoretical moments. The results of the post mortem are shown in Figs. 20 to 23.

**Fig. 17. Post-Mortem Setup**

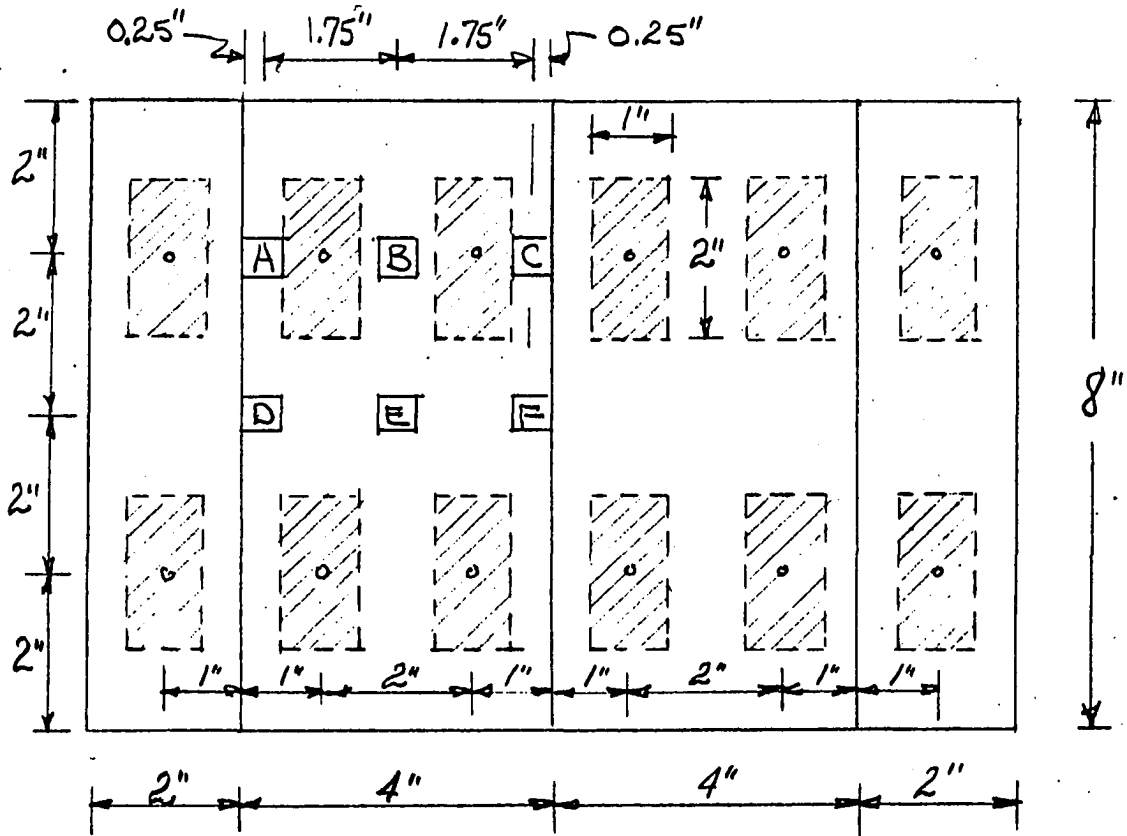


FIG. 18 GAGE LOCATION (NOT HORIZONTAL PROJECTION)

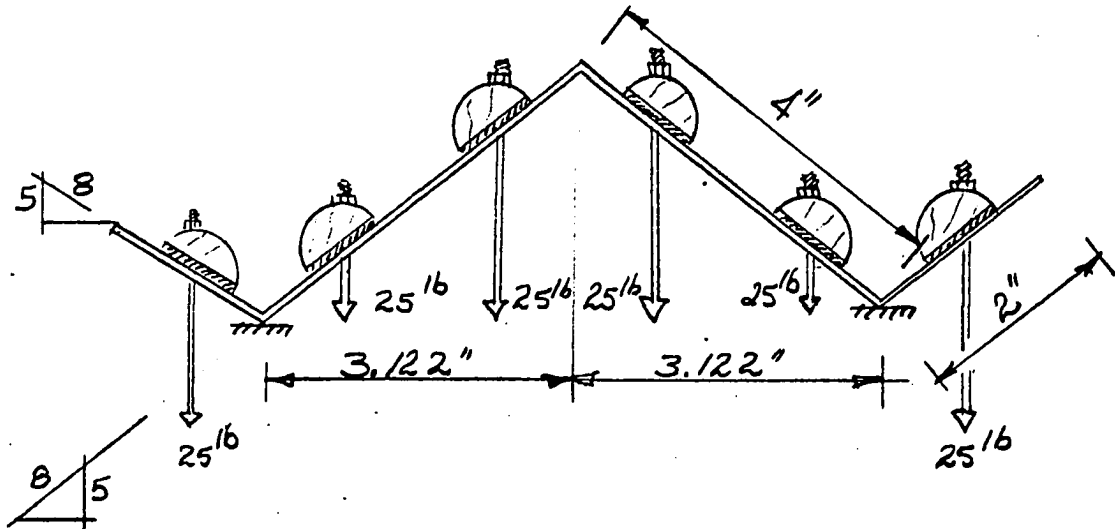


FIG. 19 LOAD PATTERN No 4



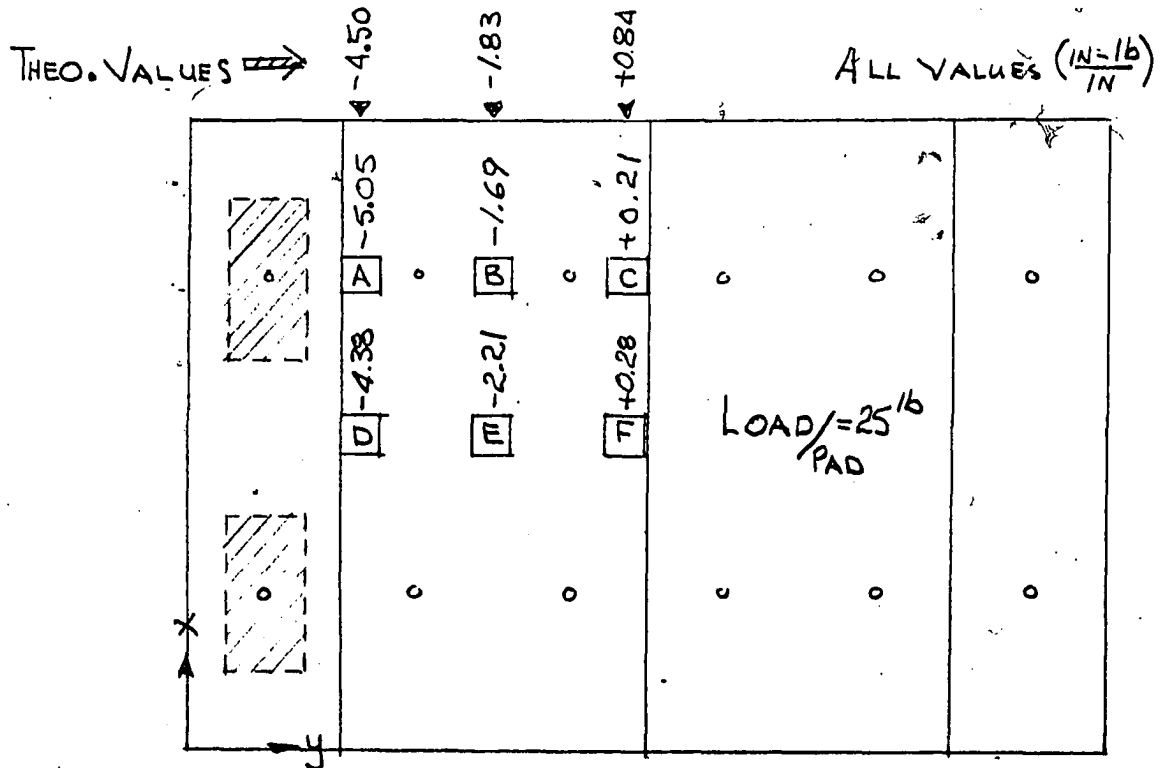


FIG. 20  $M_y$  FOR LOAD PATTERN NR 1

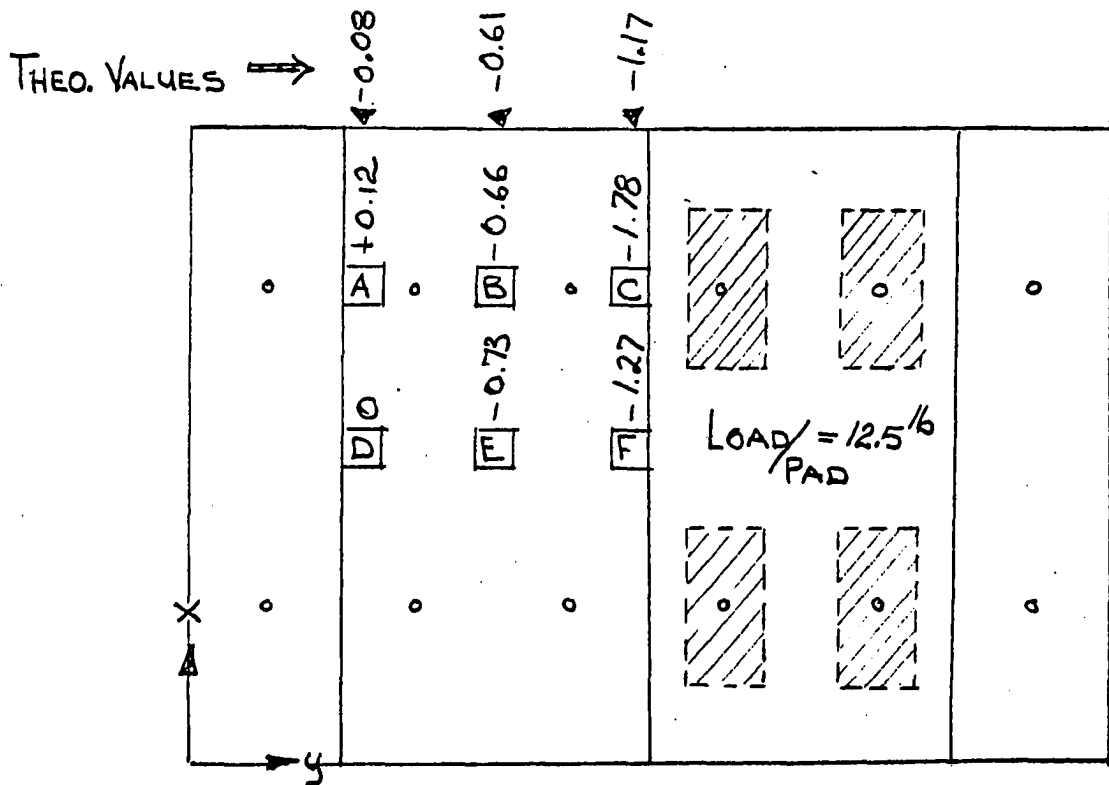


FIG. 21  $M_y$  FOR LOAD PATTERN NR 2

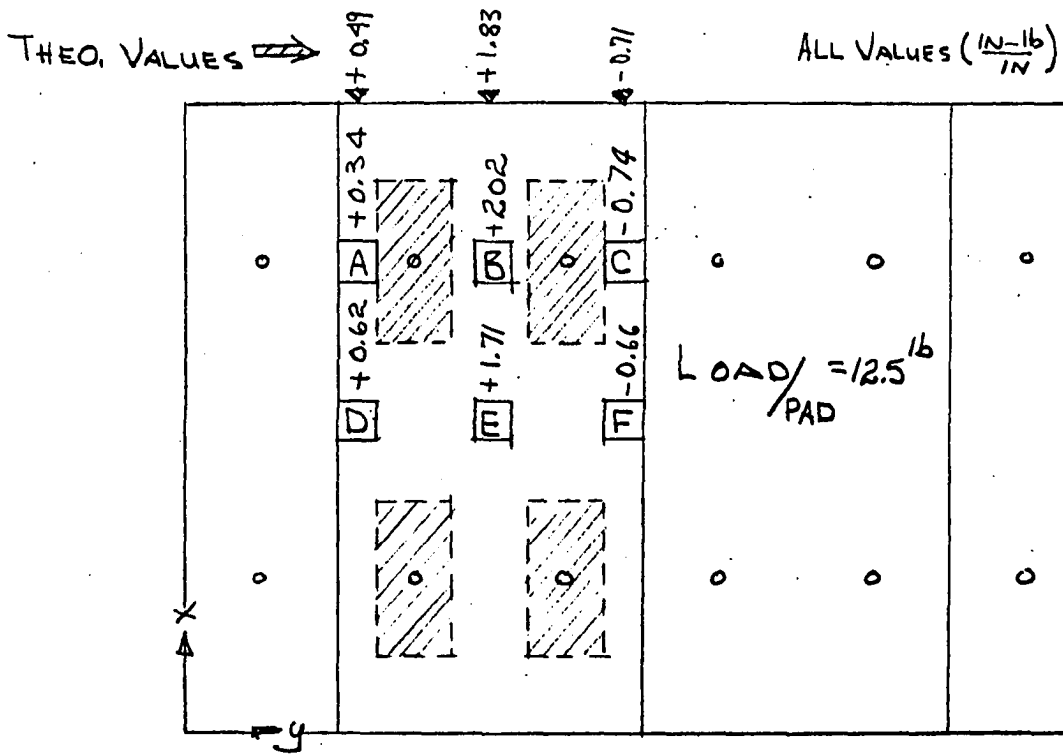


FIG. 22  $M_y$  FOR LOAD PATTERN No 3

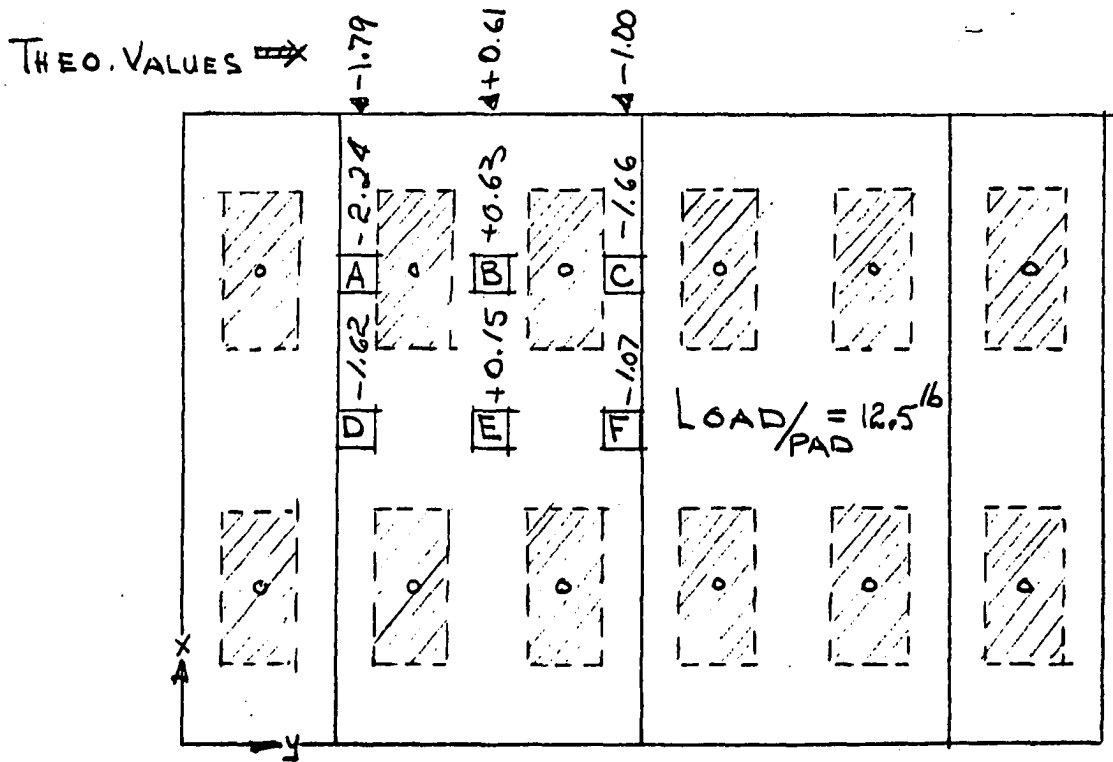


FIG. 23  $M_y$  FOR LOAD PATTERN No 4

Referring to Table 3 one will observe that the moment correlation at the first valley (B) is consistently fairly good and the experimental moment is greater than the theoretical moment. The reason for this lies in the fact that this valley moment is predominantly a function of the cantilevered load on the edge plate and therefore doesn't largely depend on the load acting directly upon the plate containing the location B.

If the post mortem information is extrapolated to effect a change in the  $m_y$  - values given in Table 3 an across-the-board improvement will be seen in the moment correlation. Qualitatively the results are very conclusive - quantitatively this extrapolation process leaves questions of degree unanswered and subsequently suggests that more extensive investigations are in order.

Another factor to be reckoned with in the  $m_y$  correlation is the fact that the folded plate theory does not account for the influence of  $m_x$  on  $m_y$ . This in itself constitutes quite an omission insofar as the  $m_x$  - values at times are greater than the  $m_y$  - values.

#### D. Experimental Observations on Buckling Behavior

All of the models tested buckled either elastically or plastically in the edge plate. In regards to the elastic buckling an attempt was made in the theoretical development to approximate the critical buckling stress in the edge plate with an equation of the form  $\sigma_{CR} = \frac{\pi^2 Et^2}{6(1-\nu^2)C_o^2 h_o^2}$ . In an attempt to derive some quantitative conclusions from the test data a plot of  $\epsilon_{x_{moment}}$  vs  $\epsilon_{x_{membrane}}$  was made for point A of each model, assuming that buckling could be detected by observing the stress level at which the moment

strains increase faster than membrane strains. Careful scrutiny of these plots revealed a strong tendency for all of the edge plates, regardless of the thickness, to buckle at an average stress level of around 5500 psi, Figs. 24 to 28. Of course the thin plates exhibited a much sharper break in linearity than the thick plates but nevertheless there were two thick plates where a break was observed at this stress level. If these limited buckling observations have any significance it means that

$$\sigma_{CR} = \frac{\pi^2 t^2}{6C_o^2} \cdot \frac{E}{(1-\mu^2)h_o^2}, \text{ where } \frac{\pi^2 t^2}{6C_o^2} = \text{a constant, } K$$

$$\text{Then } K = \frac{(\sigma_{CR})(1-\mu^2)(h_o^2)}{E} = \frac{(5500)(8/9)(4)}{10^7} = \underline{\underline{1.96(10)^{-3}}}$$

If more significance is attached to the more distinctive behavior of the thin plates,  $C_o$  can be evaluated, e.g.  $C_o^2 = \frac{\pi^2 t^2 E}{(6)(\sigma_{CR})(1-\mu^2)(h_o^2)}$

$\frac{(9.87)(0.0888)^2(10^7)}{(6)(5500)(8/9)(4)} \therefore C_o = \underline{\underline{2.57}}$ , inferring an effective length of buckle to be approximately 5-in. which is very close to the observed geometry. Additional variation of parameters will be necessary to validate this approximate formula as a design tool but it is definitely indicative of a trend.

#### E. Final Comments

It goes without saying, that as usual, more needs to be done. As evidenced by the current literature, quite a lot has been done on the mathematical model and not enough on the real model. It is the writers opinion that in the research endeavor at hand, a definite insight into the behavior of a folded plate system has been gained. In future research there are

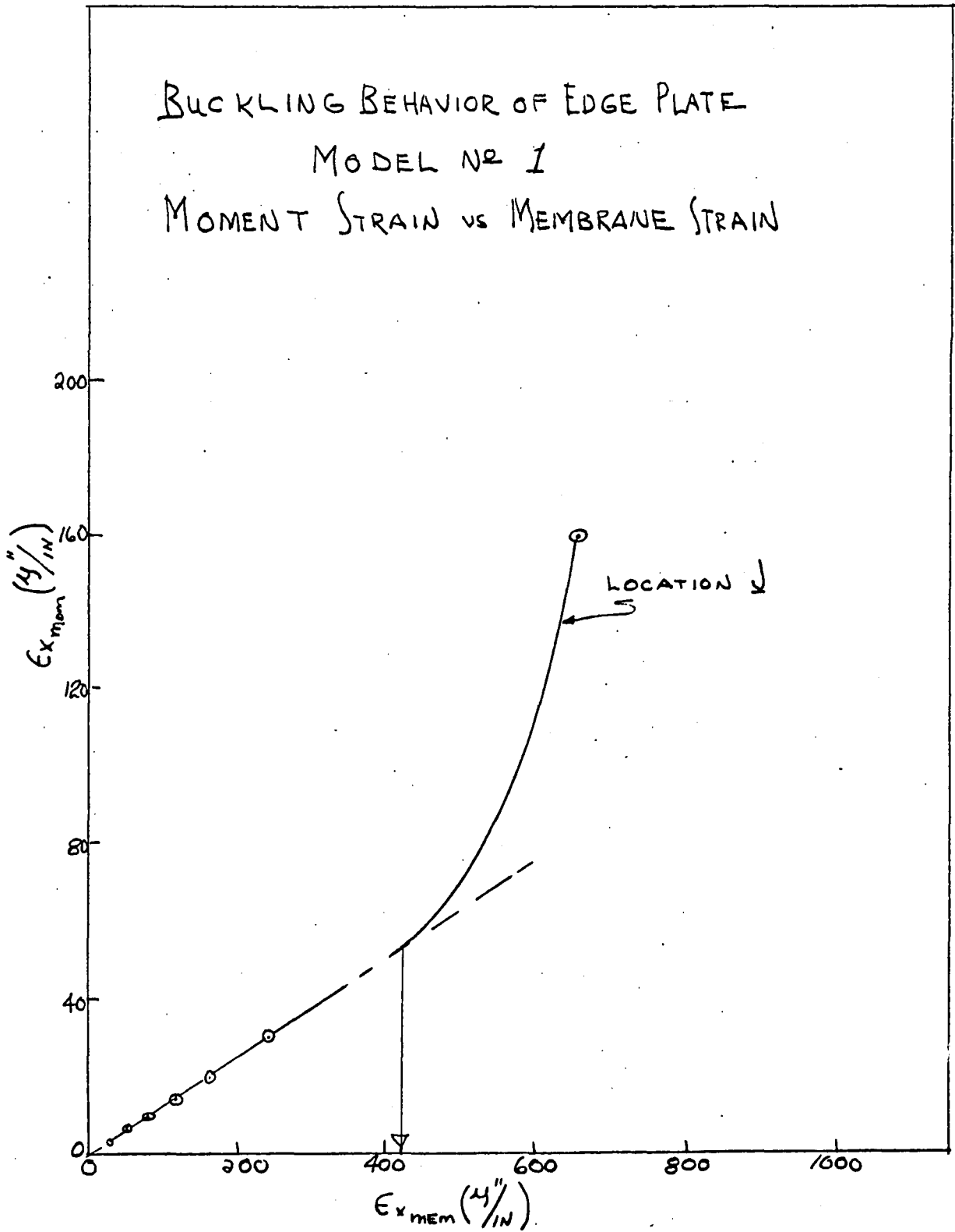


FIG.24 BUCKLING OBSERVATIONS

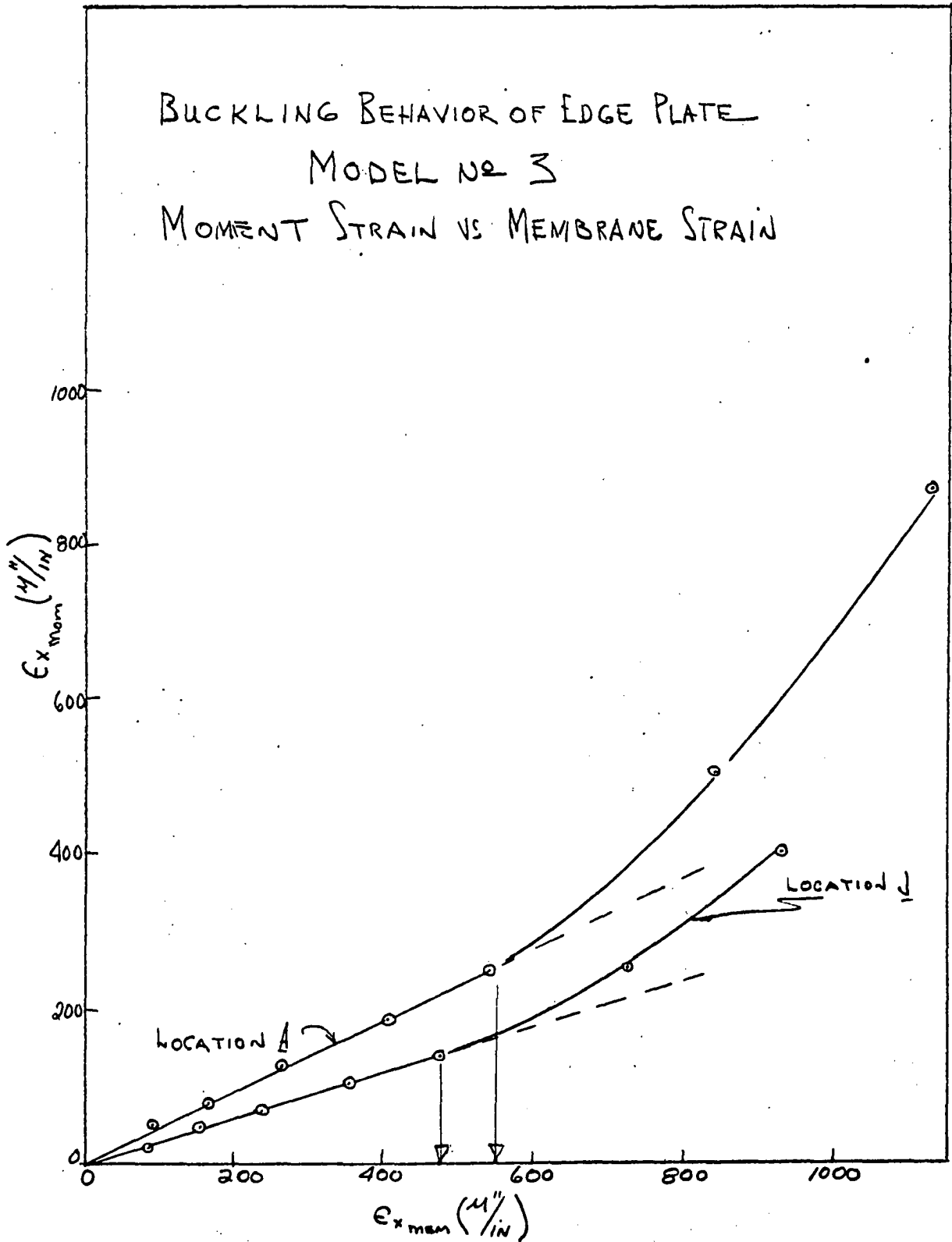


FIG 25 BUCKLING OBSERVATIONS

BUCKLING BEHAVIOR OF EDGE PLATE  
 MODEL No. 4  
 MOMENT STRAIN vs MEMBRANE STRAIN

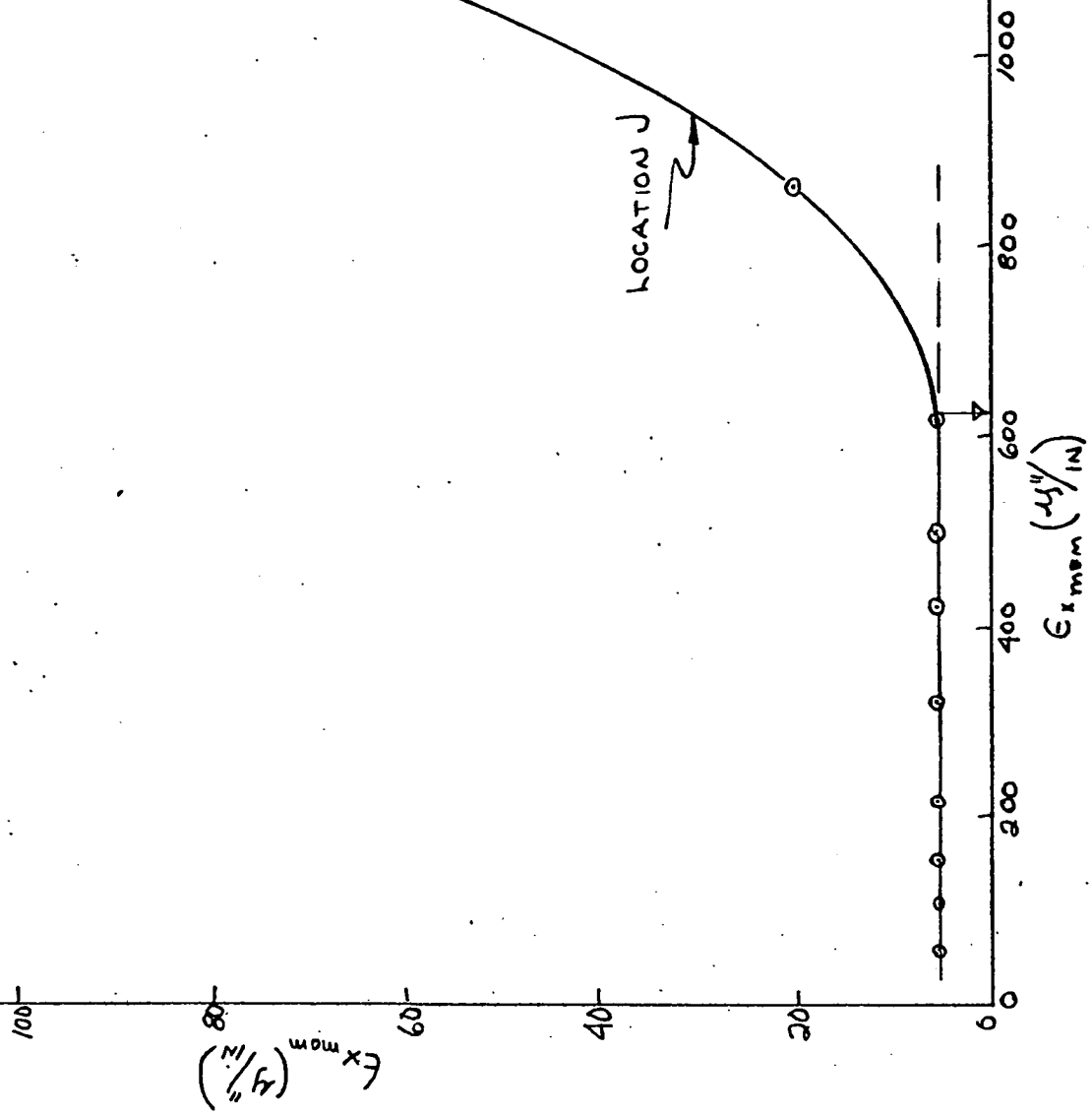
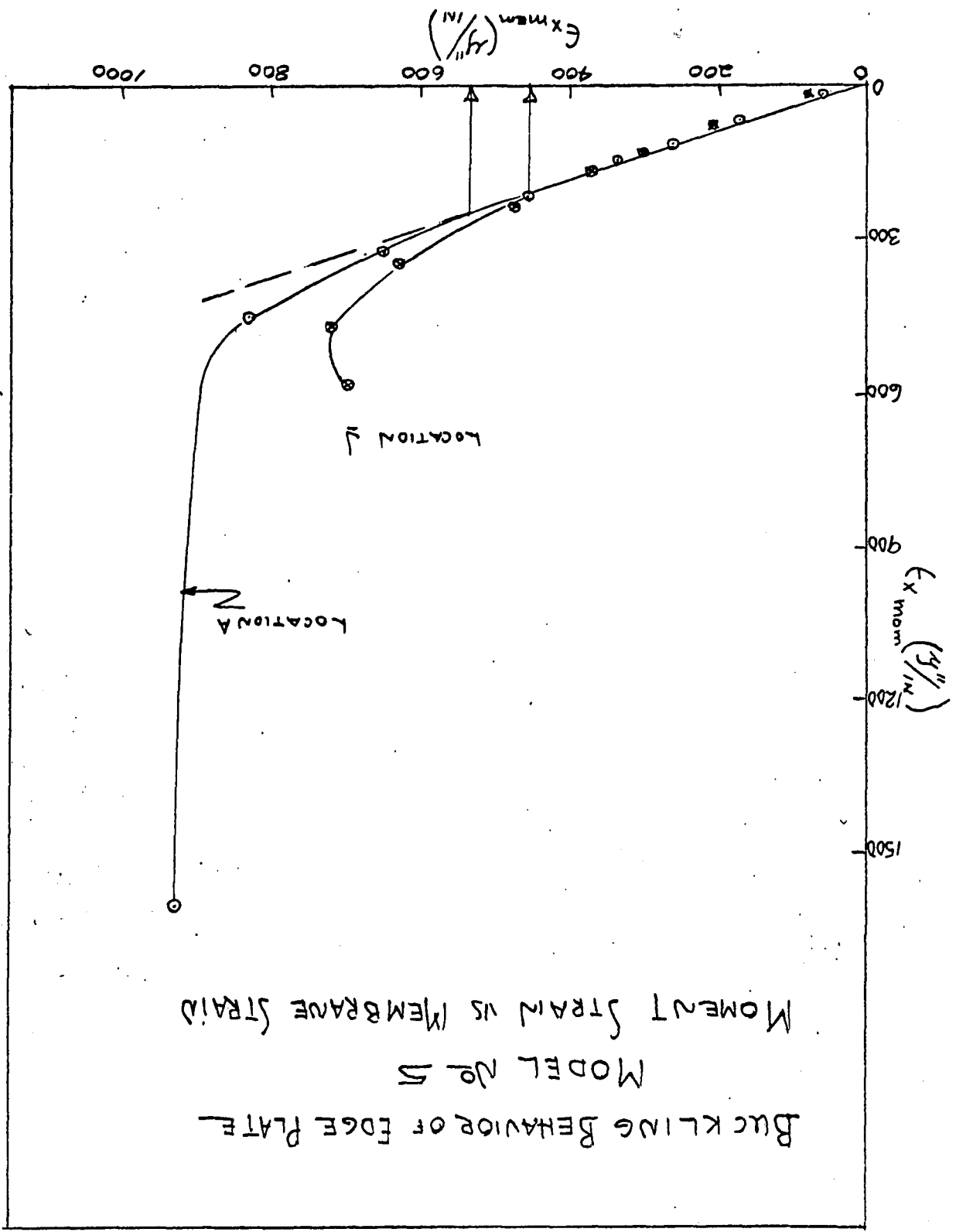


FIG 26 BUCKLING OBSERVATIONS

FIG 27 BUCKLING OBSERVATIONS





BUCKLING BEHAVIOR OF EDGE PLATE  
 MODEL NO 6  
 MOMENT STRAIN VS MEMBRANE STRAIN

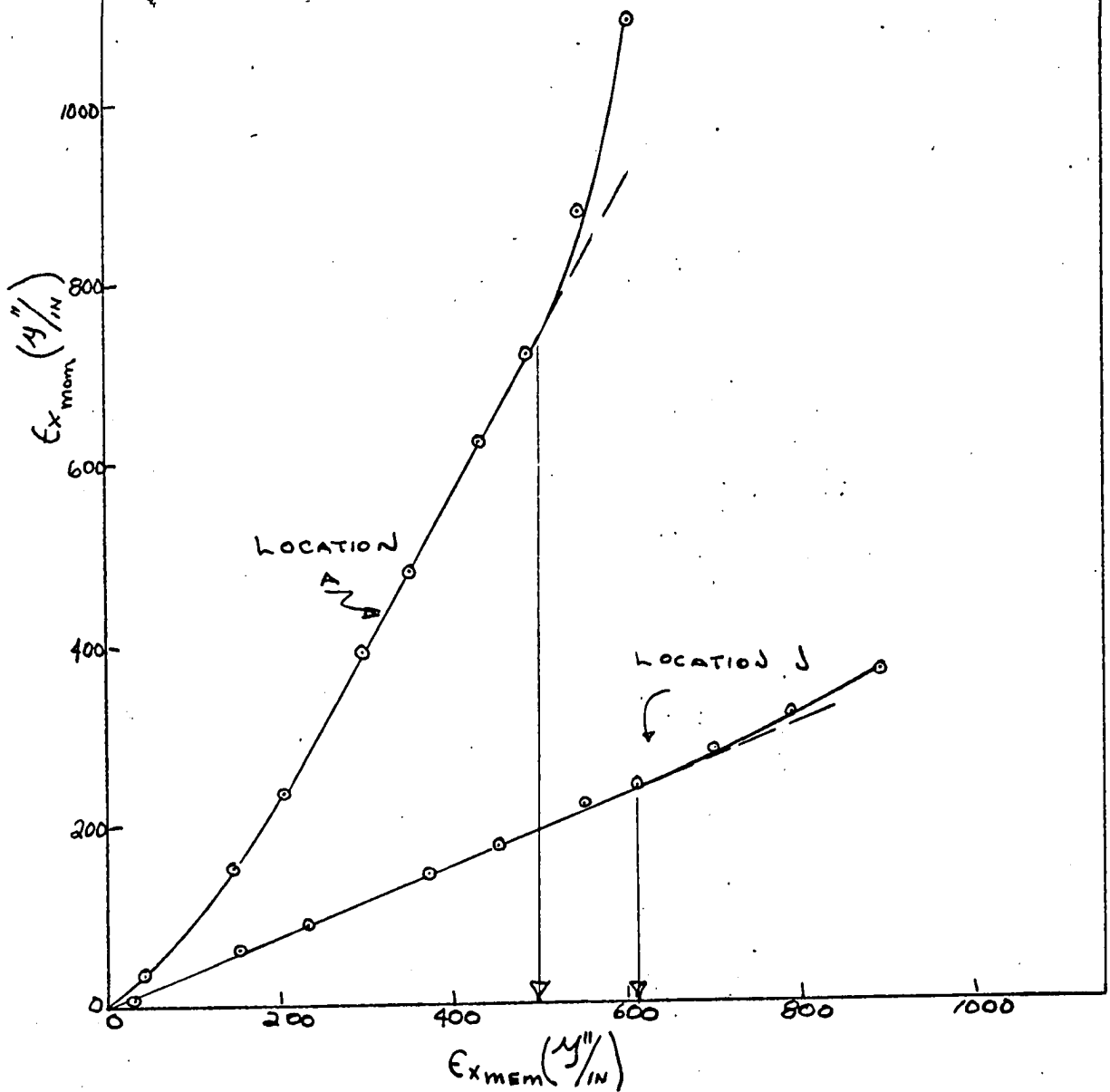
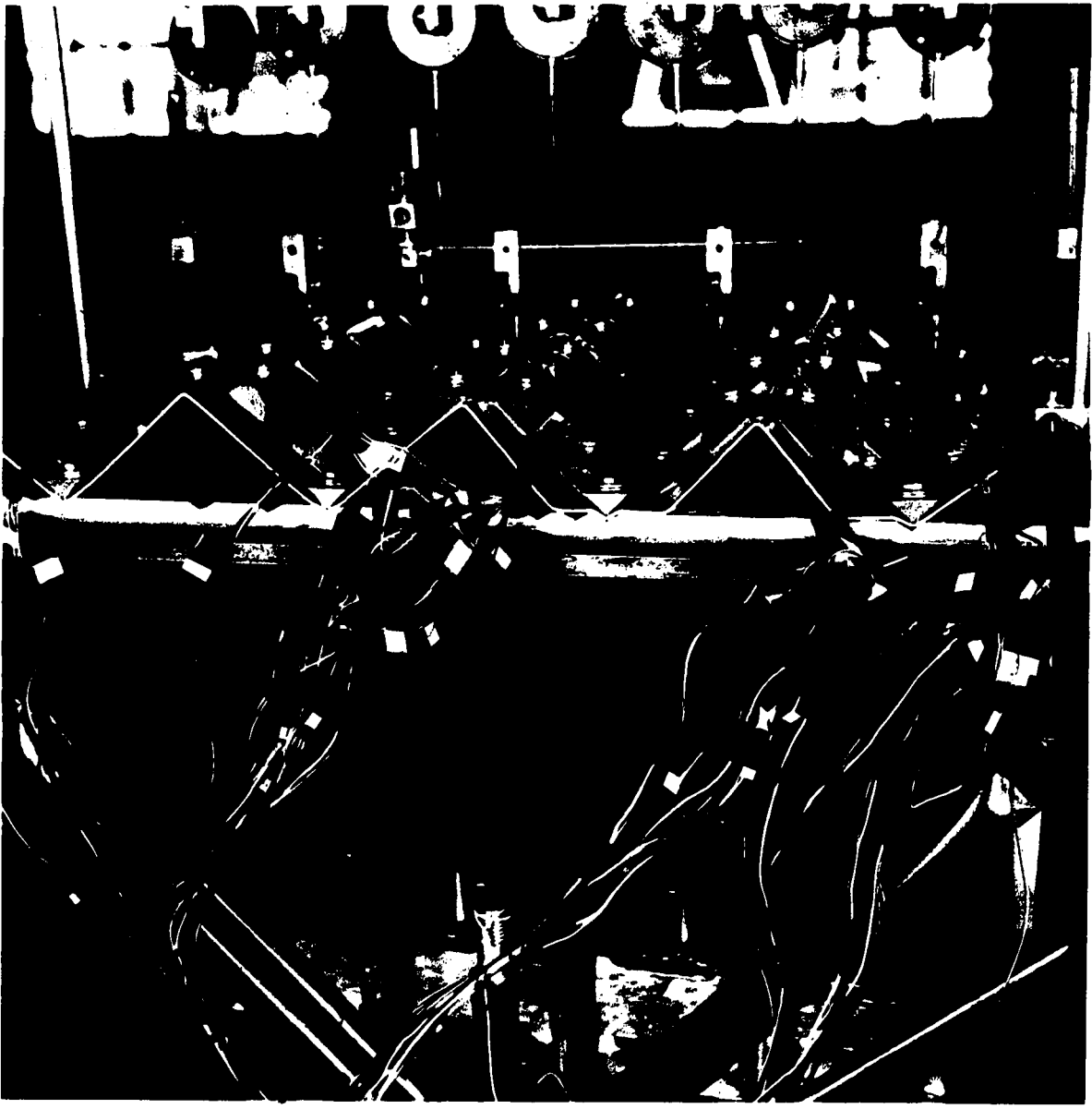


FIG. 28 BUCKLING OBSERVATIONS

**Fig. 29. Edge Plate Buckling**

**Fig. 30. Colapse by Slab Buckling**



obviously certain pitfalls to avoid, such as those relative to gage placement. The placement of gages directly on the ridges, with such spacing as to average out local disturbances should be investigated. This will also eliminate the necessity for including surface load influence in the theoretical calculations for moment, as is required when the point is not directly on the ridge. In addition to this there would probably be a distinct improvement in load continuity effect if the longitudinally discrete pads were replaced by longitudinally continuous pads.

An obvious out to these problems is to use just ridge loads, with the subsequent elimination of surface effects, but the question still looms in the mind of the writer relative to the correctness of the assumption that the surface loads are transferred to the ridges by a mechanism analogous to a continuous beam system. The results show conclusively that this trend is present but the matter of degree of precision of the assumption needs further attention. The writer would highly indorse a very basic research program that would delve into the actual validity of the fundamental assumptions. This would have to be initiated on structural systems so simple as to preclude the question of theoretical correctness of stress existing at points of interest. With such a simple system we would hopefully be able to isolate the various fundamental assumptions.

The hope of applying plastic or ultimate strength design to this particular folded plate configuration is rather remote because the plastic behavior of this system is quite frequently not a logical extension of the elastic behavior but on the contrary contains reversals of trend as evidenced by observing the test plots from model No. 5. It is therefore very dangerous to assume as we do in plastic design, that constant stress

levels are attained by successive elements of the structure with the consequent formation of a mechanism.

Finally in regards to the much sought after simplified design procedure for office practice, the writer is firmly convinced from the experimental results that there is much inherent neglected strength in this system which tends to reduce, in fact, the corrections made to the basic theoretical solution. This fact tends toward improving the validity of stresses predicted by the beam method.

Therefore a sensible design approach could be devised whereby the disturbance-producing edge plate is initially ignored or in essence, whereby we consider our structure to be of infinite lateral extent, and then replace the edge plate, assuming its stresses to be some predetermined proportion of the interior plate stresses.

## VII. SELECTED REFERENCES

1. Ashdown, A. J., The Design of Prismatic Structures. London, Concrete Publications LTD. 1951.
2. Born, J., Faltwerke, Ithr Theorie und Anwendung. Stuttgart, K. Wittwer Verlag. 1954.
3. Craemer, H., Theorie der Faltwerke. Beton und Eisen 29:276. 1930.
4. Ehlers, G., Die Spannungsermittlung in Flaechentragwerken. Beton und Eisen 29:281. 1930.
5. Gaafar, I., Hipped Plate Analysis Considering Joint Displacements. American Society of Civil Engineers Transactions 119:743-784. 1954.
6. Goldberg, J. E. and Leve, H. L., Theory of Prismatic Folded Plate Structures. Proceedings of the International Association for Bridge and Structural Engineers 87:59. 1957.
7. Gruber, E., Berechnung Prismatischer Scheibenwerke. Proceedings of the International Association for Bridge and Structural Engineers. 1932.
8. Gruber, E., The Exact Membrane Theory of Prismatical Structures Composed of Thin Plates. Proceedings of the International Association for Bridge and Structural Engineers. Vol. II. 1951.
9. Ketchum, M. S., Design and Construction of a Folded Plate Roof Structure. Journal of the American Concrete Institute Proc. 51:449. Jan. 1955.
10. Scordelis, A. C., Croy, E. L., and Stubbs, I. R., Experimental and Analytical Study of a Folded Plate. American Society of Civil Engineers Proceedings 87, No. ST8. Dec. 1961.
11. Simpson, H., Design of Folded Plate Roofs. American Society of Civil Engineers Proceedings. Paper 1508. Jan. 1958.
12. Timoshenko, S. and Gere, J., Theory of Elastic Stability. 2nd Edition. New York, New York, McGraw-Hill. 1959.
13. Timoshenko, S and Woinowsky-Krieger, S., Theory of Plates and Shells. 2nd Edition. New York, New York, McGraw-Hill. 1959.
14. Winter, G and Pei, M., Hipped Plate Construction. Journal of American Concrete Institute 43:505. 1947.
15. Yitzhaki, D., Prismatic and Cylindrical Shell Roofs. Haifa, Israel, Haifa Science Publishers. 1958.

## VIII. ACKNOWLEDGEMENTS

The writer is deeply grateful to his committee for their willingness to help whenever confronted, to Dr. Carl E. Ekberg, Jr., Head of Civil Engineering Department, who originally suggested the field of investigation and to the National Science Foundation whose fellowship created the opportunity to divert from his established routine and further his education.